PROBABILISTIC RELIABILITY ASSESSMENT OF TRANSMISSION SYSTEMS

DAWOOD ALALI

Thesis submitted to Cardiff University in candidature for the degree of Doctor of Philosophy.

School of Engineering

Cardiff University

2015

ACKNOWLEDGMENTS

I would like to thank my supervisors, Professor Huw Griffiths and Dr. Liana Cipcigan, for their guidance and input, but most of all for the constant motivation they have offered throughout my PhD. The result of this work would not be what it is without them. I would also like to acknowledge especially Professor Griffiths time, effort, and patience, and his helpful suggestions in the preparation of this thesis.

I would also take the opportunity to thank Professor Manu Haddad for giving me the opportunity to carry out my doctoral studies at the department and for the valuable discussions.

I also wish to thank all the people at the Engineering school, and especially those in the Advanced High Voltage Engineering Research Centre, for their good friendship and discussions.

In addition, I would like to thank Dubai Electricity and Water Authority for their sponsorship and for providing valuable data throughout the duration of this project.

Most importantly, I want to thank my parents, wife, children, family, and friends for their support during my work. I promise to improve my availability after my dissertation.

DECLARATION:

This work has not previously been accepted in substance for any degree and is not concurrently submitted in candidature for any degree.

Signed ……. (candidate) Date .....

STATEMENT 1

This thesis is being submitted in partial fulfilment of the requirements for the degree of PhD

Signed ……. (candidate) Date .....

STATEMENT 2

This thesis is the result of my own work/investigation, except where otherwise stated.
Other sources are acknowledged by explicit references.

Signed ……. (candidate) Date .....

STATEMENT 3

I hereby give consent for my thesis, if accepted, to be available for photocopying and for inter-library loan, and for the title and summary to be made available to outside organisations.

Signed ……. (candidate) Date .....

STATEMENT 4

I hereby give consent for my thesis, if accepted, to be available for photocopying and for inter-library loans after expiry of a bar on access previously approved by the Graduate Development Committee.

Signed ……. (candidate) Date .....

ABSTRACT

Power system reliability is defined as the ability of a power system to perform its function of maintaining supply without allowing network variables (e.g. voltage, component loading and frequency) to stray too far from the standard ranges. Traditionally over many decades, reliability has been assessed using deterministic criteria, e.g., 'N-1' or 'N-2' standards under prescribed severe system demand levels. However, using the so-called worst-case deterministic approach does not provide explicitly an assessment of the probability of failure of the component or system, and the likelihood of the outages is treated equally. On the other hand, a probabilistic security assessment may offer advantages by considering (i) a statistical description of the performance of the system together with (ii) the application of historical fault statistics that provide a measure of the probability of faults leading to component or system outages. The electrical transmission system, like other systems, is concerned with reducing different risks and costs to within acceptable limits. Therefore, a more precise algorithm of a probabilistic reliability assessment of electrical transmission systems offers an opportunity to achieve such efficiency.

This research work introduces the concept of applying the Line Overloading Risk Index (LORI) to assess one of the risks to transmission systems, namely, line overloading. Line failure or outage due to line overloading is catastrophic; they may lead to either load interruptions or system blackout. Some recent studies have focused on the assessment of the LORI; however, such research has been restricted to the analysis of system with very few intermediate demand levels and an assumed constant line thermal rating. This research work aims to extend the evaluation of the LORI through a comprehensive evaluation of transmission system performance under hour-by-hour system demand levels over a one-year period, for intact systems, as well as 'N-1', 'N-2'. In addition, probable hourly line thermal ratings have also been evaluated and considered over an annual cycle based on detailed meteorological data.

In order to accomplish a detailed analysis of the system reliability, engineering data and historical line fault and maintenance data in real transmission systems were employed. The proposed improved probabilistic reliability assessment method was evaluated using a software package, namely, NEPLAN, thus making it possible to simulate different probable load flow cases instead of assuming a single 'worst case scenario'. An automated process function in NEPLAN was developed using an extensive programming code in order to expedite the load flow modelling, simulation and result reporting. The successful use of the automation process to create multiple models and apply different contingencies, has made possible this probabilistic study which would not have been possible using a 'manual' simulation process. When calculating the LORI, the development of a Probabilistic Distribution Function (PDF) for line loading, line thermal rating and system demand was essential and useful. The developed algorithm takes into consideration the likelihood of events occurring in addition to severity, which offers opportunity for more efficient planning and operation of transmission systems. Study cases performed on real electric transmission systems in Dubai and the GB have demonstrated that the developed algorithm has potential as a useful tool in system planning and operation.

The research presented in this thesis offers an improved algorithm of probabilistic reliability assessment for transmission systems. The selected index, along with the developed algorithm, can be used to rank the transmission lines based on the probabilistic line overloading risk. It provides valuable information on the degree of line overloading vulnerability for different uncertainties.

GLOSSARY OF TERMS

GB	Great Britain
CPU	Central Processing Unit
DEWA	Dubai Electricity and Water Authority
DUBAL	Dubai Aluminium Company
FOR	Forced Outage Rate
Freq	Frequency of occurrence
HVAC	High Voltage Alternating Current
HVDC	High Voltage Direct Current
IEEE	Institute of Electrical and Electronics Engineers
LORI	Line Overloading Risk Index
N-1	Single equipment outage
N-2	Two equipment outage
PDF	Probabilistic Distribution Function
RAM	Random Access Memory
UAE	United Arab Emirates

LIST OF FIGURES

LIST OF TABLES

TABLE OF CONTENTS

CHAPTER 1. INTRODUCTION

The growth of modern society has significantly increased dependency on the availability and quality of electricity supply. Such rapid growth worldwide has resulted in many more extensive and complex national power systems which are often interconnected. The reliability and security of these important infrastructures ultimately depends on the level of redundancy or duplication so that these systems are resilient to the loss of critical component parts such as lines, cables or transformers. The level of reliability or security depends, therefore, on the level of investment and a balance must be struck between the required or desired security level and its associated cost. An evaluation of the probability of failure of a power system would help decision makers to maximize their beneficial results and minimize the associated planning and operational costs.

In this chapter, developments in national power systems are introduced, along with planning requirements for transmission systems. The aim, scope and contribution of this research will be presented.

1.1 Developments of national power systems

Modern power systems are complex networks with many generating stations often located far from load centres. These generating stations are interconnected using power transmission lines forming a power transmission network or grid. The generated electric power may be required to be transmitted over long distances to load centres through power transmission overhead lines and/or underground lines. Furthermore, the basic function of an electric power system is to supply its consumers with electrical energy as economically as possible and with a reasonable degree of continuity and quality [1].

Electric power systems have traditionally been operated and designed vertically, meaning generation, transmission, and distribution facilities are owned and/or operated by one or more

companies (Figure 1.1 a). With this structure, different power plants generate electrical power, which is transmitted to the remote load centres through transmission overhead lines and/or underground cables. This structure has existed for a long time and continues to exist in many countries. However, due to environmental and economic reasons, power systems in some countries are evolving into horizontally-designed/operated power systems (Figure 1.1 b), where distribution systems integrate both generation (e.g. renewable energy and / or distributed generation) and load. In this structure, the power flow could be bidirectional between the transmission network and the distribution network. Reverse power flows may occur when generation in the distribution system is high and the local load is low, while the transmission network transmits power to the distribution system when the local generation is low and the local load is high.

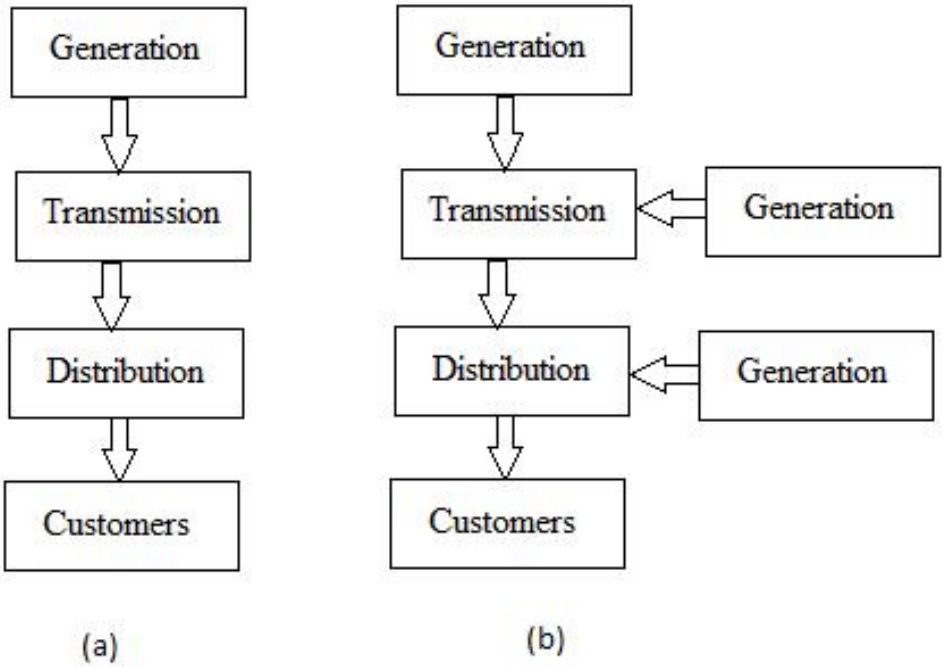

Figure 1.1: Structure of power system, (a) Traditional vertical power structure, (b) Horizontal power structure

The function of the transmission system is to transmit the energy generated by the generation system without violating the quality of supply (e.g. voltage, current). The transmission power system consists of a wide range of components that are necessary to execute its function, such as

overhead lines, underground cables, busbars, switchgears, transformers, shunt reactors, and protection systems. Generally, the voltage levels of a transmission system range from 115 kV to 750 kV [2], and the selection of the voltage level is based on power transfer requirement and cost [3]. Currently, power systems operate mainly as High Voltage Alternating Current (HVAC) systems. However, High Voltage Direct Current (HVDC) links are being integrated into modern transmission systems, due to advantages such as (i) the ability to interconnect AC systems of different frequencies, (ii) distance is not limited by stability considerations, (iii) no contribution to short circuit current infeeds in the AC systems, and (iv) cheaper where there is need for a submarine cable crossing [3].

To guarantee the reliability of the power system, several standards and criteria have been established to facilitate efficient system planning and operation. The next section reviews existing system planning methods for transmission systems.

1.2 Reliability evaluation for transmission systems and limitations of present approaches

1.2.1 Importance of transmission system and failures

The transmission system is the key to any power system; its failure could cause a minor or a major events. Transmission components may be subject to failures from a range of causes of fires, severe weather conditions (such as lightning and wind storms), component aging, lack of proper maintenance, operational human error, protection mal-operations, and high operating network variables (e.g. component loading and voltage).

As of 2009, the 400/275 kV transmission system owned and operated by GB National Grid consisted of 222 substations interconnected by 496 transmission lines and underground cables, creating a very large interconnected network. About 200 faults occur on the transmission system

every year [4]. In contrast, the 400/132 kV transmission system owned and operated by Dubai Electricity and Water Authority (DEWA) consists of 167 substations interconnected by 301 overhead lines and underground cables. According to DEWA fault records, an average of 12 line faults occurs on their transmission system every year [5]. This difference in fault rates between GB and DEWA could be attributed to the fact that GB system is spread over a wider area and susceptible to more extreme weather than that in Dubai, newer infrastructure in Dubai, and extensive maintenance in Dubai.

There is a low probability of component failures on the transmission system, in comparison with that in the distribution system. In the GB, each customer was without a power supply for an average of 86 minutes over a period of one year of 2000/2001; however only 1% of this unavailability was attributed to the transmission system or generating plants [6].

When a transmission component (e.g. line, cable, or transformer) fails, the load flowing through this component will be redirected through other components. As a result, there is a loading increase on remaining components that may exceed their capacity and result in overloading leading to a cascading failure of components and blackout. Hence the failure of a transmission component may have more wide spread and severe consequences, compared with failures on distribution systems.

1.2.2 Reliability assessment of transmission system

Consequently, transmission systems must be designed and operated to be secure against different types of failures, in order to guarantee as much as possible a continuous and high quality power supply to the consumer at low cost. Accordingly, there is interest in assessing the reliability of transmission power systems. The main purpose of assessing the reliability of a transmission power system is to estimate the ability of the system to perform its function of transmitting electrical power provided by the generating stations to the distribution system without violating the system

operational constraints. The reliability of a transmission system depends on environmental conditions in addition to the design, operation, and maintenance of the system and its restoration capabilities. Reliability analysis quantifies the system reliability based on the reliability data of its components. Such analysis can be utilized to assess past, present, and future performances of the transmission system.

Reliability assessment can be divided into two fundamental categories: system adequacy and system security. System adequacy is generally considered to be the existence of sufficient generation, transmission, and distribution facilities within the system to satisfy both consumer demand and operational constraints [1]. Security, on the other hand, is concerned with the ability of the system to respond to and withstand disturbances occurring within that system [1]. System security analysis may additionally be categorized into two types: transient (or dynamic) stability and steady-state (or static) security. Transient stability analysis evaluates system oscillations of frequency, voltage, and angle, due to a fault, which may cause a loss of synchronism between generators. Steady-state security analysis, on the other hand, determines whether, following an outage or a fault, certain components will be settling after an event into a safe level with respect to voltage and current.

Traditionally, most utilities base their investment and operation decisions by assessing the reliability of the network based on the deterministic approach developed in the 1950s, e.g., ‘‘N-1’’ (i.e. any single equipment outage) or ‘N-2’ (any two equipment outages) under prescribed severe system loading levels. With this technique, usually, a relatively small number of carefully selected and pre-specified credible contingencies (e.g. sudden removal of a generator, loss of a transmission line, or loss of system load) are selected for analysis. In using this method, the requirement is for the power system to remain stable and reach a new operating point without

loading or voltage violations following the contingency. Deterministic approaches are relatively simple and direct, and the results are easily interpreted by system planners and operators. However, such a worst-case deterministic approach has a major limitation in that it does not provide explicitly an assessment of actual system reliability as it considers only the consequences of pre-specified contingencies and does not precisely replicate the probabilistic (likelihood) nature of the system behaviour and component failures. Consequently, there is the possibility of over planning of the system [7]. The peak system demand condition, that the deterministic approach normally selects, typically, may occur only for a short periods of time during the year. Furthermore, different contingencies of transmission components occur also for only short period of time during the year. A comprehensive analysis should take into account aspects of viz. the probability and consequence of different operating scenarios. In fact, a probabilistic approach can potentially lead to great savings in investment cost without significantly increasing the risks [3].

A probabilistic reliability assessment may offer benefits by considering (i) a statistical description of the performance of the system over an annual cycle together with (ii) the application of historical fault statistics that provide a measure of the probability of faults leading to system outages [7]. This probabilistic technique assesses system reliability through the evaluation of quantitative reliability indices.

Although the probabilistic technique can offer the prediction of possible failure rates and reflect more accurately the actual level of reliability and system performance, it remains a fact that most of the present planning, design, and operational criteria of utilities are based on deterministic techniques. The main reasons cited for this situation are (i) lack of historical data, (ii) limited computational resources, (iii) difficult to use the techniques, (iv) an aversion to using probabilistic

techniques, and (v) a misunderstanding of the importance and meaning of the probabilistic criteria and risk indices [1].

1.2.3 Limitations of present reliability approaches on transmission system

Risk-based reliability assessment has been a topic for research over several decades in different aspects of power system analysis (e.g. steady state, dynamic, adequacy, transfer capability, expansion planning, and electricity market), considering a range of uncertainties in status of e.g. line and generator, and many reliability indices. As will be elaborated later in Chapter 2, a considerable amount of research has focused on the assessment of the Line Overloading Risk Index (LORI); however, such work restricted to a small number of system demand levels and single thermal rating value. The uncertainties involved in the planning and operation of the transmission system (viz. with respect to system demand, line failure, maintenance, and variable rating) are vital to assess the reliability assessment. An improved algorithm needs to be developed to assess and predict the behaviour of the transmission system through the evaluation of this LORI considering the relevant uncertainties for whole year hourly cases and whole year thermal ratings. Application of new developed tool in Dubai system could optimize the investment on infrastructure due to rapid load growth, while in GB could be useful to optimize the generation unit commitments.

1.3 Aim and scope of research

Line Overloading Risk Index (LORI) is one of the important indices used to assess transmission system performance, through analysis of probability and severity of line overloading. This research aims to extend the analysis of the LORI of transmission systems through an extensive reliability evaluation of the transmission system performance under hour-by-hour system demand levels for a one-year period, for intact systems, maintenance outage, line contingencies and thermal rating. As the consequences of line overloading depend on the frequency, duration, and magnitude of

occurrence of line loading, it is important to take into account the system demand variation over the study period, in addition to examining the effect of different contingencies. In addition, the hourly line thermal rating has also been evaluated over an annual cycle based on detailed meteorological data.

The scope of this work is limited to steady-state reliability assessment for transmission systems. This could be used both offline, to direct the power system planner, and online, to guide the power system operator in assessing the corrective actions required to prevent overloading.

1.4 Contribution of present work

During the course of the research programme, the following contributions were achieved:

- Development of an advanced probabilistic procedure for the reliability assessment of a transmission system, thus opening a path for including the risk of line overloading based on uncertainties of the system demand, line failure, maintenance outages, and variable thermal rating.
- Hourly calculation and study of thermal ratings for the transmission line for a period of one year, based on actual weather conditions and engineering parameters of real power systems.
- Development of sets of Probabilistic Distribution Function (PDF) for system demand, line thermal ratings and resultant line loading.
- Evaluation of Line Overloading Risk Index (LORI) for real systems, namely, the Dubai and GB transmission systems.
- Development of a C++ based programming code to automate modelling and multi-contingency analysis (i.e. adjust system demands, implement required unit commitment based on ranking order, apply single/double circuit outages, and report required line

loading in Amps), thus efficiently and accurately evaluating the risk of the transmission lines overloading.

1.5 Thesis outline

This thesis is organized into seven chapters. Chapter 1 introduces the developments of national power systems, in addition to the planning and operational requirements for transmission systems and the limitations of the present approaches. It also outlines the objectives, scope, and contributions of the thesis. Chapter 2 reviews, describes and compares literature on probabilistic reliability assessment of power systems, and the different technique and types of case used in such analysis. A detailed literature review was also carried out at specifically Line Overloading Risk Index (LORI), and it has been established that indices like the LORI are more appropriate to transmission system, as they provide a better and more realistic indication of the transmission system reliability. It was also found that despite its importance, the LORI has not been studied comprehensively, and the limitations of the published research works are that they use a limited number of study cases and single line thermal rating. Chapter 3 describes the deterministic approach to security assessment and its application to the Dubai transmission system. A new improved probabilistic approach to reliability assessment, in order to calculate LORI, is introduced and described in Chapter 4, considering system demand, multiple load flow simulations, line thermal rating, and reliability data. This improved algorithm was applied to two practical transmission systems (i) the Dubai (Chapter 5) and (ii) the GB (Chapter 6). Finally, Chapter 7 contains conclusions to the research work described in the thesis and presents promising future works.

CHAPTER 2. PROBABILISTIC RELIABILITY ASSESSMENT: A REVIEW

2.1 Introduction

Ensuring power system reliability has become one of the main challenges in the modern electricity industry. Thus, various approaches towards reliability evaluation and quantification have been developed.

The first section of this chapter reviews reliability in general and then specifically with regard to the power system, including different definitions offered for the term “reliability”. Then, the focus is turned to review the fundamental techniques used for reliability analysis in power systems, in particular the deterministic reliability technique, which is widely used in the utilities for system planning and operation. This is followed by a critical review of the probabilistic reliability technique. Uncertainties, reliability indices, software tools used, and test systems are described. Later, a wide variety of applications of reliability analysis are discussed. After that, different studies that have been conducted on the Line Overloading Risk Index (LORI) are reviewed. Finally, the chapter is concluded with a brief discussion that identifies the main limitations of the current approaches and provides justification for this research work.

2.2 Reliability assessment in power system

The development of reliability engineering in industry is coupled with various industries such as (i) the aerospace industry, (ii) military, (iii) the nuclear industry, (iv) electricity supply, and (v) continuous process plants, such as steel plants and chemical plants. A number of these industries have experienced severe catastrophic failures, e.g., aerospace (Challenger space shuttle in 1986 and many commercial aircraft accidents), nuclear (Chernobyl in 1986), and electricity supply

(New York blackout in 1977) [8]. These failures have caused significant social and environmental consequences that have increased the need to assess reliability more thoroughly.

A widely used definition for 'reliability' is 'the probability of a component and system performing its purpose adequately and securely for the length of time intended under the operating conditions encountered' [8]. It is important to differentiate between hazard and risk i.e. a hazard is an event that can be classified in terms of its severity but does not take account of its likelihood, while risk considers not only the hazardous event but also the likelihood of it occurring [8].

In power systems, as system demand increases, so the required or standard levels of redundancy increase [3], thus improving the system reliability. A common method of improving the reliability performance of a system is through component redundancy [8]. In practice, a power system consists of a network of components that are connected together either in a radial or meshed formation or combination of the two. Power systems are normally supplied by at least two or more normally-closed circuits connected in parallel (redundant) (Figure 2.1 b) or by one circuit (radial) with or without supervisory or automatic switching provision of alternative circuits which are switched into operating mode when a normally operating component fails (Figure 2.1 a) [3, 8]. A transmission network is designed to be fully redundant, which is effective, but is usually quite expensive. Increasing the number of components connected in radial formation decreases system reliability whilst increasing the number of components connected in meshed network increases system reliability [8]. Failure in radial system will result if any component fails, however, failure any component in meshed system will not cause system failure, hence more reliable.

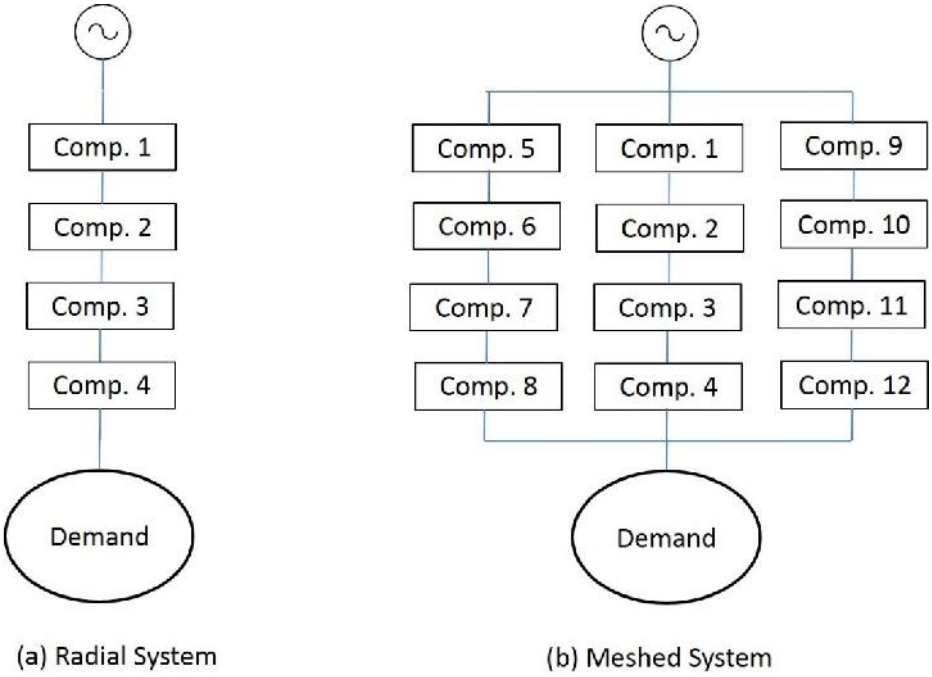

Figure 2.1: Radial and meshed networks

2.3 Reliability assessment techniques used in transmission power system

Two main techniques were found to be widely used for assessing the reliability of electric power systems, namely, the deterministic and probabilistic techniques, each with its own advantages and disadvantages. As early as 1905, improvements in the reliability of power systems were achieved by enhancing service reliability through the duplication of electrical apparatus [9]. The probabilistic assessment of power system reliability was found to be discussed as early as 1963 [10], in which the probabilistic method was used to evaluate the reliability and reserve benefits for interconnecting two power systems.

The deterministic technique evaluates whether the system can withstand the loss of any major single or multiple component, with consideration of an anticipated set of worst case system condition (e.g. at system peak demand, the probability of which may be small). In order to ensure that a single contingency ‘N-1’, double contingencies ‘N-2’, and/or even higher order ‘N-x’ contingencies do not result in problems in the transmission network, contingency analyses may be

run to study all credible “what-if” cases and check for consequences. Conducting an ‘N-x’ contingency analysis is challenging due to the huge number of contingency combinations which require extremely large amount of computational time. While the deterministic approach has traditionally provided an acceptable reliability level in the planning and operation for transmission power systems, one main weakness is the absence of any assessment of the likelihood of failure [1, 7]. Probabilities of important uncertainties, such as system demand, generator outputs, maintenance outages, and component failures, are ignored in the deterministic approach, thus, leading to over estimation of system planning reinforcement and operational requirements, and a corresponding excessive system security. If a component fails very rarely, for instance, but causes system loading to reach near or above maximum capacity, then according to the deterministic approach, its probability is ignored and severity is considered, which may result in costly operational measures or reinforcement in a future design.

The probabilistic method for security assessment aim to overcome disadvantages of simple deterministic method by consideration of probabilistic nature of component failures. This probabilistic approach represents inputs and outputs of power system through Probabilistic Density Function (PDF), thus considering the random nature of component failures and evaluating different operating conditions (e.g. thermal overloading). Considering probabilistic nature of power system and component results in a deeper insight into system performance, since likelihood and severity of limit violation are two main aspects to evaluate the security level. The probabilistic reliability assessment process in a power system consists of quantifying the possible limit violation (i.e. severity of the consequences) and the probability (or likelihood) of occurrence [1]. Power systems, like any other type of system, are vulnerable to various types of component failures and they are affected by environmental or operational uncertainties e.g. fire, tower collapse, extreme weather,

etc.. The main advantage of the probabilistic approach is the ability to quantify the environmental and operational uncertainties affecting the components and systems as a whole [7].

Accordingly, deterministic approach assess the power system and the results are based on the severity evaluation, while the result of probabilistic approach is based on both the severity and likelihood of component failure. In this research work, the results were benchmarked against the deterministic approach

Over the past 20 years, there has been growing recognition of the importance of the probabilistic aspect of different uncertainties [12-27]. These studies have been carried out using the probabilistic approach for security assessment of transmission systems, different techniques have been applied and risk indices derived.

Previous studies have investigated the influence of uncertainties on a practical and test power system for the evaluation of reliability. In such evaluations, the uncertainties were quantified using time varying system demands [12-18], generator outages [15, 19], line failure [18-27], and ambient temperature [25].

Once the uncertainties of interest have been selected and their probabilities have been found, they can be used to evaluate the probability of different power system states. The most widely used methods for assigning probability to different system states are (i) the analytical method (sometimes called 'enumeration' method) and (ii) the Monte-Carlo simulation (MCS). The analytical method calculates risk indices through defining and analysis of probabilities of all possible system states, while the MCS method estimates the reliability indices by simulating the actual process and random behaviour of the system according to their probability distributions [8]. According to literature, most studies have focused on the MCS method [28-46], and only a few

have used the analytical approach [22]. This is could be attributed to the size of the study cases and computational burden.

Due to the complexity of required computations for reliability evaluation, many software packages have been used for system modelling and for the calculation of various risk indices. Examples include MATLAB [12, 30, 32, 47, 48], NEPLAN [22, 49, 50], Power System Analysis Toolbox (PSAT) [51], DIgSILENT [24], PROCOSE [52], Physical and Operational Margins (POM) [53], PRA [53], and 'NH2' [51].

Previous work has proposed a number of reliability indices, which are calculated using the probability of the states and the resultant severity. Examples include (i) voltage performance [19, 20, 27, 53, 55-58] that express voltage limit violations, voltage collapse, and voltage instability; (ii) line overloading [18-20, 22, 27, 38, 45, 49, 51, 53, 57-61], which are demonstrated through e.g. thermal overload and security margin; (iii) load curtailment [16, 17, 23, 24, 26, 27, 42-44, 53, 54, 60, 62-68], which is calculated as duration, frequency, and probability of power (or load) and energy curtailment (or interruption or shedding or loss); (iv) cost [16, 18, 24, 52, 70-78], which is evaluated as interruption cost, remedial action cost, benefit cost ratio, investment cost, operating cost, and social cost; and (v) combined severity indices [19], which comprises both the overload and voltage severity indices.

In terms of the types of systems studied, a range of simplified test and real systems were used for the probabilistic reliability analysis of transmission systems, as can be seen in Table 2.1.

2.4 Applications of probabilistic assessment in transmission systems

Reliability assessment of transmission systems is the key in decision making regarding the new investment, maintenance, design, and operation of a system. Studies have been carried out into the probabilistic-based reliability assessment and have been applied in different particular areas of a

Table 2.1: Study case systems used in probabilistic approach studies in transmission system

Study Case Name	No. of buses	System demand (MW)	Study Features	Type of System
5-bus reliability test system [58]	5	230	System power loss	Test
IEEE 6-bus reliability test system [43-44]	6	185	Frequency and duration of load and energy interruption	Test
IEEE 9-bus reliability test system [79]	9	Not mentioned	Line flow probability evaluation	Test
IEEE 14-bus reliability test System [12, 25, 37]	14	Not mentioned	(i) Transfer Capability, (ii) Thermal limit violations,	Test
22-bus reliability test system [38]	22	11,525	Line flow	Test
IEEE 24-bus reliability test system [16, 18, 20, 23, 27, 28, 35, 36, 40, 44-47, 52, 63, 67, 80, 81]	24	2850	(i) Frequency, duration and cost of load and energy interruption (ii) Severity index for voltage violation, overload, load loss, and frequency deviation (iii) Transfer Capability (iv) Market bid energy cost	Test
IEEE 30-bus power system [26, 30]	30	Not accurately specified	(i) Loss of load (ii) Transfer Capability	Test
IEEE 96-bus reliability test system [58, 82]	96	8550	(i) Overload and voltage severity indices (ii) Transfer Capability	Test
IEEE 118-bus reliability test system [19, 31, 34, 41, 48, 59, 61, 79, 83, 84]	118	Not clearly specified	(i) Line flow probability, (ii) Overload, voltage and composed severity indices (iii) Transfer Capability (iv) Cascading Blackout (v) Probabilistic load flow	Test
IEEE 145-bus test system [21]	145	Not mentioned	Contingency Analysis	Test
WSCC 9-bus system [33]	9	315	Transfer Capability	Real
Western Electricity Coordinating Council (WECC) system [32]	179	Not mentioned	Transfer Capability	Real
Great Britain (GB) (Figure 2.9) [22, 49]	322	25,850	Security Margin	Real
Romanian Power System [47]	145	Not mentioned	Transfer Capability	Real
Taiwan Power Company [85]	122	Not mentioned	Transfer Capability	Real
Italian power grid [86]	Not mentioned	Not mentioned	Transfer Capability	Real
Brazilian South/ Southeast/ Central West system (BSSW) [82]	1629	31,920	Transfer Capability	Real
Northern Region Electricity Board, India (NREB) system [20]	Not mentioned	Not mentioned	Contingency Analysis	Real
New England test system [21, 39]	39	Not mentioned	Contingency Analysis	Real
New York power system [39]	Not mentioned	Not mentioned	Blackout hazard	Real
Khorasan Regional Electric Company (KREC) [41]	125 substations	3000	Cascading Blackout	Real
Electricite du Laos (EDL) [24]	38	Not mentioned	Frequency, duration and cost of load and energy interruption	Real
Egyptian Transmission Company [65]	Not mentioned	17,300	Frequency, duration and cost of load and energy interruption	Real
Korea power system [53]	1668	Not mentioned	Overload, Voltage and load loss indices	Real
Part of Korea system [66]	21	Not mentioned	Load interruption	Real
Brazilian Southern/Southeastern (SSE) system [54]	660	27,895	Loss of load	Real
Saskatchewan Power Corporation (SPC) system [67]	41	1802.90	Frequency, duration and cost of load and energy interruption	Real

transmission power system, in order to evaluate the cascading failure, blackout, transfer capability, load flow, contingency analysis, line thermal rating and others, as will be explained in this section. In many of these applications, the probabilistic technique has become essential to the decision making, especially because of the benefit it provides in assessing the reliability with sufficient accuracy.

2.4.1 Evaluation of the cascading outages and blackout

Transmission power systems could suffer intervallic disturbances that may activate cascades of component failures, which, in turn, can result in blackouts of different scales. A cascading failure is a single or sequence of events which causes a sequence of component outages and leads to massive disruptions to the electricity service [79]. Some of the uncertainties which have been considered in probabilistic investigations into cascading failures include effects of the different sources of failures (e.g. cascading overloads, failures of protection devices, and voltage collapse) [40], long-term effects of reliability policies (e.g. standard 'N-1' criterion) and system demand growth [61]. Many methods and models have been developed to study cascading failures probabilistically, for instance, using (i) the branching process [83, 84, 88-91], which uses high level probabilistic models to describe complicated cascade failures, starting from some initial distribution of failures that then propagate in stages, (ii) Monte Carlo Simulation (MCS) [39, 41], (iii) Metropolis algorithm [92] in order to easily specify a uniform search distribution in rare event simulation, and (iv) Exponentially Accelerated Cascading (EAC) model [93], which is used to evaluate the probability of high-order cascading contingencies.

2.4.2 Evaluation of the Transfer Capability

The Transfer Capability (TC) of a transmission system indicates the maximum real power that can be exchanged between different areas [28]. Many studies have calculated the TC using the

probabilistic method to consider different uncertainties. For instance, [12, 31, 32, 36, 37, 81] calculated TC based on the MCS method to consider the impact of uncertainties of system demand, while [31, 33] incorporated security constraints in their TC studies. The characteristics of TC were obtained through its probability distribution function in [34, 85]. TC analysis using the probabilistic method gradually came to have a wide application in industry. It was used to quantify the importance of each component [49], ranking outage events [50], congestion management [47, 86], and wind farm management [28].

2.4.3 Load flow algorithms

Most uncertainties in the application of the probabilistic method on the load flow algorithm are found to be stochastic generation output [21, 94], generation unit outages [59, 95, 96], wind generation output [95], fluctuation of loads [59, 94, 95], branch outages [59, 97-99], and node data [100]. Different techniques of applying the probabilistic approach to load flow equations were (i) Gaussian mixture models [101] to represent non-Gaussian correlated input variables, such as wind power output or aggregated load demands; (ii) method of moments [79, 102] in which power flow equations are solved in the moments domain (without knowledge of the specific PDF of the input variables beforehand but using only the expected value and standard deviation of input variables), for simple, high speed and accurate calculation; (iii) the cumulant method [103] to obtain the cumulants of the input random variable that has complex distribution function, considering the correlation between input random variables; (iv) convolution [104-106], for getting a probabilistic load flow solution dealing with the linear correlation between input random variables; (v) point estimation [107] to estimate the uncertainties of bus injections and line parameters, through probability distribution fitting; (vi) Monte Carlo Simulation (MCS) [108-111], and (vii) dependence between input nodal powers [112, 113].

2.4.4 Calculation of the line thermal rating

When applying the conventional deterministic approach to determine the line thermal rating, 'worst-case' weather conditions are assumed. However, weather conditions vary frequently in certain periods and areas; thus, this conventional method may under-estimate the thermal line rating. In the probabilistic approach, actual detailed data of prevailing weather conditions are used to determine the line thermal rating. Calculation of the line thermal rating was estimated probabilistically considering historical environmental conditions at a certain time [114-120].

2.5 Evaluation of Line Overloading Risk Index (LORI)

A system reliability evaluation normally begins with the calculation of the failure rate of a component followed by an analysis of the severity effect of failure. From this, the calculation of reliability indices follows. Distribution utilities commonly use indices associated with load interruption includes e.g. System Average Interruption Duration Index (SAIDI), System Average Interruption Frequency Index (SAIFI), and the Customer Average Interruption Duration Index (CAIDI). Such indices attempt to capture the impact of interruptions on customers and loads for distribution system. Often, these indices are incorporated in software tools, e.g. NEPLAN. However, these indices are not so useful for transmission system reliability since the load interruption due to failure of components is very rare in the comparison with distribution system. It has been recognized that indices required to assess transmission system performance should be pivoted towards other aspects, rather than the impacts on load interruption. The acceptable service quality of a transmission system could be tied to several parameters, e.g., voltage level, component loading, and so on. Accordingly, it has been established that indices like the Line Overloading Risk Index (LORI) are more appropriate, as they provide a better and more realistic indication of the transmission system reliability.

Many similar terminologies have been used for LORI, such as security margin [22, 49, 50], transfer capability [12, 31-37, 80-82, 85, 86], thermal overloading risk [18], overloading severity [20, 58], power severity index [19], thermal limit violation [25, 27], line overload risk [45, 51], and overload reliability index [53]. The terminology used in this research is 'Line Overloading Reliability Index' (LORI) since it is related to one of the main objectives in a transmission system, i.e., maintaining line loading within prescribed limits.

Although considerable researches have been devoted to evaluate the LORI, they have been limited to consideration of only one or two uncertainties in the transmission system, such as 'N-1' component outage [12, 19, 21, 22, 25, 31, 32, 37, 51, 58, 81, 86], up to 'N-2' component outage [18, 27, 34, 50, 53, 80], multiple component outage [45, 49], up to four system demand levels [12, 22, 31, 35-37, 45, 50], annual system demand [18], system demand forecast error [12], weather [18, 25], generator output [31, 37, 86], and power transactions in electricity market [85]. Indeed, little or no attention has been paid to the combined uncertainties of system demand, line outages/maintenance, and variable thermal rating for whole year in hourly basis.

The main methods used in selecting study states, which are of great use in evaluating the LORI, are the enumeration method [22, 27, 50, 80, 81] and the MCS method [12, 21, 25, 34-37, 45]. The MCS method, on the other hand, generates some states based on a provided PDF, but does not generate all states. The approach followed in this research involves studying all possible cases systematically by assigning a probability. Using this technique, as will be shown later, makes it possible to study all states, instead of selecting and studying the states randomly (as is the case in MCS).

As previously shown in Table 2.1, the LORI was evaluated using a range of test and real systems. This research has focused on two real transmission systems, namely, those of Dubai and the GB,

to apply a new algorithm for calculating the LORI. These real systems, rather than test systems, were selected for the following reasons:

(i) The Dubai and GB power systems provide good examples of a small and large transmission system respectively and provide useful contrast in load and temperature characteristic.

(ii) Detailed system data was available for both systems.

(iii) The adoption of real systems allows a realistic local meteorological data for calculation of thermal ratings.

(iv) In GB, introduction of renewables can lead to more heavily overloading and there are difficulties of building new lines. In Dubai, repaid expansion is seen. Hence different circumstances are studied.

As described in Section 2.3, several tools have been previously used in studies to calculate the LORI. In this thesis NEPLAN was chosen as the software platform which has the facility to carry out power flow calculation and incorporates a programming facility based on C++ to enhance detailed control of computations and import and export data handlings.

2.6 Conclusions

This chapter has set out the challenge for evaluating the reliability of industrial systems as a means of preventing sectional or even catastrophic failures as much as possible within economic constraints. The application of reliability assessment techniques to transmission systems has been reviewed and it was found that numerous investigations have been carried out on a range of 'test' and real system models using enumeration, Monte Carlo techniques, and many different softwares have been used in such studies. Application of the probabilistic technique was used in assessment of blackout, power transfer capability and voltage assessment under contingencies. It was found

that the results of deterministic approach that is based solely on the severity evaluation, was not compared with the probabilistic approach which is based on both the severity and likelihood of component failure. It will be shown in the subsequent chapters that the proposed method could be superior to deterministic approach due to consideration of both severity and likelihood that may result in the most efficient operation and design of the transmission system. Specifically, for transmission systems, work has been carried out in the evaluation of the Line Overloading Risk Index (LORI). In the various approaches of reliability assessment for the transmission systems studied in this review, it was found that despite its importance, the LORI has not been studied extensively, and the limitations of the published works appear to be that they utilize only a limited number of system demands and one line thermal rating. It has been found that there is a need for further research into a comprehensive evaluation of the LORI taking into account combined uncertainties of system demand, line failures and line thermal ratings.

CHAPTER 3. DETERMINISTIC APPROACH TO SECURITY ASSESSMENT AND ITS APPLICATION TO THE DUBAI TRANSMISSION SYSTEM

3.1 Introduction

The deterministic approach is widely used by many utility companies for planning and operation purposes. The main purpose of this method is based on maintaining adequate and secure services under most probable outages without considering the probability of different uncertainties. The deterministic approach is used for the purpose of identifying operational and design limits. Under the deterministic method, an operating condition is identified as secure if it can withstand the effects of a pre-specified contingency, i.e., not to violate loading, voltage, or stability.

This chapter presents a detailed description of the deterministic reliability assessment procedure and reports the results of a preliminary deterministic security assessment on the Dubai Electricity and Water Authority (DEWA) transmission network. This will allow later a comparison to be made with the results of the probabilistic assessment of the same network, as described in Chapter 5.

3.2 Deterministic reliability assessment

The main purpose of a transmission system security assessment is to study the reinforcement and operational requirements of the existing system (which includes substations, circuits, generations, etc.) excluding the distribution system, for a specific horizon time duration. The deterministic approach is widely used by utilities worldwide to ensure adequate and secure operation under most probable outages (i.e. without considering the likelihood of occurrence of different uncertainties). Many standards were established to properly shape the deterministic study. Different AC and DC

load flow calculation techniques were also developed to calculate the required power system parameters. Consequently, many software packages were also developed to ease and expedite such load flow calculations.

This section describes in detail the deterministic procedure and reviews relevant standards, along with techniques and software.

3.2.1 General procedure for the deterministic approach study [11]

The first step in conducting a deterministic security assessment is selecting appropriate network configurations (i.e. network topology and unit commitment), power system operating conditions, outage events, and performance evaluation criteria. Sometimes, there is a large number of possible network configurations and contingencies and a wide range of operating conditions; thus, an exhaustive study of all combinations of configurations, contingencies and operating conditions is generally not considered reasonable. Therefore, the deterministic approach should provide useful results while limiting the amount of computation required.

This technique depends on applying two criteria for selecting study cases: (i) credibility, in which the network configuration, system operating conditions, and outage event are reasonably likely to arise; and (ii) severity, that is, the extent to which the study parameters are violated. The network configuration, system operating condition, and outage events must be the most severe state, i.e., there should be no other credible combination that results in a more severe state. Sometimes, sensitivity studies are also performed in order to select (i) credible network configurations, (ii) credible operating conditions, and (iii) credible outage event.

Application of the deterministic technique consists of the following simple steps (Figure 3.1):

1. The development of a base case that reflects (i) the study time period (year, month, week, and day) and (ii) the loading conditions (peak, intermediate peak, and off peak). Accordingly, the generators and component are arranged.

2. Selection of the study parameters and identification of their accepted ranges of operating conditions.

3. Selection of the credible contingency events whereby reliability performance could be affected by the violation of the studied parameters.

4. Identification of the event/s and system operating condition/s that result in reliability performance violations and recommend remedial actions. If there are no violations, the system is considered to be secure and reliable.

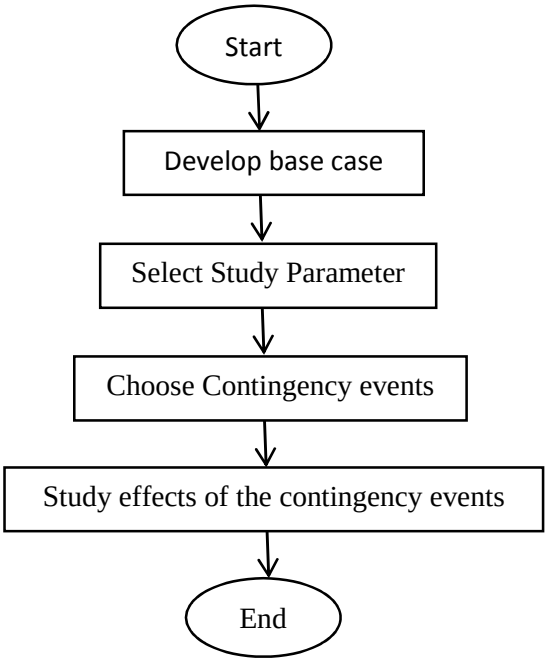

Figure 3.1: General deterministic approach of security assessment

Based on the deterministic approach, the successful operation and design of an electrical power system should fulfil the following general conditions [121]:

1) Generation must supply the demand plus the losses.
2) Bus voltage magnitudes must remain close to the rated values.
3) Generators must operate within specified real and reactive power limits.
4) Transmission lines and transformers should not be overloaded beyond their rated values for short or long periods.

The present and commonly applied deterministic approach, developed in the 1950s [3], however, does not sufficiently reflect the levels of risk that network users actually face. This is due to the following reasons: (i) it does not explicitly provide an assessment of the probability of failure (i.e. the likelihood of the outages is treated equally) as it considers only the consequences of pre-specified contingencies, (ii) it is difficult to account for continual changes in system performance and the adoption of suitable cases depends heavily on the engineer experience and perception (iii) the binary approach to risk (i.e. state is considered to be at no risk if the occurrence of outage does not violate pre-specified limits, while the system is considered to be at an unacceptable level of risk if the occurrence of outages cause violations of the limits) is fundamentally problematic as the system is sometimes highly exposed to the risk of system failure even if no outage leads to violations of limits, (iv) the current deterministic approach may significantly over estimate reliability risks (leading to an over secure network operation/design), and thus system operation and design with uneconomical costs, and (vi) this method does not deal suitably with renewable generation (e.g. wind, solar, etc.) which have many intermittent uncertainties [7, 11, 77].

Most transmission planning and operation practices, however, are still in accordance with the traditional deterministic approach for transmission network reinforcement and operation. Networks that are designed and operated based on these deterministic standards have delivered

secure and reliable supplies. However, the degree of this security and reliability can vary widely depending on the contingency states.

3.2.2 Security standards adopted for transmission systems design / operation

One of the main objectives of a security standard is to be used as a guideline by system operators and planners. The transmission security standard considers variations in the power flow across the transmission network caused by variations in demand and generation in particular areas or zones, due to e.g. weather, generation unavailability, etc. Examples of system conditions that may cause a departure from the normal state are capacity deficiencies, energy deficiencies, loss of generation or transmission facilities, transmission facility overloads and voltage violation, and abnormal power system frequency. The transmission network must be capable of transmitting the planned power, i.e., there must be a balance between the system demand and the generation for the zone or area being considered, plus any difference due to any unplanned conditions that may arise. The latter is sometimes referred to as the “interconnection requirement’ [3], which was found to be used in GB system planning.

The transmission power system must be operated and designed with sufficient transmission capability prior to any fault such that there shall not be any of the following: (i) equipment loadings exceeding the pre-fault rating, (ii) voltages outside the pre-fault voltage limits, or (iii) system instability [121]. The transmission power system should also be planned and operated with sufficient transmission capability to withstand the loss of any pre-specified contingencies of any of the following: (i) single transmission circuit, (ii) single generation circuit, (iii) double circuit overhead line, (iv) section of busbar, and (v) loss of power infeed. In general, regarding the application of these criteria, the contingencies should not result in any parameter violations, the

loss of a major portion of the system, or the unintentional separation of a major portion of the system.

Various standards and criteria could be applied in an analysis related to demand estimates, generating plant requirements, transmission and substation requirements, and other system developments. Based on these standards, planners and operators can set out alternative designs and make decisions. For example, the GB follows the Security and Quality of Supply Standard (SQSS) [77, 121], while the Dubai utility follow the North American Electric Reliability Corporation (NERC) standard [5].

It is essential to consider possible outages of transmission components that would reduce the capability of the network to transmit the required planned power. In the deterministic approach for the transmission system of a lower voltage level (e.g. 132 kV and below), the 'N-1' rule, where events are limited only to those involving the loss of one main component (mainly a line, a transformer, or a generator), is often used [3, 5, 121]. Sometimes, the 'N-2' rule is used at the higher voltage level (e.g. 400 kV and above); this rule considers the simultaneous failure of two lines. These 'N-1' and 'N-2' contingencies should not cause a supply interruption to consumers or any criteria violation [3, 5, 121]. DEWA currently uses an 'N-2' deterministic security criteria assessment for the 400 kV network and an 'N-1' criteria for the 132 kV network, for planning and operational purposes. While in GB, 'N-2' criteria is adopted at 400 kV, while 'N-1' is used for the 275 kV system.

3.2.3 Load flow calculation techniques [122]

The load flow is the essential calculation tool for studying the power system performance for the design and operation of a power system.

In the load flow, there are four potential independent variables associated with each bus: voltage magnitude (V), voltage angle (δ), active power (P), and reactive power (Q); and three types of buses are defined: load buses (or PQ buses), generation buses (or PV buses), and a slack bus (or swing or reference bus). The solution to the power flow study determines the magnitude and phase-angle of the voltage at each bus, and the active and reactive power flowing in each component, for a given set of operating conditions, and network topology. Two of the variables associated with each bus must be specified (i.e. given known values), while other two variables are free to vary (unknown values) during the solution process.

A power system is physically complicated, and power flow problems cannot be solved linearly, but instead must be solved by numerical iterations. There are four methods that commonly used to carry out the iterative process: the Gauss-Seidel method, the Newton-Raphson method, the Fast Decoupled method, and the DC method. The Gauss-Seidel method is an early formulation of the load flow problem and is usually slower than other methods. The Newton-Raphson method is a more powerful technique that incorporates first-derivative information based on Taylor's series expansion and the Jacobian matrix when computing voltage updates. Normally, with this method only three to five iterations are required to solve the load flow problem, regardless of the system size. The Fast Decoupled method is an efficient approximation based on the Newton Raphson method. In the DC load flow, a linear approximation (i.e. phase angles, voltages and reactive power are not considered) is implemented for situations where many estimates of load flow are needed in a short time. The DC power flow is approximately 10-100 times faster than the conventional load flow, but may have associated errors [123], and it is frequently used for solution to carry out multiple contingency studies.

In this thesis, the DC load flow calculation is selected due its speed and because the emphasis here is on the calculation of line power loading and on the performance of the system.

3.2.4 Commercial software packages

NEPLAN is a program used for flow calculation on electrical, gas, and water networks. The electrical model of the software provides a power system analysis tool for planning, optimisation, and simulation for transmission, distribution, and industrial networks. It was developed by BCP Busarello + Cott + Partner Inc. in cooperation with ABB Utilities and the Swiss Federal Institute of Technology. It is used by more than 750 companies worldwide, including the European Organisation for Nuclear Research (CERN) and other major European electricity utilities. [123, 124].

The NEPLAN has been adopted in the thesis work. It has NEPLAN Programming Library (NPL) that contains a set of C++ functions which allows to (i) access project files, (ii) execute any analysis function (e.g. load flow analysis) (iii) modify any variable of all element types (e.g. length of a line and component outages), (iv) add and remove elements from the network, and (v) access the results; through a user written C++ program. With this set of library functions, it is possible to manipulate NEPLAN projects through a normal C++ program with the Microsoft compiler Visual .NET 2005. [123]. In addition, the GB transmission model was already available at Cardiff University in NEPLAN format, while a model of DEWA transmission system was able to be migrated from 'PSS/E' format to NEPLAN format relatively easily.

3.3 Description of Dubai transmission system [5]

DEWA transmission network was selected as a case study for a security assessment investigation using the deterministic approach. This transmission system was built, owned, and operated by the

Dubai government. It transmits the necessary power for Dubai city in the United Arab Emirates (UAE), which in 2011, served a population of more than 1.9 million. The power demand in Dubai has been developing at a rapid rate since the setup of the utility in 1959. To cope with this huge demand growth, the power system infrastructure has also augmented greatly. Initially, the system voltages were at 6.6 kV; then, in 1969, a higher voltage of 33 kV was introduced, which remained as the primary transmission voltage until 1977 when a 132 kV system was introduced. Then, in 1993, a transmission network comprising 400 kV lines and substations was established.

A simplified 400 kV schematic diagram, together with the corresponding detailed model in NEPLAN of the DEWA transmission system for 2011 are shown in Figure 3.2(a) and Figure 3.3(a), respectively. It should be noted that the network is undergoing a programme of rapid expansion and reinforcement over the period of research work and that the current network shown in this thesis represents one configuration approximating to a December 2011 timeline. It has been assumed that the 400 kV network for the year 2011 is sufficient to deliver forecasted system demand for up to the year 2015. For purpose of this research, it was also necessary to create conditions that resulted in line overloadings. Hence, a modified model was also adopted to 2021 so that system demand was increased up to a forecast load, thus producing a ‘stressed’ system. For the year 2021 to cope with forecasted system demand, it was required to include new generation, called as (Q), together with two proposed 400 kV substations (i.e. R and S) and line modifications, shown in Figure 3.2(b) and Figure 3.3(b).

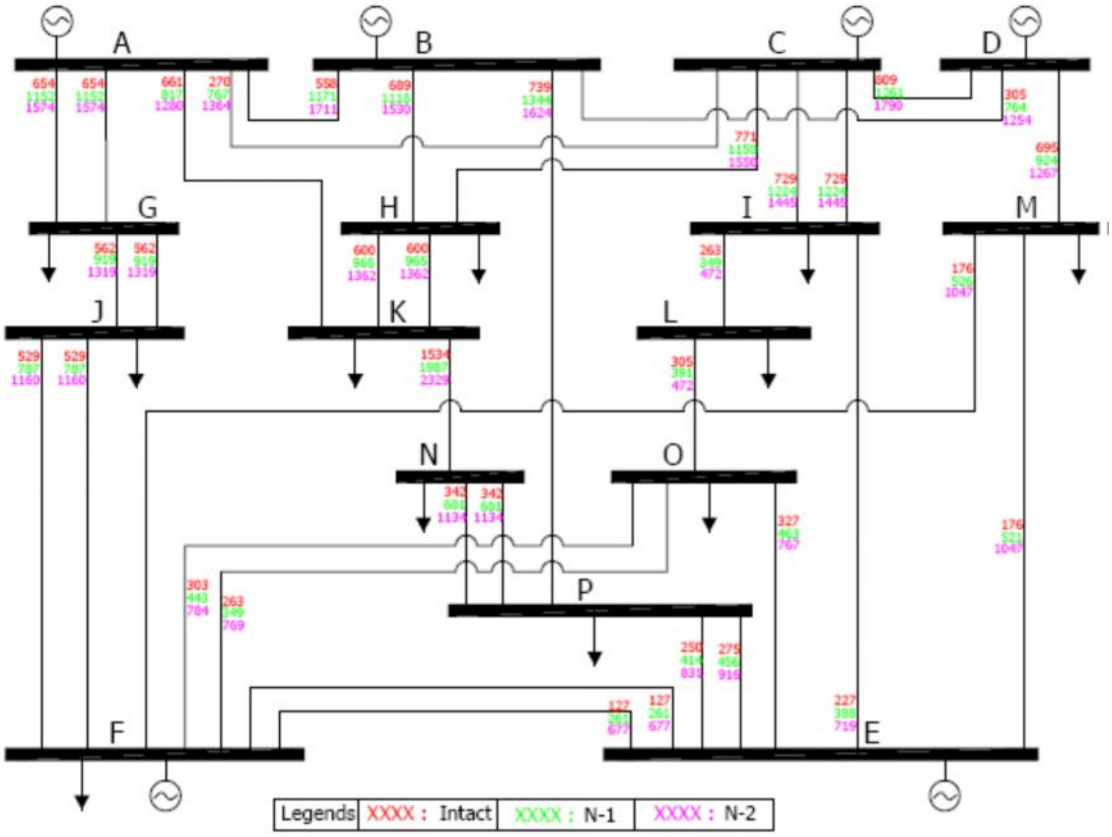

(a) For year 2011

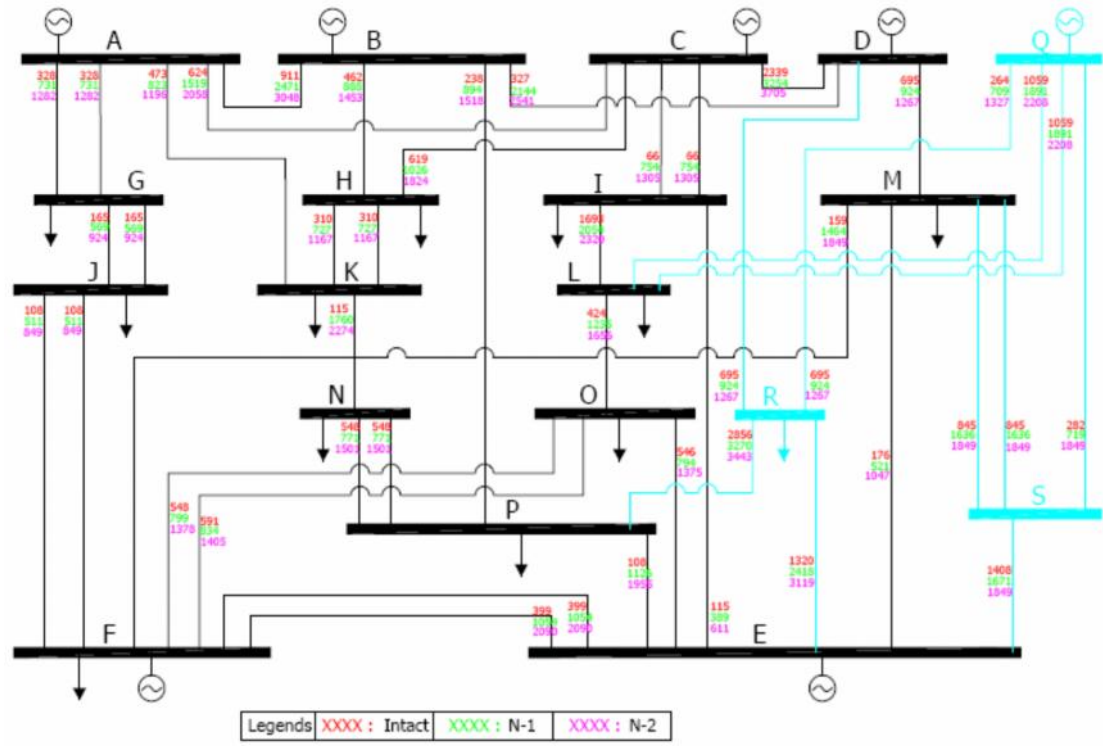

(b) For year 2021

Figure 3.2: Dubai 400 kV transmission system

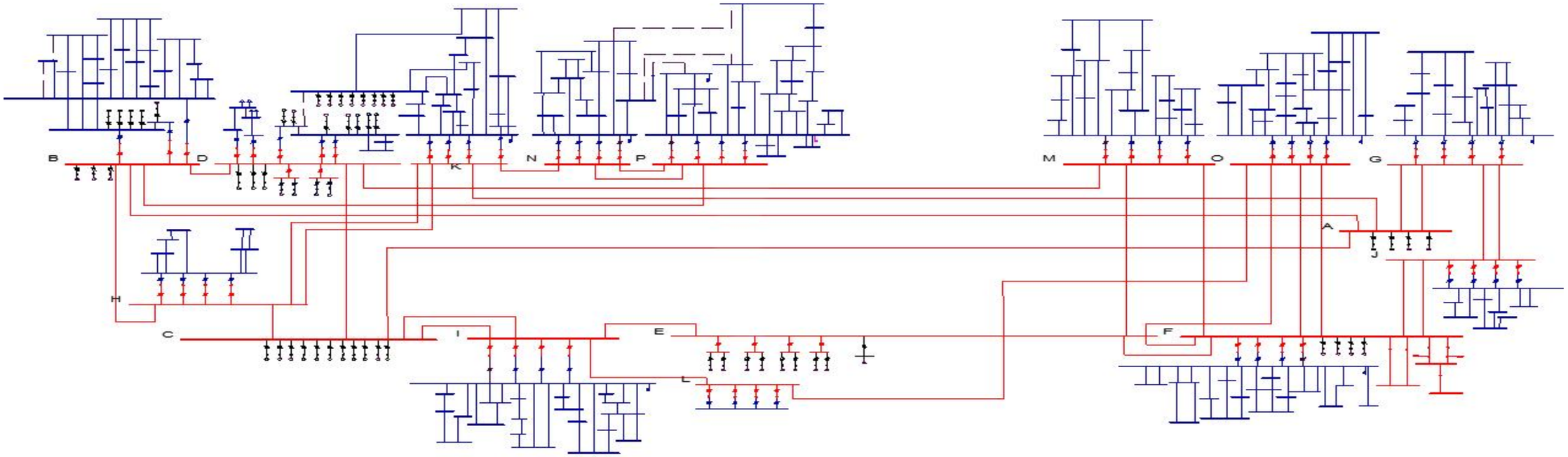

(a) 2011

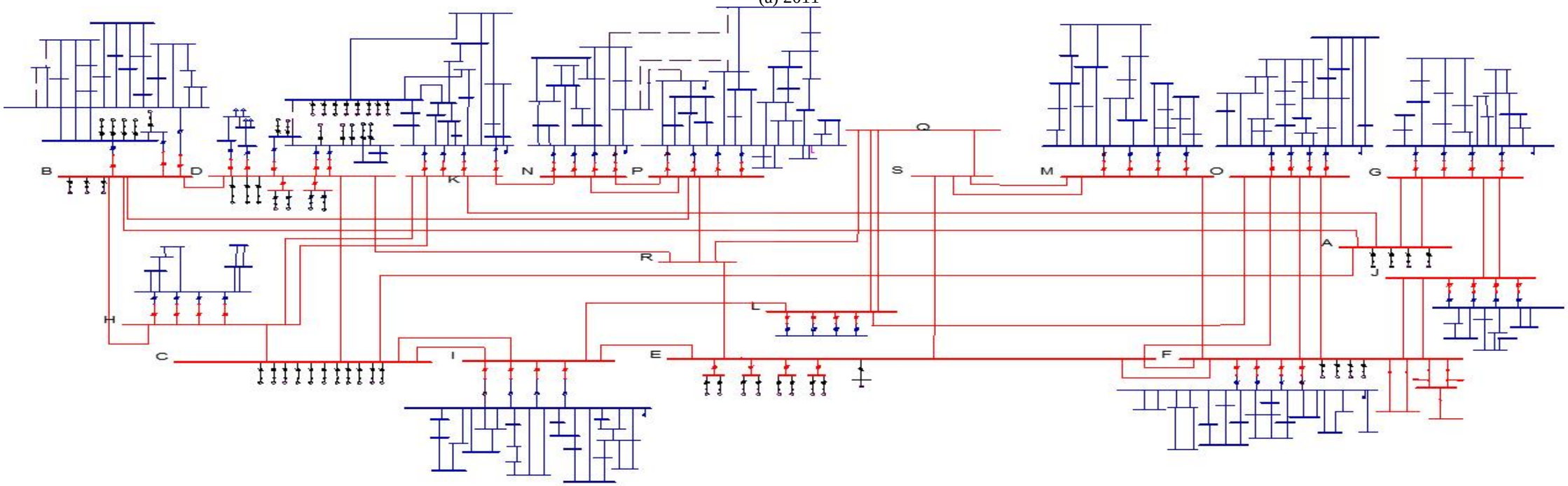

(b) 2021

400 kV circuits *132 kV circuits* *400kV/132kV Transf.* *Generating unit*

Figure 3.3: Detailed Dubai transmission system as modelled

The generators are located in two main areas: (i) along the coast at the Jebel Ali Power Plant (A, B, C and D) and (ii) inland at Awir (E and F). Generators are located not only at 400 kV stations, but also at 132 kV and 33 kV stations. The generating sources include both gas and steam turbines. DEWA uses both combined cycle and open cycle generation arrangements. The fuel source is primarily natural gas with heavy oil as a back-up fuel. All existing generating units have a dual fuel firing capability (i.e. power plants are designed to operate on natural gas as the primary fuel and diesel oil as the secondary or standby fuel). However, DEWA recently considered the option of future coal-based power plant and renewable solar park. DUSUP, the authority responsible for the supply of fuel gas in Dubai, arranges gas supplies from various sources. The maximum generation capacity as of December 2011 was 9,172MW (summer) and 10,717MW (winter).

The power generated at DEWA generating stations is transmitted through a 132 kV and 400 kV network. Since the end of 2011, it consisted of sixteen 400 kV substations and thirty-four double-circuit 400 kV lines, with a total transformation capacity of about 22,000 MVA. Table 3.1 summarizes the statistics of the DEWA transmission system as of December 2011. The existing 400/132 kV transformers and their capacities are listed in Table 3.2. The 400 kV circuits are constructed of overhead power lines employing either 'Zebra' ACSR 4x484.5 or 'Yew' AAAC 4x479.9 conductors in a 'quad' formation, with a total length of about 870 km. The 400 kV lines from the Jebel Ali power plant are the major carriers of bulk power to the load centres in Dubai city. In the case of the 2011 study, thirteen 400 kV circuits from the Jebel Ali power plant are in parallel operation. Table 3.3 tabulates detailed conductor constructions along with their calculated seasonal ratings for 400 kV circuits. It should be noted that some of

the 400 kV circuits are gas-insulated lines (GIL), above the ground, with a relatively short distance, which have a higher capacity.

Table 3.1: Summary of the Dubai transmission system as of December 2011

Number of 400 kV substations	16
Number of 132/33 kV substations	17
Number of 132/11 kV substations	134
Number of 400 kV circuits	34
Number of 132 kV circuits	268
Installed generation capacity	9,172MW (Summer) 10,717MW (winter)

Table 3.2: Transformation capacity of the DEWA 400 kV power network

400/132 kV substation	**Installed Capacity (MVA)**
D	3x450 and 2x300
K	4x300
M	4x450
O	4x450
N	4x450
B	3x305
P	4x450
I	4x450
F	4x450
G	4x505
J	4x505
H	4x505
L	4x505

In addition, the system under study had seventeen 132/33 kV substations with a total transformation capacity of about 3,795 MVA. There were a hundred and thirty-four 132/11 kV substations with a transformation capacity of 20,580 MVA. At 132 kV, there is about 459 km of 132 kV overhead lines and about 1,137 km of underground cables.

Table 3.3: Detailed thermal rating for 400 kV circuits in DEWA

#	Circuit	Types	Thermal Rating (MVA)	
			Summer	Winter
1	O-L	Yew AAAC 4x479.9	2280	2690
2	E-I	Yew AAAC 4x479.9	2280	2690
3	E-M	Yew AAAC 4x479.9	2280	2690
4	F-O-1	Yew AAAC 4x479.9	2280	2690
5	F-O-2	Yew AAAC 4x479.9	2280	2690
6	F-J-1	Yew AAAC 4x479.9	2280	2690
7	F-J-2	Yew AAAC 4x479.9	2280	2690
8	F-M	Yew AAAC 4x479.9	2280	2690
9	F-E-1	GIB/GIL	2385	2830
10	F-E-2	GIB/GIL	2385	2830
11	O-E	Yew AAAC 4x479.9	2280	2690
12	E-P	Yew AAAC 4x479.9 and Zebra ACSR 4x484.5	2280	2690
13	G-A-1	Yew AAAC 4x479.9	2280	2690
13	G-A-2	Yew AAAC 4x479.9	2280	2690
15	G-J-1	Yew AAAC 4x479.9	2280	2690
16	G-J-1	Yew AAAC 4x479.9	2280	2690
17	N-K	Yew AAAC 4x479.9 and Zebra ACSR 4x484.5	2280	2690
18	N-D	Yew AAAC 4x479.9	2280	2690
19	L-I	Yew AAAC 4x479.9	2280	2690
20	N-P-1	GIB/GIL	2545	2770
21	N-P-2	GIB/GIL	2545	2770
22	H-K-1	Yew AAAC 4x479.9	2280	2690
23	H-K-2	Yew AAAC 4x479.9	2280	2690
24	A-K	Yew AAAC 4x479.9	2280	2690
25	C-I-1	Yew AAAC 4x479.9	2280	2690
26	C-I-2	Yew AAAC 4x479.9	2280	2690
27	C-A	Yew AAAC 4x479.9	2280	2690
28	C-H	Yew AAAC 4x479.9	2280	2690
29	C-D	Yew AAAC 4x479.9	2280	2690
30	D-M	Yew AAAC 4x479.9	2280	2690
31	B-H	Yew AAAC 4x479.9	2280	2690
32	B-P	Yew AAAC 4x479.9	2280	2690
33	B-A	Yew AAAC 4x479.9	2280	2690
34	B-D	Yew AAAC 4x479.9 and Zebra ACSR 4x484.5	2280	2690

It should also be noted that DEWA 400 kV network is interconnected to other power networks, such as the Abu Dhabi network, the federal network, and the Dubai Aluminium Company DUBAL. The four 400 kV interconnectors with Abu Dhabi and federal networks are connected to a 400/132 kV F-substation (two circuits are connected to Abu Dhabi and the other two are

connected to the federal network). Similarly, interconnectors to DUBAL are through two 400kV lines connected to 400/132 kV D-substation. However, in the present study, the presence of these interconnectors has been ignored for the sake of simplicity and due to the fact that normally the transfer between areas is zero.

DEWA uses an 'N-2' deterministic security criteria assessment for the 400 kV network and an 'N-1' criteria for the 132 kV network for planning and operational purposes. The reliability, voltage, and stability quality standards/guidelines used in DEWA system, which are based on NERC standard [5], are shown in Table 3.4, Table 3.5, and Table 3.6, respectively.

Table 3.4: Reliability standard in DEWA

	400 kV	**132 kV**
Lines	N-2	N-1
Transformers	N-1	N-1

Table 3.5: Voltage quality standard in DEWA

	Normally				**Contingency**			
	Min >		**Max <**		**Min >**		**Max <**	
	kV	**%**	**kV**	**%**	**kV**	**%**	**kV**	**%**
400 kV	380	-5	420	+5	360	-10	420	+5
132 kV	125	-5	138	+5	120	-10	145	+10

Table 3.6: System frequency quality standard in DEWA

Nominal Frequency	**Normally**				**Contingency**			
	Min >		**Max <**		**Min >**		**Max <**	
	Hz	**%**	**Hz**	**%**	**Hz**	**%**	**Hz**	**%**
50	49.9	-0.2	50.1	0.2	49.6	-0.8	50.3	0.6

3.4 Application of the deterministic approach to the Dubai transmission system

The deterministic approach was conducted considering carefully selected operating parameters. The aim was to evaluate the existing system capabilities and identify any

deficiencies. This was done by (i) developing a base case, (ii) conducting a power flow and contingency analysis, and (iii) analysing the result as described previously in Section 3.2.1.

3.4.1 Development of base case

A base case, which is consistent with (i) a time period (year, month, week, and day), and (ii) the system demand conditions (i.e. peak and off peak) was developed for the study. In this chapter, two cases for two study cases of the year 2011 and the 'stressed' year 2021 – one for winter (off-peak time) and one for summer (peak time) – were studied. In each base case, the generation arrangements and component conditions were set based on the historical data and expected conditions. For the network under 2011 study, a peak system demand of 6,081 MW and an off-peak system demand of 1,997 MW were selected. For 2021, the 'stressed' network study, a peak system demand of 11,000 MW and an off-peak system demand of 3,600 MW were used. This is implemented because it was found that no overloading will occur in 400 kV system due to upto N-2 contingencies and upto year 2021. Hence, the system of 2021 was further stressed, by increasing the system demand level close to full generation capacity.

Generator unit commitments were managed in this study according to the ranking order, which is based on operational and cost efficiency for both study cases. Table A.1 in Appendix A gives salient information on the power plants under study, along with their ranking order, based on operational and cost constraints, which was adopted for the '2011' study.

The system demand reported at the peak in 2011 was around 6,080 MW at around 3 pm, while the off-peak demand was reported to be around 2,000 MW in the early morning, around 33% of the peak demand. Normally, the peak time occurs in the summer, while the off-peak time occurs in the winter. The model provided by DEWA was for the case with a system demand of 3,273 MW. The active and reactive powers of each load substation were arranged and modelled

as a proper proportion of 6,080 MW for the peak time and then scaled down to 2,000 MW for off-peak time. For the provided network, there were 209 load points (i.e. consumer loads and station auxiliary loads). Table A.2 in Appendix A shows the calculated active and reactive powers for each load point located in the NEPLAN model at 11 kV and 33 kV for the year 2011.

In order to reduce the short-circuit levels in the 132 kV system, some of the 132 kV busbars in the power plants were split. Furthermore, some of the 132 kV lines are kept open at one end, due to operational constraints to avoid circulation through 132 kV loops.

The pre-fault continuous thermal ratings for winter and summer for the 400 kV overhead lines typically range from 2,280 MVA up to 2,770 MVA per circuit, as shown in Table 3.3.

3.4.2 Contingency Analysis

For the deterministic study case, a security checking study was conducted in order to assess the study parameters of branch flows and to assess the impact of outages. All single ‘N-1’ and double ‘N-2’ outages for circuits operating at 400 kV of the DEWA transmission system were considered in a contingency analysis for all cases of the studied years. Transmission line loadings were observed for post-contingency and compared with relevant line thermal loadings.

3.4.3 Results for 2011 case study

The detailed study conducted was only for the loading assessment for the 400 kV network during intact conditions, ‘N-1’ and ‘N-2’ contingencies. Common thermal ratings for all lines of 3,290 Amps and 3,880 Amps were considered for peak and off-peak periods, respectively [5].

Figure 3.4 shows the 400 kV lines loadings during intact conditions for the peak and off-peak study cases and the corresponding adopted thermal ratings. The maximum line loadings were found to be on the 400 kV line 'K-N', i.e., 1,534 Amps during the peak period and 479 Amps during the off-peak period. These maximum loadings are well below the thermal rating.

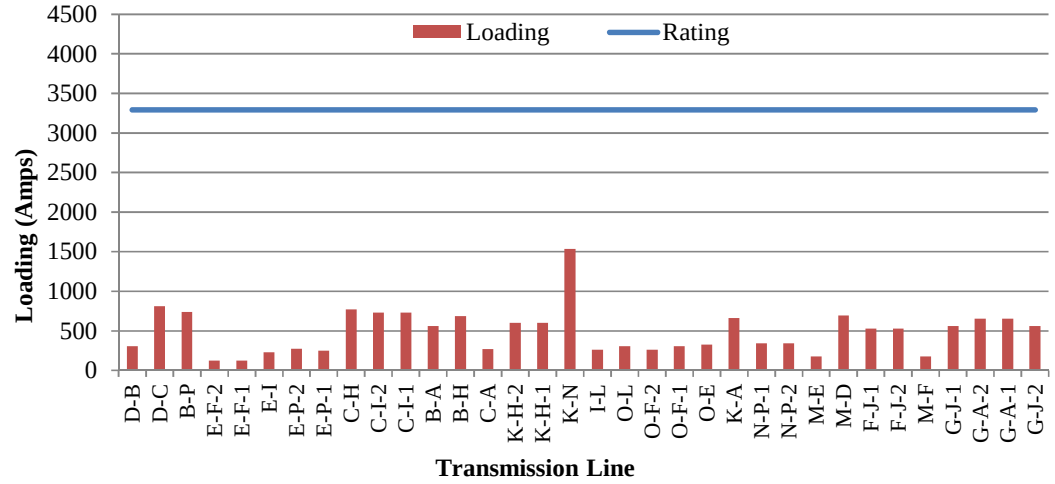

(a) Peak study case

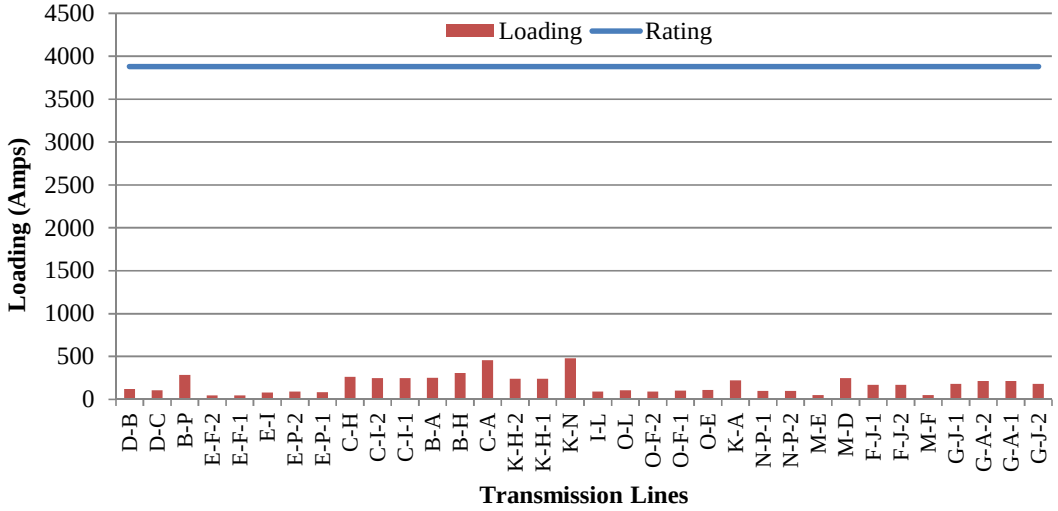

(b) Off-peak study case

Figure 3.4: 400 kV lines loadings during intact condition for the study case of year 2011

Figure 3.5 displays the 400 kV line loadings for ‘N-1’ contingencies during peak and off-peak study cases. The 400 kV line of ‘K-N’ has a maximum line loading of 1,987 Amps during the peak period for the outage of single line of ‘B-P’, while the 400 kV line of ‘C-A’ has a maximum line loading of 679 Amps during the off-peak period for the outage of a single line of ‘B-A’. These resultant maximum loadings due to single line outages are also well below the thermal rating.

Figure 3.6 shows a detailed 3-D representation of the 400 kV line loadings for ‘N-2’ contingencies during peak and off-peak study cases. The most heavily loaded 400 kV line is ‘K-N’ with 2,329 Amps due to simultaneous outages of the 400 kV lines ‘B-P’ and ‘M-D’ in the peak period, while the 400 kV line ‘C-A’ will be loaded with 781 Amps due to simultaneous outages of the 400 kV lines ‘B-A’ and ‘M-D’ in the off-peak period. The calculated maximum line loadings are well below the seasonal thermal ratings of 3,290 Amps in summer and 3,880 Amps in winter.

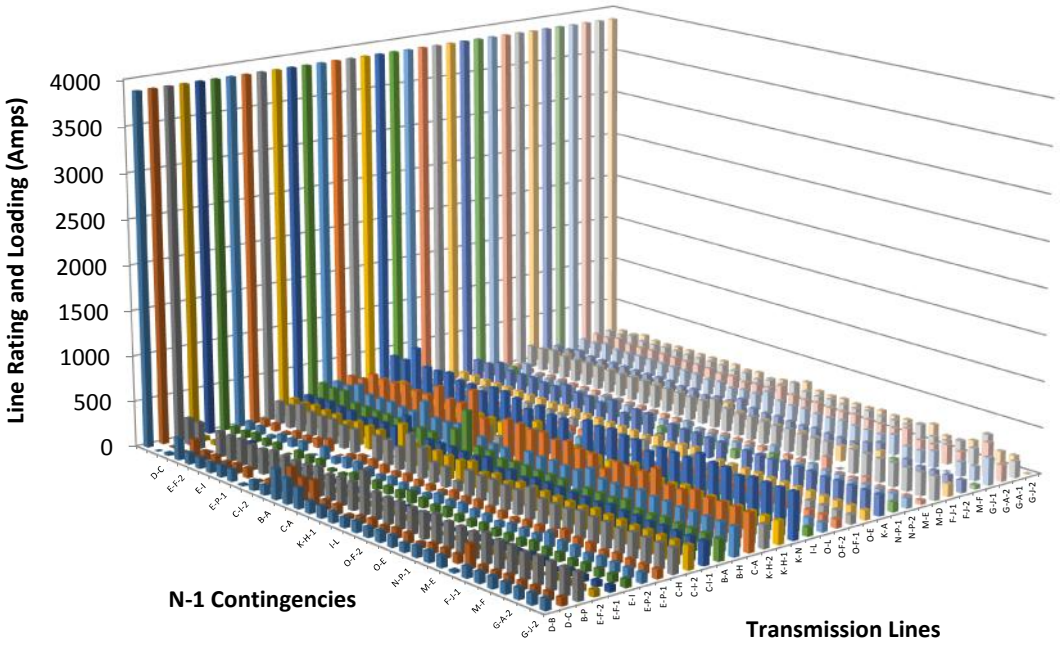

(a) Off Peak study case

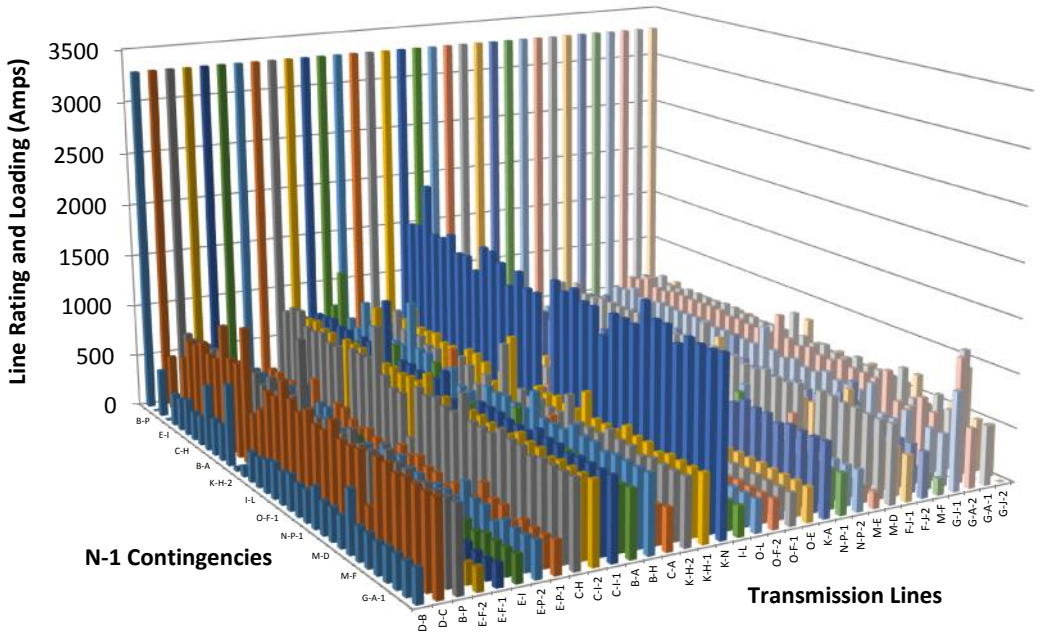

(b) Peak study case

Figure 3.5: 400 kV line loadings during 'N-1' contingencies for the study case of year 2011

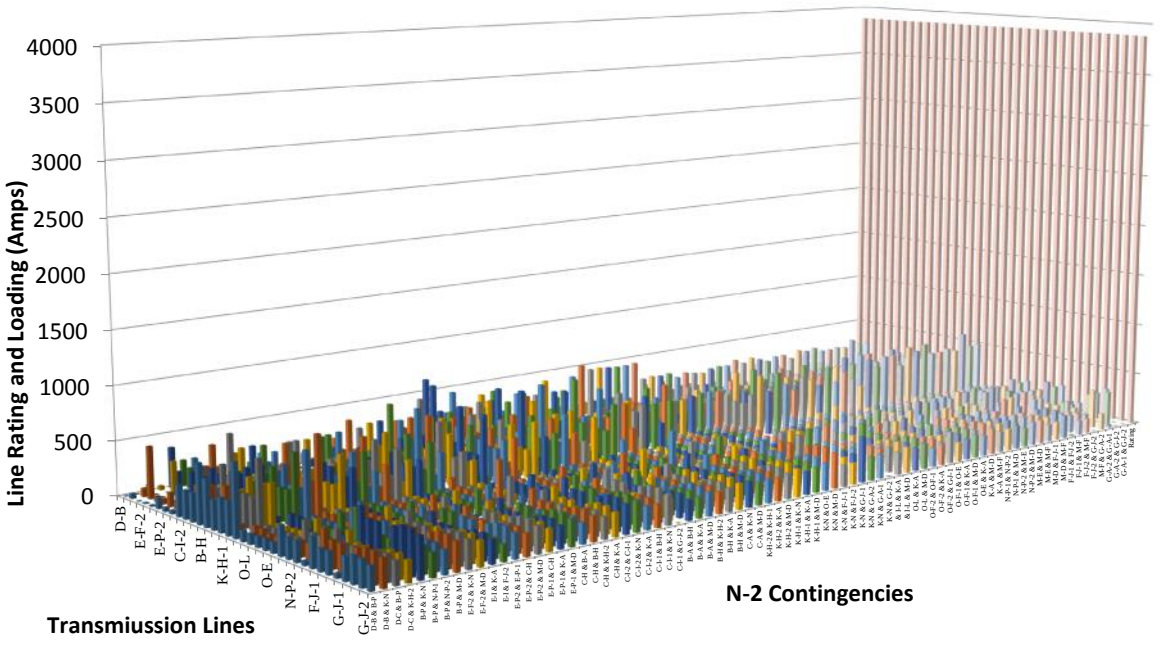

(a) Off Peak study case

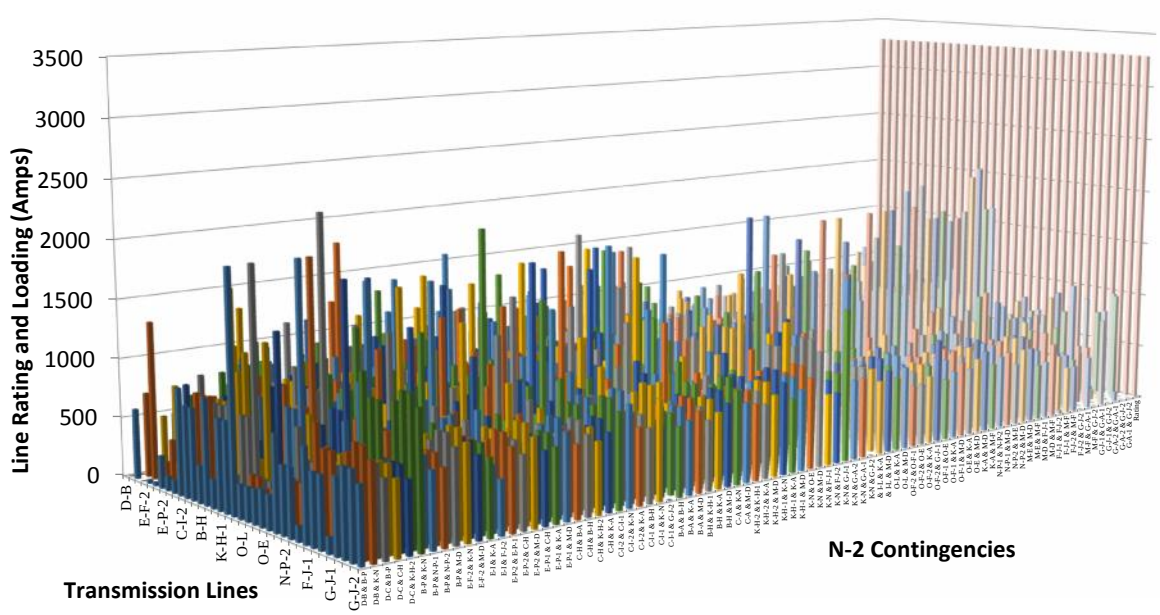

(b) Peak study case

Figure 3.6: 400 kV line loadings during 'N-2' contingencies for the study case of year 2011

Figure 3.7 shows a 2D representations of the worst case 400 kV line loadings (i.e. highest line loading) for an intact system, ‘N-1’, and ‘N-2’ contingencies during peak and off-peak study cases.

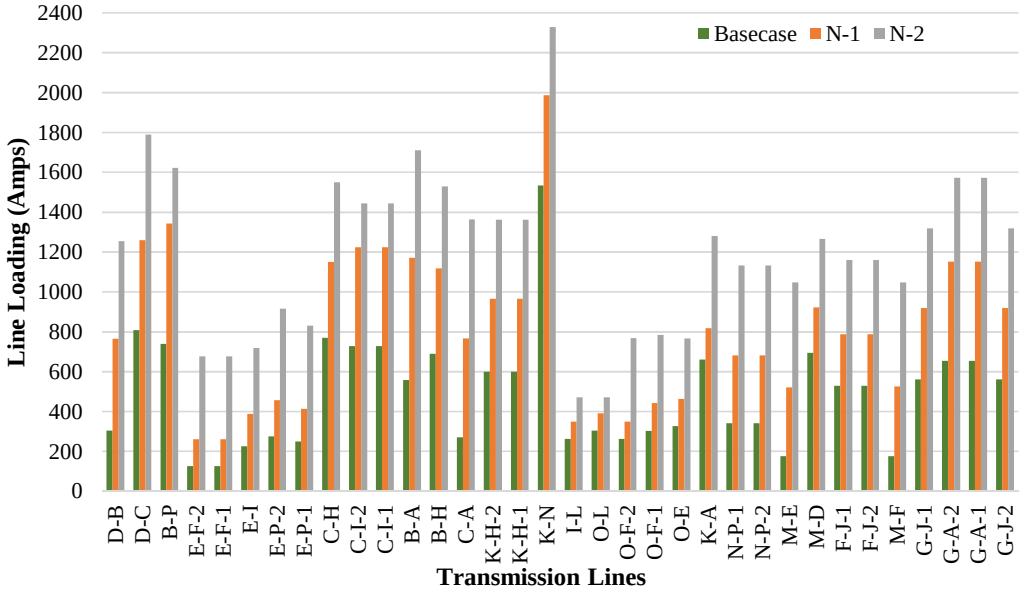

(a) Peak study case

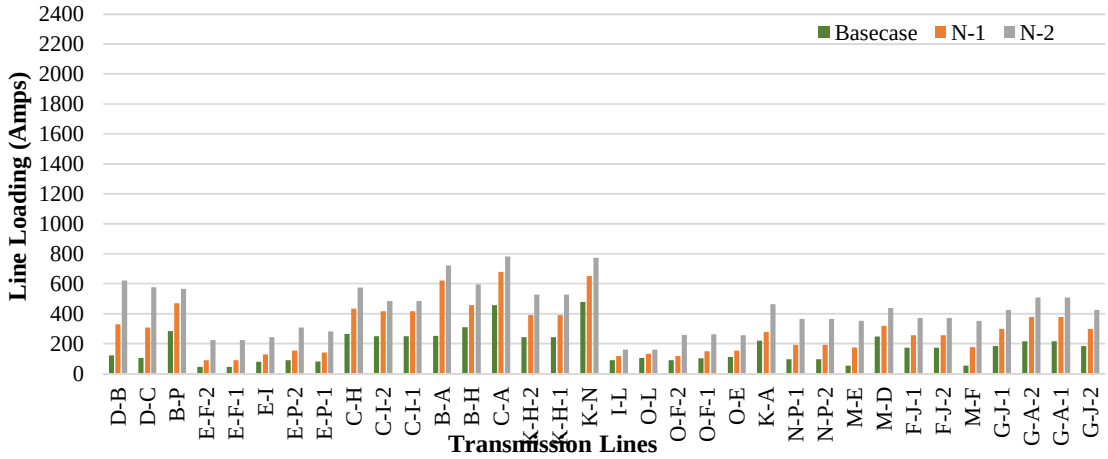

(b) Off-peak study case

Figure 3.7: Worst case 400 kV line loadings for the study case of year 2011

It can be observed that for the studied range of outages, the loading of all 400 kV lines falls well within their rating under intact conditions, ‘N-1’ and ‘N-2’ contingencies. It is clear that

the system would be maintained with respect to all ‘N-1’ and ‘N-2’ contingencies. This result could be attributed to a ‘high’ security policy adopted in a utility in order to avoid the risk of power interruptions and to facilitate rapid future development of load and generation. These results also illustrate that different system demand conditions and contingencies yield quite different patterns of flow. It should be noted that these results may also change with different unit commitments.

3.4.4 Results for ‘stressed’ system 2021 case study

The simplified topology of the ‘stressed’ 400 kV system was shown in Figure 3.2 for 2021. For the network under study, a peak system demand of 11,000 MW was considered.

Figure 3.8 illustrates a 2D representation of the highest line loadings for intact system, ‘N-1’, and ‘N-2’ contingencies during peak and off-peak study cases. It can be noticed clearly that line loadings are drastically higher than that of year 2011. Furthermore, two 400kV lines of ‘D-C’ and ‘P-R’ get overloaded due to ‘N-2’ contingency during peak hour. However, some lines are almost close to their thermal ratings due to either ‘N-1’ or ‘N-2’ contingencies e.g. lines ‘D-C’, ‘P-R’, ‘B-A’ and ‘E-R’. However, during off-peak period, the loading of all 400 kV lines falls well within their rating under intact conditions, ‘N-1’ and ‘N-2’ contingencies. It can be seen although there is some overloading occurs here, but could not notice their probability of occurrence.

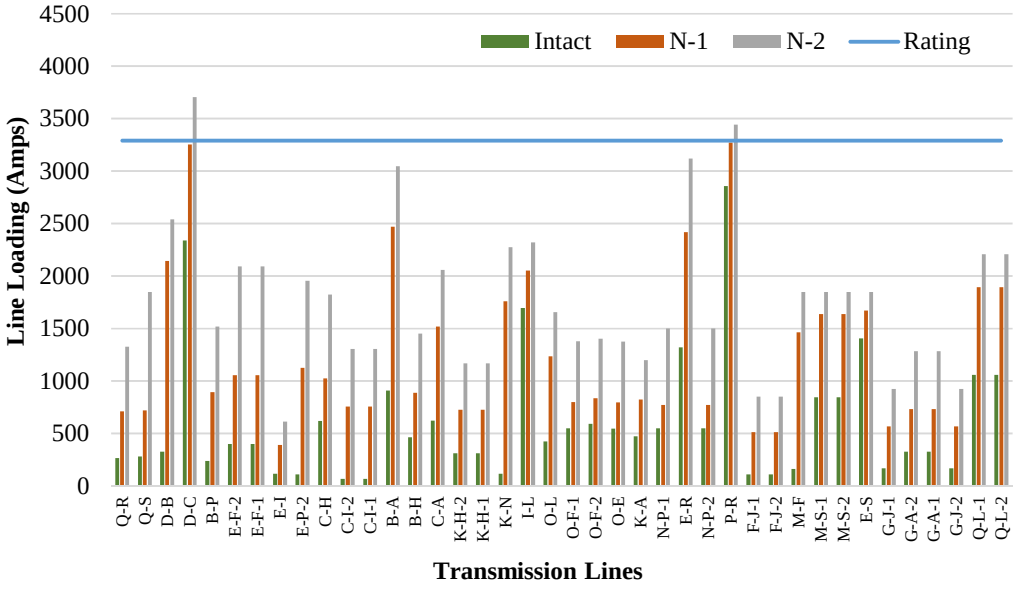

(b) Peak study case

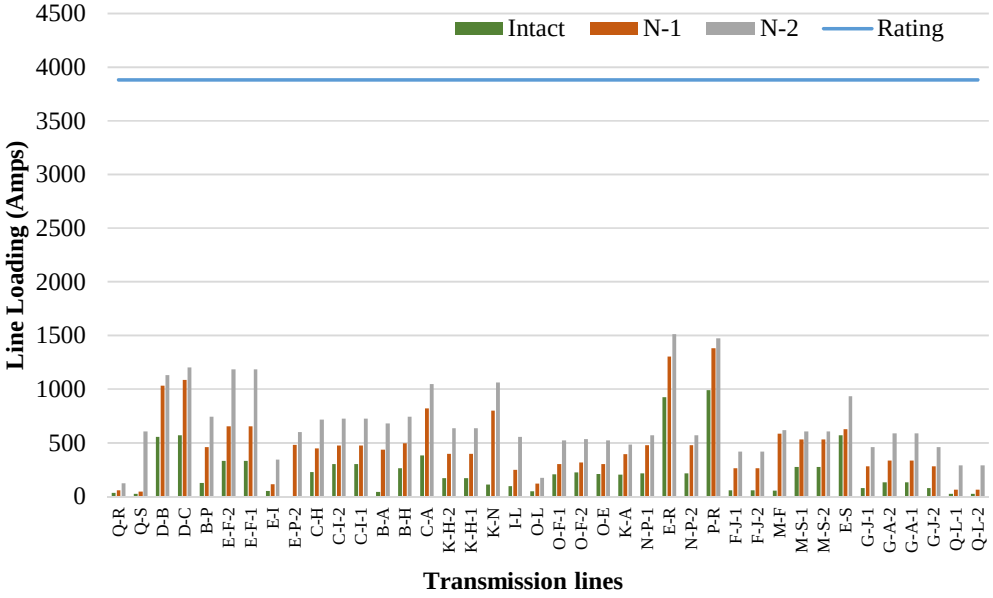

(b) Off-peak study case

Figure 3.8: Worst case 400 kV line loadings for the study case of 'stressed' year 2021

3.5 Conclusions

The details of established procedure for carrying out a deterministic assessment for a transmission system have been described along with examples of industry application of such procedure.

The Dubai transmission network has been set up and modelled in NEPLAN software, and contingency analysis based on the deterministic approach (i.e. under a range of intact conditions, 'N-1' and 'N-2' outages) carried out for 2011 and so-called 'stressed' system projected to 2021. It was found that no overloading will occur in 400 kV system due to upto N-2 contingencies and upto year 2021. Hence, the system of 2021 was further stressed, by increasing the system demand level close to full generation capacity. It was found that the 2011 system has a high degree of surplus transmission capacities even for all studied 'N-2' contingencies. This reflects the high levels of investment that have been made in the transmission infrastructure. For the specifically created 'stressed' system for year 2021, it was found that two transmission lines were overloaded for particular 'N-2' outages.

It is clearly shown that this deterministic approach does not consider the likelihood of different uncertainties, which may lead to the power system being designed and operated inefficiently. The following chapters will show how studies on the existing network were extended to include a picture of the full range of system demand over an annual load cycle and taking into account uncertainties in system demand, network conditions, and variable thermal ratings. In this way, a probability distribution of line loadings and thermal ratings could be obtained to form a platform for risk assessment.

CHAPTER 4. NEW APPROACH FOR PROBABILISTIC RELIABILITY ASSESSMENT

4.1 Introduction

As mentioned in Chapters 2 and 3, traditionally, most utilities base their investment decisions for design and operation by continuously and closely studying the security of the network using the deterministic approach, i.e., the application of 'N-1' (i.e. any single equipment outage) or 'N-2' (any two circuits outage) circuit depletion under prescribed severe system conditions. With this technique, usually, a small number of carefully selected pre-specified credible contingencies (e.g. sudden loss of generator, transmission line, transformer, or system load) are identified and analysed. As can be seen from Chapter 3, this approach is relatively simple and direct and the results are easily interpreted by system planners and operators. However, such a worst-case deterministic approach has a main drawback in that it does adequately reflect levels of operational and planning risk that network users face, as it considers only the severity of pre-specified contingencies and not the probabilistic feature of the system behaviour and component failures. Also the likelihood of the outages is assumed to be equal. Consequently, this may result in the possibility of over system planning and operation and excessive degree of reliability. Furthermore, the degree of security provided by the deterministic approach, using general rules applied to all cases, will not be optimal as the cost of providing the suggested level of redundancy is not compared with the cost delivered [77].

The deterministic approach can be supplemented through a probabilistic method that is able to account for the different uncertainties of the power system. The probabilistic security assessment may offer advantages by considering (i) a statistical description of the performance of the system over an annual cycle together with (ii) the application of historical fault statistics

that provide a measure of the probability of faults. The relative merits of the two methods are shown in Table 4.1 [3].

Table 4.1: Merits of deterministic and probabilistic approach

Deterministic Rules	**Probabilistic Analysis**
Simple rules make for easy application	Criteria appropriate to circumstances must be selected
Extra computer analysis, if required, easily and automatically applied. Little data needed.	Computer analysis of each case given in detail. Programs and extensive database required.
Cannot predict failure rates.	Can predict possible failure rates.
Cost/benefit assessments are not possible.	Cost/benefit figures can be calculated for all variants.
Cannot respond to continual changes in plant and system performance	Is able to incorporate effect of shorter-term changes in plant and system performance
Can lead to unnecessary installation of plant and therefore can be costly.	Permits system to be designed to closer limits and is therefore less costly.

In any transmission power system, there are numerous sources of uncertainties, such as changes in system demand, generation output, component failure, thermal ratings of transmission lines, etc. Thus, a different type of risk depends on these uncertainties. Normally, in any reliability assessment, uncertainties can be categorized as an uncertainty regarding the occurrence of a contingency (e.g. component failure) or uncertainty in the actual operating conditions (e.g. system demand and thermal rating). The uncertainties involved in the planning of a system have increased, and thus, new processes need to be developed to assess and predict the behaviour of the transmission system. Probabilistic distributions provide a practical way to describe the variation of different uncertainties and indices.

The severity of violations also needs to be quantified. Severity is the degree of the violation of the study parameter, either for an intact system or following an outage event. It can be evaluated based on voltage violations, component overloads, system frequency deviation, generation reserves, system stability margin, etc. In this chapter, the severity for the intact system and for ‘N-1’ and ‘N-2’ contingencies was computed with respect to the line overloading.

Probabilistic techniques should calculate the risk indices that can be used to evaluate the reliability of a system and provide some indication of the required remedial actions in order to maintain the required reliability. A risk index therefore should reflect the probability of the occurrence of uncertainties that may result in a violation in a study parameter. There are a number of different indices that could be selected. As outlined in Chapter 2, indices have been developed relating to (i) voltage performance, (ii) line overloading, (iii) load curtailment, and (iv) combined indices. These indices may be useful to rank contingencies and components, especially when considering different uncertainties. They can be used to compare the effects of various operation, design, and maintenance strategies on the system reliability.

In the probabilistic analysis performed in this thesis, an index that reflects the security level for a transmission system, namely, the Line Overloading Risk Index (LORI), was chosen. This index is expected to be useful for operational and design decision making.

This chapter provides details for the evaluation of the LORI through an extensive systematic evaluation of the steady state performance under hour-by-hour loading levels over a one-year period.

4.2 New algorithm to calculate the Line Overloading Risk Index (LORI)

Transmission reliability analysis evaluates the variations in load flow across a transmission system due to different uncertainties. A risk of line overloading may arise from the following uncertainties, which can be represented by probabilistic distributions: (i) hourly variations in system demand, and (ii) 'N-x' line outages, considering respective variation in line thermal rating. The flow chart in Figure 4.1 outlines the proposed new method to calculate the LORI and to develop the Probabilistic Distribution Function (PDF) of the resultant line loading and line thermal rating. Starting with the actual historical annual system demand curve (on an

hourly basis), a PDF of the system demand is obtained and a range of discrete system demand levels identified. For each system demand level, the corresponding generation unit commitment is determined according to a ranking order. DC load flows are carried out for each discrete system demand level from which the corresponding line loadings are obtained in order to determine the severity, for the intact system and 'N-x' contingencies. The power flow computations are performed using the NEPLAN load flow program, and the systematic multiple study execution and data handling is achieved using a developed C++ based programming code. For each hourly system demand, corresponding hourly line thermal ratings are calculated based on local meteorological data. Finally, the PDFs for the resultant line loadings are compared with the PDFs for the thermal ratings of each line and the LORI is determined. The following sections describe in detail each of the flow chart elements shown in Figure 4.1.

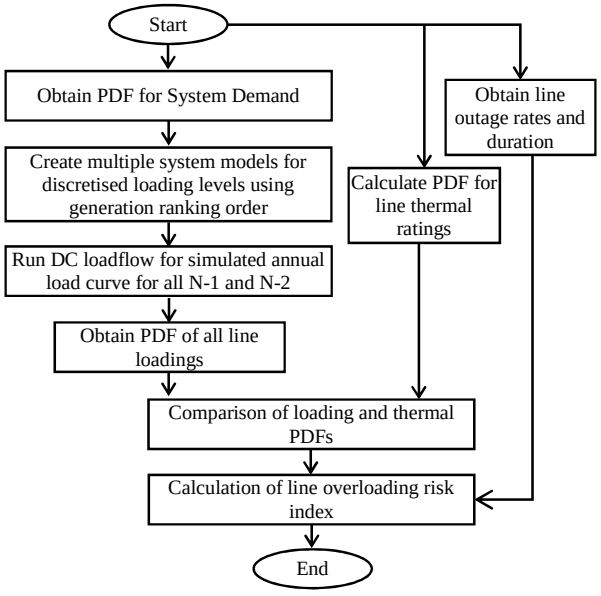

Figure 4.1: Procedure to calculate PDFs of line loading and line rating along with LORI

4.3 Probabilistic Distribution Function (PDF) of system demand and selection of system demand levels

Uncertainties of system demand can be considered in a probabilistic security assessment by distribution function, which can be divided into several discrete intervals. In order to reduce the potential number of simulation studies, a suitable number of discrete system demand levels (bins) may be identified. For the hourly annual range of system demand, the system demand range can be divided, as an example, into 100 units (bins) each with a bin size of 100 MW. The frequency of occurrence of each system demand level can be evaluated and then expressed as a relative frequency. For each range of recorded system demand, the probability of occurrence of this range was determined using Equation 4.1 [8].

$$P(of\ particular\ event\ occuring) = \lim_{n\to\infty}\left(\frac{f}{n}\right) \qquad \text{Equation 4.1,}$$ where

f denotes the number of times event is occurred, and

n represents total number of occurrences of event.

Figure 4.2 illustrates the hourly total system demand over an annual cycle for the Dubai power system. This chronological system demand can be represented by a 43-state distribution model, as shown in Figure 4.3. This chronological system demand can be represented by a 43-state distribution model, according to range of 100 MW and bin size that determined the number of states, as shown in Figure 4.3. It can be observed that the chronological system demand curve was changed into a multi-step system demand curve. The relative frequency of occurrence of each system demand level is shown on the right axis, while its probability is shown on the left axis.

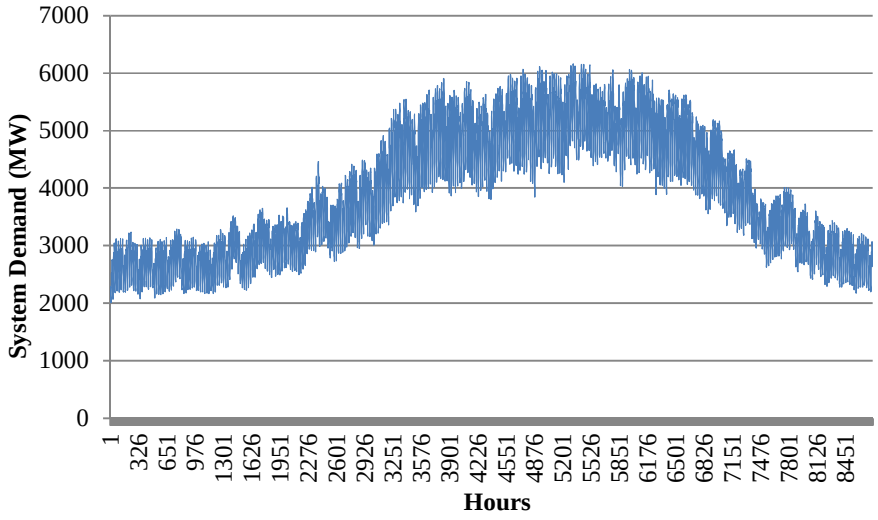

Figure 4.2: Hourly system demand variation along a year

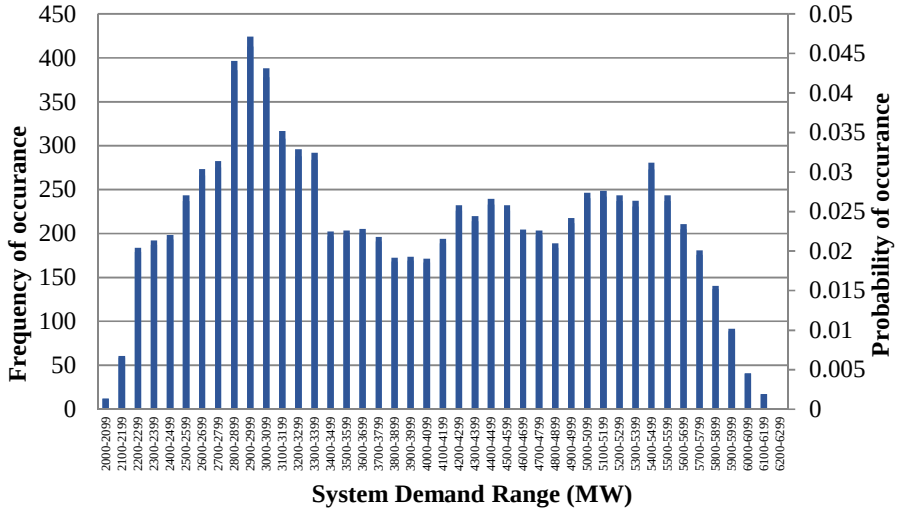

Figure 4.3: 43-state system demand probabilistic model

4.4 Multiple load flow simulations

In the evaluation of the LORI, as proposed in this research, the NEPLAN software programme package [123, 124] was used for the power system load flow computations. This software has a controlled multiple study facility, which was achieved using the C++ programming code. The

NEPLAN Programming Library (NPL) is a C++ based interface that includes functions to access NEPLAN data and calculation algorithms. This allows the automation of almost any function in NEPLAN. Although there are some important functions in NEPLAN, without use of the NPL, they are less useful. For example, using the 'Contingency Analysis' tool, the user can select elements (or nodes) to experience outage, and customisable results can be obtained; however, the analysis is limited to taking only one line out of service at a time and/or manually specifying the combinations for N-2 contingencies (outage of any two lines). The NPL was used here in order to automate network modelling and contingency simulation. Microsoft visual studio 2008 was used to write the C++ code and generate dll files which are able to be expanded by NEPLAN.

An NPL code was written according to the flow chart shown in Figure 4.4 to carry out the following functions: (i) to adjust the system load to each of the identified system demand levels, i.e., loads at each load bus are scaled proportionately; (ii) for each system demand level, to match the required generation unit commitment according to the ranking order (Figure 4.5); (iii) for each system demand level, to run the DC load flow and store line loadings; and (iv) to repeat such studies at each system demand level for all N-1 contingencies (N_1) and every combination of N-2 contingencies ($\frac{(N-1)N}{2}$) (See Figure 4.5 for snapshot of the developed code).

The flow chart shown in Figure 4.6 illustrates the process used in NPL programming code to set unit commitment based on utility's agreed ranking order so that the slack bus will be maintained to certain level (for GB it was assumed ± 1000 MW). In this process, for each system demand level, load flow runs and noting the power on slack bus. If the power on slack bus is higher than maximum limit (i.e. + 1000 MW), then a generator unit based on ranking

order will be switched on, otherwise will be switched off again based on ranking order. The process will be repeated until the power on the slack bus is within the agreed limit.

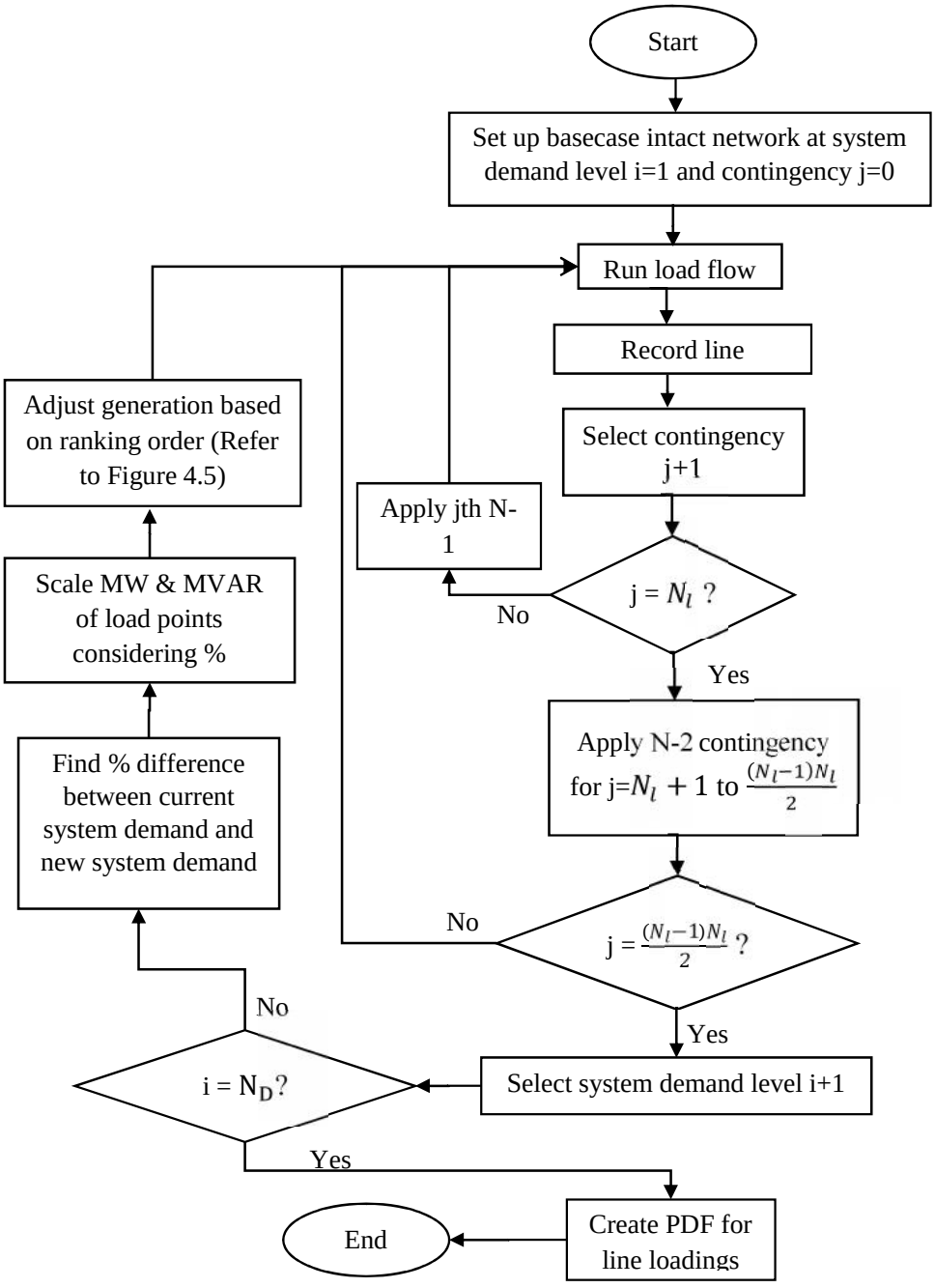

Figure 4.4: Developed NPL code to create line loading PDF

```
GetElements(_T("LINE"),numElementsL,pElementIDsL);
for(int count1=0;(count1<numElementsL);count1++)
{
	SwitchElement (pElementIDsL[count1],FALSE);
	for(int count2=0;(count2<numElementsL);count2++)
	{
		if (count1<count2)
		{
			SwitchElement(pElementIDsL[count2],FALSE);
			RunAnalysisLF();
			GetElements(_T("LINE"), numElements, pElementIDs);
			for (int i=0; i<numElements; i++)
			{
				unsigned long lineID = pElementIDs[i];
				GetResultDouble(lineID,_T("I-x1"),MW);
				swprintf_s(cMessageText, _T("%.3f"),MW);
				WriteMessageToLogFile(cMessageText);
			}
			FreeElements(pElementIDs);
			SwitchElement (pElementIDsL[count2],TRUE);
		}
	}
			SwitchElement (pElementIDsL[count1],TRUE);
}
```

Figure 4.5: A snap shot of C++ code for N-2

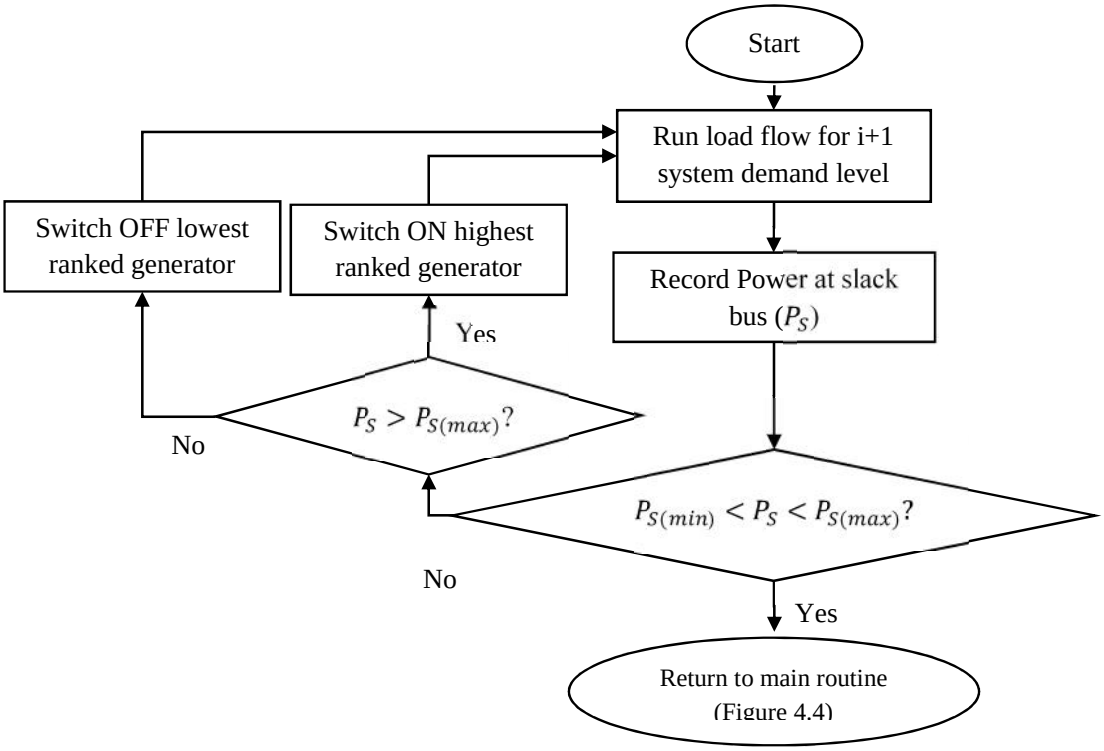

Figure 4.6: Adjust generation in the NPL code

4.5 Probabilistic Distribution Function (PDF) of line thermal rating

For overhead lines, the conductor comprises bare wire suspended between two supporting structures and exposed to the surrounding weather conditions. For secure system operation and design, the overhead line operating temperature or current flow must not be exceeded in order to avoid excessive sag or damage to the overhead lines. The maximum load current that can be carried by the conductor is called the conductor thermal rating (sometimes known as the Ampacity, current-carrying limit, or thermal capacity). Thermal ratings of overhead high voltage transmission lines are crucial parameters for assessing the capability of an electrical transmission network to ensure its reliable operation and design. A steady-state thermal rating has been calculated in this work in preference to dynamic ratings since this would provide the maximum allowable thermal rating for long-term system operation and planning (compared to short term e.g. within six hours of a fault).

Examples of aluminium-based conductors in use in transmission system are categorized as tabulated in Table 4.2 [125].

Table 4.2 : Different Aluminium based conductors

AAC	All-Aluminium Conductors
ACSR	Aluminium Conductors Steel Reinforced
AAAC	All-Aluminium Alloy Conductors
AACSR	All-Aluminium Alloy Conductors Steel Reinforced
ACAR	Aluminium Conductors Alloy Reinforced

Two main standards relating computational methods have been developed and utilized widely in the power industry to calculate the thermal rating, in Amperes (or MVA), of transmission overhead lines conductors, i.e., CIGRE-22.12 [126] and IEEE Std. 738 [127]. These two standards use slightly different formulas to calculate the thermal rating of the conductor; however, it was found that the differences in the resultant calculated thermal ratings were

minimal. For the purposes of this study, the method described in IEEE Standard 738 was used as a computation method to calculate hourly thermal ratings.

The thermal rating is restricted by the conductor's maximum allowable temperature, which determines the suitable conductor type. Depending on weather conditions, conductor type, and load flow duration, conductor heating may result in one or both of the following: (i) loss of clearance and (ii) loss of strength. Since metal expands with an increase in temperature, the length of conductor between supporting structures also increases, which results in greater conductor sag and reduces ground clearance, and in extreme cases, the line may touch an underlying body, resulting in a short-circuit and subsequent outage. The lines maximum operating temperature (generally between 50 °C and 100 °C for different conductors) is the highest temperature at which the conductor can operate and still maintain the minimum clearance requirements for safe line operation. Other constraints limiting the allowable current ratings are conductor loss of strength through annealing, and inadequate compression fittings, in which the recrystallization of metal occurs causing a loss of tensile strength. [5].

Electrical current passing through a conductor experiences resistance, which generates energy in order to overcome that resistance to complete its path from the energy source to the load; this is translated into thermal energy gain (or heat gain I^2R) within the conductor, thus raising the conductor's overall temperature. The conductor is also assumed to be exposed to the sun, with an associated solar heat gain (q_s). Heat loss is primarily driven by temperature differences between the conductor and its surrounding environment. Figure 4.7 illustrates the different heat gains and losses.

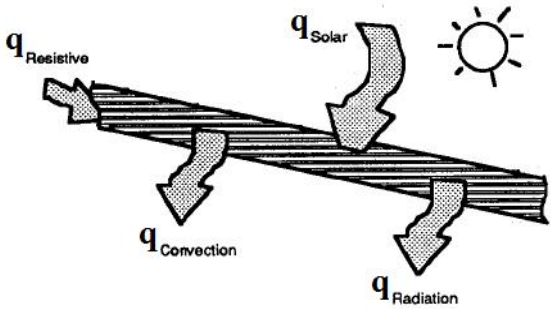

Figure 4.7: Steady-state conductor heat flow [116]

According to the approach outlined in IEEE 738 standard, the maximum allowable current rating that transmission lines can carry, are derived under assumed steady-state conditions. The line thermal rating is determined using a steady-state heat balance equation between the heat produced inside the conductor and the heat exchange on its surface, involving convective heat, radiated heat loss, solar heat gain, and conductor Ohmic resistance. The heat flow out of a conductor should balance its internal heat generation and the heat flow into it.

The equations used to calculate the thermal rating of the transmission overhead lines, based on heat balance, are associated with the material properties of the conductor, surface properties, geographical conditions, and ambient weather conditions. The required specific input parameters include ambient temperature, maximum conductor temperature, wind speed and direction, azimuth of the line, conductor height, latitude, day and hour, emissivity, and solar absorptivity. Conductor characteristics are defined by diameter and calculated resistance at 25 ^{o}C and 75 ^{o}C. Compared with underground cables, the ratings of overhead lines are significantly affected by weather variations. Historical records of ambient temperatures (T_a), wind speeds (V_w), and wind directions (φ) over a one-year period were obtained from a meteorological office. These are measured at specified locations. Under steady-state conditions, the current flowing in the conductor can be determined from the conductor

temperature (or vice versa) if the ambient temperature, solar radiation, and effective wind speed can be accurately quantified.

The heat balance equation was used to calculate the conductor's maximum allowable temperature when the conductor's electrical current is given, or, conversely, to calculate the electrical current given the maximum allowable conductor temperature. In a steady-state calculation, the "heat balance" is calculated using the Equation 4.2, while the thermal rating current can be calculated using Equation 4.3. Using the weather conditions, the conductor's electrical and physical parameters, and the maximum allowable conductor temperature, values of q_s, q_c and q_r can be obtained.

$q_s + I^2R = q_c + q_r$ Equation 4.2 , where

q_s: the solar heat gain.

I^2R: the heat gain due to line current, sometimes known as Joule effect.

q_c: the heat loss due to convection.

q_r: the heat loss due to radiation.

$I = \sqrt{\frac{q_c + q_r - q_s}{R}}$ Equation 4.3

Convection is heat transfer by the movement of air when the heated air is caused to move away from the source of heat, carrying energy with it. Convection above a hot surface occurs because hot air expands, because it is less dense, and so rises. Furthermore, convection varies widely according to whether the conductor is exposed to high or low speed wind. Convection heat loss is divided into forced convection heat loss and natural convection heat loss. Forced convection heat transfer from an overhead conductor is the function of many variables, the primary one being wind velocity and direction. Equations for forced convection heat losses during low wind

speed and high wind speed are shown in Equation 4.4 and Equation 4.5, respectively. Natural convection occurs during zero wind speeds. The equation for natural convection heat loss is calculated using Equation 4.6. The largest of the calculated convection heat losses is used. Parameters in these formulas are explained in Table 4.3.

$$q_{c1} = \left[1.01 + 0.0372\left(\frac{D\rho_f V_w}{\mu_f}\right)^{0.52}\right] k_f k_{angle}(T_c - T_a) \qquad \text{Equation 4.4}$$

$$q_{c2} = \left[0.0119\left(\frac{D\rho_f V_w}{\mu_f}\right)^{0.6}\right] k_f k_{angle}(T_c - T_a) \qquad \text{Equation 4.5}$$

$$q_{cn} = 0.0205\rho_f^{0.5} D^{0.75}(T_c - T_a)^{1.25} \qquad \text{Equation 4.6}$$

Table 4.3: Parameters used to calculate convection heat

D	Conductor diameter, in (mm)
ρ_f	Density of air, in (kg/m^3), and calculated using $\rho_f = \frac{1.293 - 1.525*10^{-4}H_e + 6.379*10^{-9}H_e^2}{1 + 0.00367T_{film}}$
V_w	Wind speed, in (m/s)
μ_f	Dynamic viscosity of air, in (Pa-s), and calculated using $\mu_f = \frac{1.458*10^{-6}(T_{film}+273)^{1.5}}{T_{film}+383.4}$
k_f	Thermal conductivity of air, in $(W/(m-{}^oC))$, and calculated using $k_f = 2.424*10^{-2} + 7.477*10^{-5}T_{film} - 4.407*10^{-9}T_{film}^2$
K_{angle}	Wind direction factor, and calculated using $K_{angle} = 1.194 - \cos(\varphi) + 0.194\cos(2\varphi) + 0.368\sin(2\varphi)$
T_c	Conductor temperature, in (^oC)
T_a	Ambient air temperature, in (^oC)
T_{film}	Average temperature, and calculated using $\frac{T_c + T_a}{2}$, in (^oC)
H_e	Elevation of conductor above sea level, in (m)
φ	Angle between wind direction and conductor axis, in (^{o})

The formula for radiated heat loss of the conductor is calculated using Equation 4.7.

$$q_r = 0.0178D\varepsilon\left[\left(\frac{T_c+273}{100}\right)^4 - \left(\frac{T_a+273}{100}\right)^3\right] \qquad \text{Equation 4.7, where}$$

ε: Emissivity.

Equation 4.8 below is used to calculate Solar Heat Gain, and parameters needed in this equation are listed in Table 4.4.

$q_s = \alpha Q_{se} sin(\theta) A'$ Equation 4.8, where

Table 4.4: Parameters used to calculate solar heat

	Solar absorptivity
	Total solar and sky radiated heat flux rate with corrected elevation, in (W/m^2), and calculated using $Q_{se} = K_{solar} Q_s$
θ	Effective angle of incidence of the sun's rays, in (^{o}), and calculated using $\theta = arcos[cos(H_c)cos(Z_c - Z_1)]$
	Projected area of conductor per unit length, in (m^2/m), and calculated using $A' = \frac{D}{1000}$
	Solar altitude correction factor
	Total solar and sky radiated heat flux rate, in (W/m^2), and calculated using $Q_s = A + BH_c + CH_c^2 + DH_c^3 + EH_c^4 + FH_c^5 + GH_c^6$
	Altitude of sun, in (^{o}), and calculated using $H_c = arcsin[cos(Lat).cos(\delta).cos(\omega) + sin(Lat).sin(\delta)]$
	Degrees of latitude, in (^{o})
	Solar declination, in (^{o}), and calculated using $\delta = 23.45 sin[\frac{284+N}{365} 360]$
	Days of the year
	Hour angle which is the hour from noon 15°, in (^{o})
A, B, C, D, E, F, G	Constants, which depend on clear or industrial atmospheres. Their values are given in Table 4.5
	Azimuth of sun, in (^{o}), and calculated using $Z_c = C + arctan(\chi)$
	Azimuth of line, in (^{o})
	Solar azimuth constant (^{o}), which is a function of μ and i, as shown in Table 4.6
χ	Solar azimuth variable and calculated using $\chi = \frac{sin(\omega)}{sin(Lat)cos(\omega) - cos(Lat)tan(\delta)}$

Table 4.5: Coefficients for total solar and sky radiated heat flux rate

Clear atmosphere	
A	42.2391
B	63.8044
C	−1.9220
D	3.46021×10^{-2}
E	-3.61118×10^{-4}
F	1.94318×10^{-6}
G	4.07608×10^{-9}
Industrial atmosphere	
A	58.1820
B	14.2110
C	6.6138×10^{-1}
D	-3.1658×10^{-2}
E	9.4654×10^{-4}
F	1.3446×10^{-5}
G	-1.3236×10^{-5}

Table 4.6: Solar azimuth constant

"Hour Angle," ω (degrees)	C if $\chi \geq 0$ (degrees)	C if $\chi < 0$ (degrees)
$-180 \leq \omega < 0$	0	180
$0 \leq \omega \leq 180$	180	360

Transmission lines have traditionally been operated and designed according to the thermal rating calculated using deterministic methods based on set of most conservative assumptions (i.e. bad cooling conditions): high ambient temperature and low wind speed with small angle direction e.g. 20 °. Thermal rating determined this way usually results in underutilization of transmission line capacity. [128-135].

Wind may hit a conductor at an angle other than 20° with respect to the line, although it is this particular angle that is generally assumed in current thermal rating methods as the conservative assumption in DEWA [5, 128-133]. As shown in Figure 4.8, wind speed (*V*), may be in a plane at varying wind angles (φ) measured from a normal to the conductor axis. Wind direction is changeable at low wind speed [130]. Conductor thermal rating, as will be illustrated in the next chapters, is very sensitive to the wind angle of incidence. A wind direction perpendicular to the conductor increases turbulence around the conductor and thus increases the heat exchange on its surface, whereas a wind direction parallel to the conductor would minimize heat exchange. Furthermore, the direction of the transmission overhead line may vary over its length. Wind speed also fluctuates with time and location along transmission overhead lines [5].

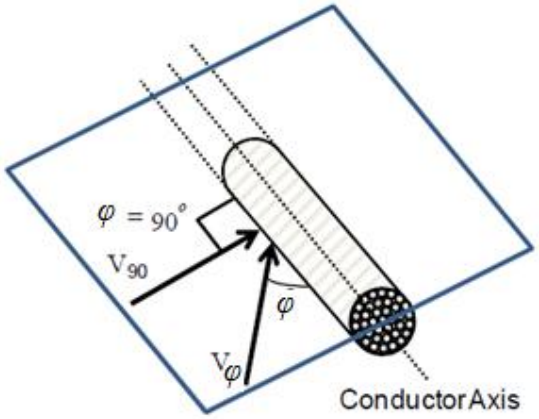

Figure 4.8: Wind direction, conductor orientation and velocity profile [5]

Since weather conditions change frequently, the thermal rating of transmission overhead lines also changes. In this thesis, hourly thermal ratings were calculated in order to develop its Probabilistic Distribution Function (PDF).

Actual historical hourly weather observations are used to calculate the range of thermal rating of a transmission overhead line over a year. Using Heat Balance equations, the hourly thermal rating for overhead transmission lines were calculated. This formula is expected to provide a higher range of thermal ratings than those derived from the traditional 'conservative' method.

In this work, a time-varying thermal rating model is developed to study the resultant hourly thermal ratings and find their uncertainties as defined by a distribution function, which can be divided into several discrete intervals. A number of discrete thermal ratings (bins) were identified. Over an annual period, the thermal rating range was divided into 30 units (bins), each with a bin size of 30 Amps. The frequency of occurrence of each thermal rating range was evaluated and then expressed as a relative frequency. For each range of thermal rating, the probability of occurrence of this range was determined using Equation 4.1. Figure 4.9 illustrates a sample of the resultant hourly thermal rating variation for a period of one year for

a sample of 'Zebra' conductors used in the Dubai network. Thermal ratings used by DEWA in each season (i.e. 3550 Amps, 3,825 and 4,100 Amps for summer, Spring/autumn and winter respectively) is shown in Figure 4.10. This chronological thermal rating is represented by a probabilistic model, as shown in Figure 4.10.

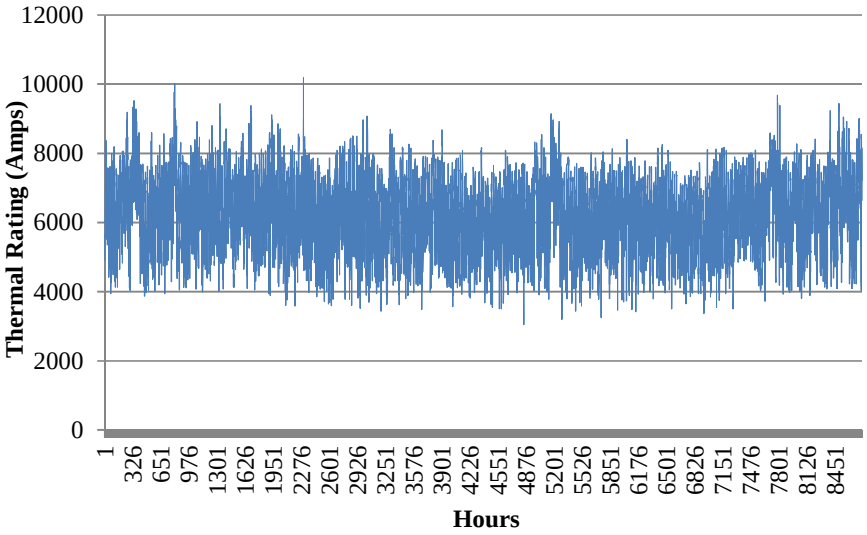

Figure 4.9: Hourly thermal rating variation along a year

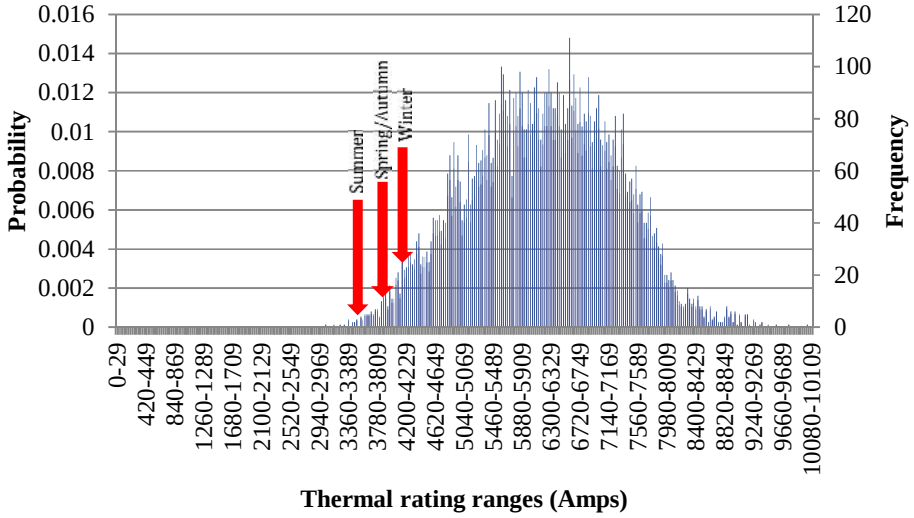

Figure 4.10: Thermal rating probabilistic model

4.6 Reliability data of transmission line

The term “failure” refers to outages in which the component is unavailable to transmit power (or to function properly) either temporarily or permanently. Faults on a transmission component are usually due to severe weather conditions (such as lightning and wind storms), component ageing, high operating network variables, and the lack of proper maintenance. Component failure of transmission network is quite rare due to the inherent high reliability of such components. However, it is a more regular occurrence for these types of components to be temporarily outaged from service, due to for example protection maloperations, operational human error, or severe weather conditions. Although component failures on a transmission system have a low probability, they have a relatively high impact. Moreover, blackouts typically involve sequences of component failures.

In 2000, and according to GB National Grid, about 200 faults occur on the GB’s transmission system every year [4]. Each customer was without supply in GB for average of 86 minutes, while problems due to transmission system or generating plants accounted for only about 1% of this unavailability [6]. Furthermore, since 2011, the 400/132 kV transmission system operated by Dubai Electricity and Water Authority (DEWA), faces approximately 12 lines faults each year [5].

4.6.1 Probability of first and second order contingency

When a main transmission component (e.g. line, cable and transformer) fails, the load is transferred elsewhere. This leads to a rise in the load on some of the remaining components. If this rise exceeds pre-specified ratings, it will result in overloading and possibly cause a cascading failure, or it might cause a blackout depending on the type and condition of the failures. Depending on the rules and standards followed, lines may either be allowed to carry

an overload for a short duration or alternatively, they may be removed from service or the system demand may be reduced [5].

Clearly, analysis of all possible network configurations is impracticable for real power networks due to the huge amount and complexity of computing involved. Therefore, some methods have been developed to reduce the number of analysed configurations.

In a transmission system, the main components include transmission overhead lines, underground cables, and transformers. These components are generally represented by a two state down-up model as shown in Figure 4.11, where an on-state indicates that the element is in an operating state, and an off-state implies that the element is shut down due to failure or maintenance. This model is known as the Markov model. For the purpose of this thesis, only reliability data for the component failure of a transmission line was used. Failures of other component (such as generators, cables, transformers, and busbars) have been neglected and assumed to be 100 % reliable.

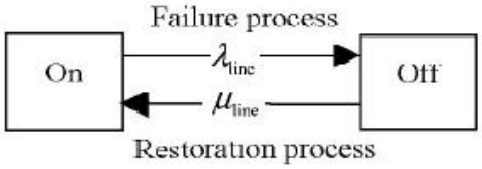

Figure 4.11: Markov two-state model of transmission line

The outages of various components are classified as (i) independent when the outage of one component does not affect the outage probability of others, and (ii) dependent when the outage of a component does affect the outage probability of others. Dependent component failures on transmission systems can be categorized into common mode and substation-originated failures. Common mode failures are events with one external source resulting in multiple component

failures, such as the failure of a transmission tower supporting two circuits. A substation-originated outage is an event that depends on a post-fault protection system, such as breaker failure, bus section failure, stuck breakers, bus bar failure, etc. [136].

To conduct a reliability assessment effectively, it was necessary to consider the probable outages of transmission lines that would reduce the capability of the transmission system to transmit the required power. A complete set of probable contingencies should be selected systematically. In this respect, the outages considered were single and double circuit failure outages, in addition to maintenance outages. Based on the GB SQSS standard [5, 121], no single or double circuit fault should cause any remaining line loading to be greater than its thermal rating.

Component performance indices, such as the frequency (sometimes called failure rate in event/year) and duration (sometimes called repair rates in duration/year) of component failure/s, have been reported by utilities [5]. They quantitatively describe components reliability and thus, the system reliability. It is practical to use these component-performance indices to assign a probability to every occurrence and thus obtain an overall probability. The probability of line failure in a system can be determined using Forced Outage Rates (FORs). To calculate FOR for a transmission line, failure rates (λ) and failure duration (r), in addition to restoration rates and restoration duration, are required.

For a transmission line, the probability of the N-1 contingency $Pc_{(N-1)}$ (i.e. FOR) was obtained from either actual historical statistical or anticipated reliability data of line failure rates and duration for the studied system, as shown in Equation 4.9 [22, 50].

$$Pc_{(N-1)} = \frac{^{a}r}{T} \quad \text{Equation 4.9, where}$$

λ: the failure rate (i.e. number of N-1 outages per annum) that can be interpreted as the number of times the outages occurs during an observation time of 8,760 hours.

r: the average duration of the outages.

T : the total period of study; this is 8,760 hours for a year.

The failure rate of two coincident and unrelated 'N-1' outages (all the 'N-2' contingencies except double circuit cases) was calculated as the product of the probabilities of individual 'N-1' outages, which is a reasonable approximation when the duration of the outages is very small in comparison with the total time of study. In absence of 'N-2' outage data, the probability of 'N-2' double circuit contingencies was considered to be 7.5 % of the 'N-1' case as has been assumed in [137]. The probability of an event in which two independent line outages overlap is very small.

4.6.2 Probability of high order contingency

Practically, the probability of a large number of transmission lines experiencing outages at the same time is very rare. However, probabilistic approach, up to only N-2 or even N-3 or beyond, may not adequately describe the real physical threats to the system. The challenge is to build up a probability of not only independent N-1, N-2, N-3 ... etc contingencies but also the probability of dependent high-order multiple trippings. Cascading failures in practice can be very sophisticated chains of rare events. Rare events with high severities, potentially may lead to blackouts in power systems. Blackouts become widespread by initial failures expanding in a complicated cascade of rare events. High-order cascading failures and blackouts in power systems are rare, but they have formidable consequences such that neglecting their probability of occurrence may result in a degree of exposure to unforeseen failure. Cascading failures are generally assumed to be distributed according to the Poisson probability distribution function

(pdf) [89, 91]. The Poisson distribution is an approximation when each initial failure propagates to a large number of components [89, 91]. Initial failures could be represented by Poisson distribution and each initial failure produces more failures according to poisson distribution. Based on the Poisson distribution, probability of failure occurring 'x' times in interval 't' can be calculated using Equation 4.10, with given failure rate λ [8]. Given that the possible number of rare events is excessively large and it is neither possible nor necessary to do analysis for all of them, it will become extremely difficult for electric transmission utilities to rationalize capital expenditures on basis of possible interruptions caused by rare contingencies. Many system states are very rare, hence trade-off is sought between objective accuracy and computational burden. Thus, although could be considered in future, in this study high order contingencies were not taken into consideration.

$$Px(t) = \frac{\lambda_t{}^x e^{-\lambda_t}}{x!} \qquad \text{Equation 4.10}$$

4.7 Probabilistic Distribution Function (PDF) of the calculated line loadings

The probabilistic distribution of the resultant loading of a line, for all system demand levels and all studied contingencies, is the summation of the product of (i) the probability of the contingency that considers probability of system demand ranges, and (ii) the relative frequency of the line loading for all contingencies over the annual cycle, as shown in Equation 4.12, where $Pc_{(j)}$ is the probability of the jth contingency that takes into account probability of system demand ranges, and $Fl_{(i,j)}$ is the relative frequency of line loading for the ith system demand and jth contingency. The number $N_L(N_L + 1)/2$ is the summation of the number of single line outages (N_L) and the number of double line outages is $N_L(N_L - 1)/2$ for a system of N_L lines. It is $\frac{N_L(N_L-1)}{2} + N_L = N_L(N_L + 1)/2$.

$$Pl_{(i,j)} = \Sigma_{i=1}^{N_D} \Sigma_{j=1}^{N_L(N_L+1)/2} Pc_{(j)} Fl_{(i,j)} \quad \text{Equation 4.12}$$

Uncertainties in line loading were considered in a probabilistic security assessment using a distribution function, which was divided into several discrete intervals. The line loading range was divided into 30 units (bins) each with a bin size of 30 Amps. The frequency of occurrence of each line loading range was evaluated and then expressed as a relative frequency to obtain the PDF of the line loading for each line. For each range of the resultant line loading, the probability of occurrence of this range was determined using Equation 4.1. The PDF for a sample of line loadings with a distribution function, for an intact system, and for N-1 and N-2 contingencies, is shown in Figure 4.12. This figure does not necessarily show overload occurs due to coincidence of day to day loading and rating.

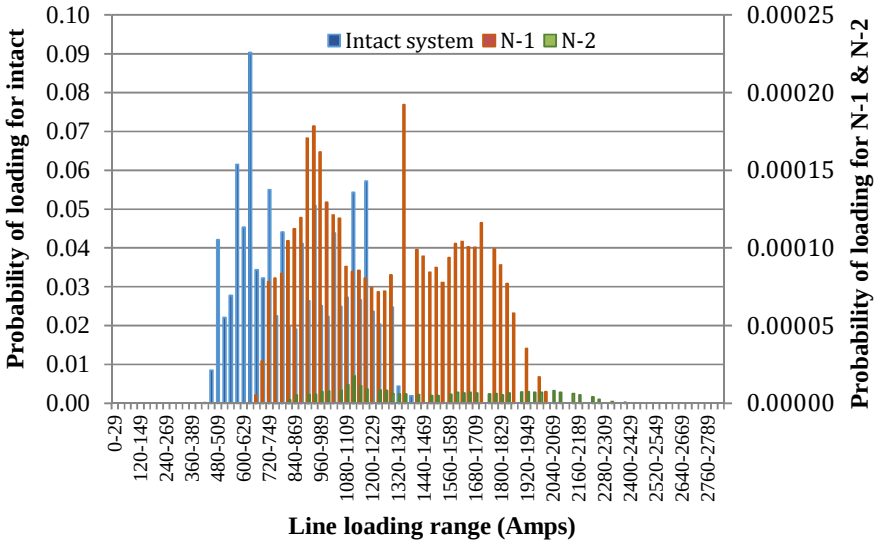

Figure 4.12: PDF for a sample of line loadings for intact system, N-1 and N-2 contingencies

4.8 Calculation of the Line Overloading Risk Index (LORI)

The LORI risk index in this work was selected because it is required to reflect the probability and severity of line overloading in a transmission power system. Generally, the risk index can

be evaluated using the following formula as shown in Equation 4.13, where, $\mathrm{Sev}(E_j, X_i)$ is the severity of event E_j for operating condition X_i, while $\Pr(E_j)$ is the probability of occurrence of event E_j [58]. In this particular application, the Line Overloading Risk Index (LORI) is defined by Equation 4.14 as the summation of product of the line loading probability and the line loading severity, $Sl_{(i,j)}$.

$$Risk(X_j) = Sev(E_j, X_i) * Pr(E_j) \qquad \text{Equation 4.13}$$

$$\mathrm{LORI} = \Sigma_{i=1}^{N_D} \Sigma_{j=1}^{N_L(N_L+1)/2} Pc_{(j)} Fl_{(i,j)} Sl_{(i,j)} \qquad \text{Equation 4.14}$$

$Sl_{(i,j)}$ is defined and used in this research work as equal to zero up to 90% of the line thermal rating and increasing linearly from 0 to 1 as the line loading increases from 90 % to 100 % of the rating. Also, the severity function increases linearly beyond the 100 % of rating, as shown in Figure 4.13. This function is referred to as continuous severity. An alternative severity function uses a zero value for 0 to 100 %, and 1 for all values above 100 %. A disadvantage of this so-called discrete severity function is that it does not express extent of violation and neither does it provide any indication of when the system is close to reaching its limit [138].

For a particular values of i and j, $Pc_{(j)}.Fl_{(i,j)}$ gives the probability of that particular loading, then there may be a number of lines during the year that could produce this condition. Therefore, there may be more than one possible loading, so we should account for possibilities of different loadings.

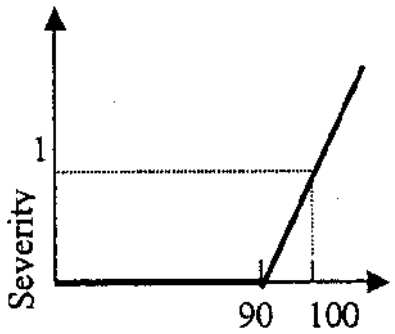

Figure 4.13: Overload continuous severity function [138]

The probability of line overloading, in a simple way, which varies according to the distribution functions of the system variables can be illustrated graphically , as shown in Figure 4.14. In the figure, line loading and thermal rating are shown as variable quantities, and depending on extent of the overlap of these two distributions, the associated inadequacy and security risk occurs.

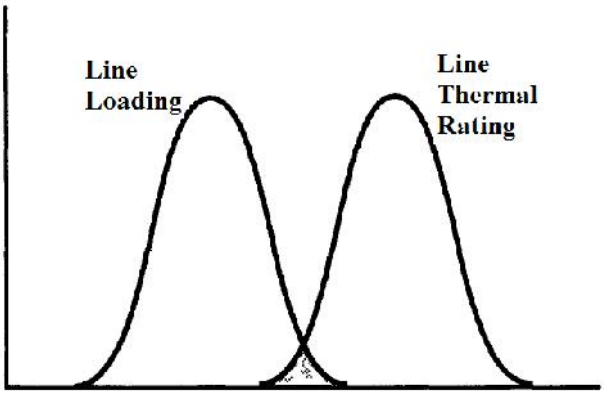

Figure 4.14: Typical line loading and thermal rating distribution [8]

4.9 Conclusions

This chapter has described the application of Line Overloading Risk Index (LORI) to assess systematically transmission line overloading and an improved algorithm for its calculation, is proposed. The LORI is calculated using a probabilistic method that determines the likelihood

and severity of line overloading, under hour-by-hour system demand levels over a one-year period, for intact conditions and all N-1, N-2 and maintenance outages. For each possible event or state of the system, the corresponding probability of line thermal rating has been calculated, considered over an annual cycle and based on detailed meteorological data, which were provided by official MET offices in Dubai and UK. In order to accomplish this, the proposed improved probabilistic reliability assessment method was evaluated using NEPLAN software package with NPL code programming, thus making it possible to simulate a very large number of different load flow cases, using an automated process. Work on calculating the LORI has led to the development of Probabilistic Distribution Functions (PDF) for line loading, line thermal rating and system demand.

Each line risk can be calculated and used as a benchmark for the comparison of different system operations and designs. In this research, this developed algorithm will be applied to the Dubai and GB real transmission systems, presented in the next two chapters.

CHAPTER 5. APPLICATION OF NEW PROBABILISTIC RELIABILITY APPROACH TO THE DUBAI TRANSMISSION SYSTEM

5.1 Introduction

A transmission probabilistic reliability analysis should consider and evaluate certain relevant parameters, e.g. the variations in load flow, across a transmission system due to different uncertainties. A risk of line overloading may arise, and include but not be restricted to, the following relevant uncertainties: (i) hourly variations in system demand, (ii) maintenance outages, and (iii) 'N-x' line outages, taking into account respective variations in the thermal rating.

Chapter 4 introduced an improved method to calculate the Line Overloading Risk Index (LORI) and to develop the Probabilistic Distribution Function (PDF) of the resultant line loading and line thermal rating. Starting with the actual historical annual transmission system demand curve (on an hourly basis), a PDF of the system demand was obtained and a discretised range of system demand levels were identified. DC load flows, using a commercial load flow program and associated programming code, were carried out for each discrete system demand level from which the corresponding line loadings were obtained in order to determine the severity for the intact system, 'N-x' contingencies, and maintenance outage. For each hourly system demand, corresponding hourly line thermal ratings were calculated based on local meteorological data. Finally, the PDFs for the resultant line loadings were compared with the PDFs for the thermal ratings of each line and the LORI was determined. Hence, the LORI was calculated based on the probabilistic method, which determines the likelihood and the severity of the line overloading.

Accordingly, this chapter aims to apply the proposed LORI algorithm to the Dubai Transmission System. Details of the Dubai transmission system were provided in Section 3.3.

5.2 System demand for Dubai power system

Based on the ambient temperature, the calendar year in Dubai can be divided into the two main seasons of summer and winter. Summer is normally considered to be the months of April, May, June, July, August, and September; while winter comprises the remaining months of the year. Figure 5.1 illustrates the hourly system demand variation during 2011. It can be noted that for this system, the maximum demand occur during the summer period (middle of graph) due to the high usage of air conditioning units, while lower system demands happens in the winter months (start and end of graph). The maximum system demand for 2011 was 6,162 MW, which occurred during the summer period at 15:00 hrs on 10 August 2011, while the minimum system demand was 2,005MW, which occurred during the winter period at 05:00 hrs on 01 January 2011.

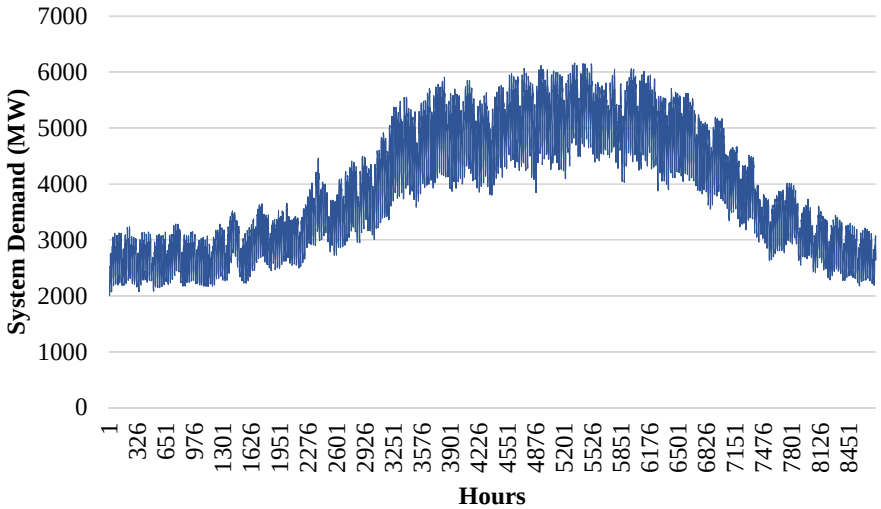

Figure 5.1: Hourly system demand variation during 2011 for the Dubai power system

In order to reduce the potential number of simulation studies, a number of discrete system demand levels (bins) were identified. System demand range was divided into 100 units (bins), each with a bin size of 100 MW. Hence, actual chronological hourly system demands were converted into different state models, with a distribution function corresponding to a one-year period.

Table 5.1 shows the resultant system demand ranges along with their frequencies and probabilities. As can be seen, system demand in Dubai city for the year 2011 ranged from 6,162 MW to 2,005 MW. The most frequent range of the system demand was 2,900 – 2,999 MW, which occurred for 413 hours in the year (its probability is 0.047). On the other hand, the least frequent range of system demand was 2,000 – 2,099 MW, which occurred for only 12 hours in the year (its probability is 0.001). The frequency and PDF curves are shown in Figure 5.2. This figure shows the frequency of occurrence of each range of system demand on the left-hand scale, and the corresponding probability on the right-hand scale, for the complete annual load cycle in 2011 with a bin size of 100 MW.

Table 5.1: Ranges of the system demand of the year 2011 with their frequencies and probabilities of occurrence

#	**Ranges**	Freq	Prob.	#	**Ranges**	Freq.	Prob.	#	**Ranges**	Freq	Prob.
1	**2000-2099**	12	0.001370	**16**	**3500-3599**	198	0.022603	**31**	**5000-5099**	240	0.027397
2	**2100-2199**	59	0.006735	**17**	**3600-3699**	200	0.022831	**32**	**5100-5199**	242	0.027626
3	**2200-2299**	179	0.020434	**18**	**3700-3799**	191	0.021804	**33**	**5200-5299**	237	0.027055
4	**2300-2399**	187	0.021347	**19**	**3800-3899**	168	0.019178	**34**	**5300-5399**	231	0.026370
5	**2400-2499**	193	0.022032	**20**	**3900-3999**	169	0.019292	**35**	**5400-5499**	273	0.031164
6	**2500-2599**	237	0.027055	**21**	**4000-4099**	167	0.019064	**36**	**5500-5599**	237	0.027055
7	**2600-2699**	266	0.030365	**22**	**4100-4199**	189	0.021575	**37**	**5600-5699**	205	0.023402
8	**2700-2799**	275	0.031393	**23**	**4200-4299**	226	0.025799	**38**	**5700-5799**	176	0.020091
9	**2800-2899**	386	0.044064	**24**	**4300-4399**	214	0.024429	**39**	**5800-5899**	137	0.015639
10	**2900-2999**	413	0.047146	**25**	**4400-4499**	233	0.026598	**40**	**5900-5999**	89	0.010160
11	**3000-3099**	378	0.043151	**26**	**4500-4599**	226	0.025799	**41**	**6000-6099**	40	0.004566
12	**3100-3199**	308	0.035160	**27**	**4600-4699**	199	0.022717	**42**	**6100-6199**	17	0.001941
13	**3200-3299**	288	0.032877	**28**	**4700-4799**	198	0.022603	**43**	**6200-6299**	0	0.000000
14	**3300-3399**	284	0.032420	**29**	**4800-4899**	184	0.021005				
15	**3400-3499**	197	0.022489	**30**	**4900-4999**	212	0.024201		**Total**	8760	1

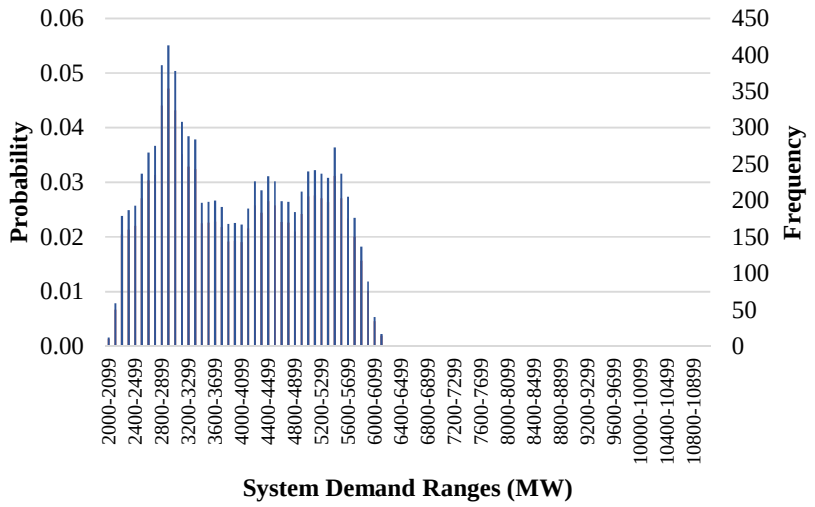

Figure 5.2: Frequency Distribution and PDF for system demand for the year 2011

The study cases were extended to consider the forecasted system demands of the years 2015, 2021 and the 'stressed' system for 2021. It is forecasted that the system demand will be around 8,000 MW, 9,500 MW and 11,000 MW for the years 2015, year 2021, and the 'stressed' year 2021, respectively. Figure 5.3 shows the system demand growth based on official forecast of DEWA master plan. Thus, the equivalent scaling percentage, with respect to the actual system demand of 2011 was used to derive the hourly system demand for the forecasted years. As temperature, humidity and social patterns are expected to be very similar over the period to 2021, it is not expected to be a significant change in daily or seasonal shape of system demand. Therefore, the annual system demand for future years has been considered using the same system demand shape as for year 2011 but scaled to the respective predicted maximum.

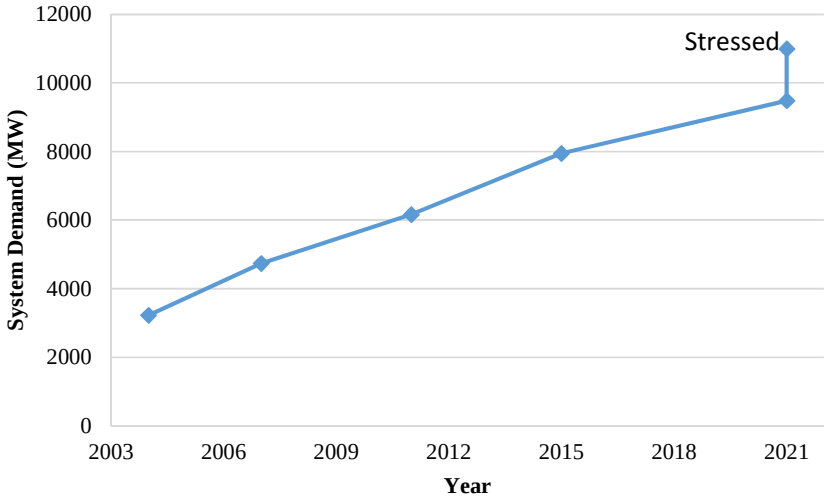

Figure 5.3: System demand growth for Dubai power system

Graphs of the hourly variation of and PDF for the system demand for years 2015 and 2021 were developed and analysed. The system demands in 2015 are expected to vary from 7,947 MW to 2,585 MW, with the most frequent range of the system demand is expected to be 3,700 – 3,799 MW, while the least frequent range of system demand is 2,500 – 2,599 MW. For the 2015 study, the number of system demand states increased to 55 while maintaining the same bin size of 100 MW. In 2021, the system demands are forecasted to range from 9,482 MW to 3,085 MW, with the most frequent range is 4,400 – 4,499 MW and the least frequent range is 3,000 – 3,099 MW. The number of system demand states further increased to 65 with similar bin size of 100 MW.

As stated previously, it was required to stress year 2021, and thus the system demands ranged from 11,000 MW to 3,600 MW (Figure 5.4). Figure 5.5 shows that the most frequent range of the system demand is 5200-5299 MW, which is expected to occur 245 hours in a year, while the least frequent range of system demand is 3,500 – 3,599 MW, which is expected to occur for one hour in a year. Number of resultant state is 76.

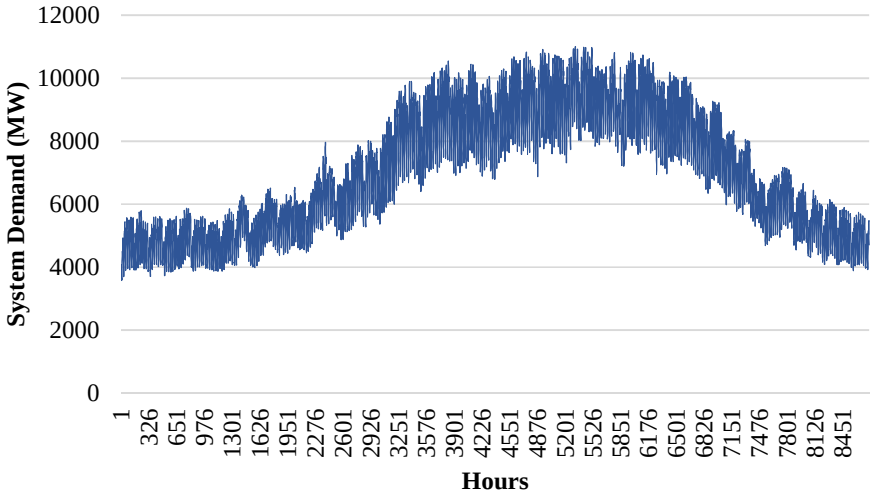

Figure 5.4: Hourly system demand variation along a 'stressed' year of 2021 for Dubai power system

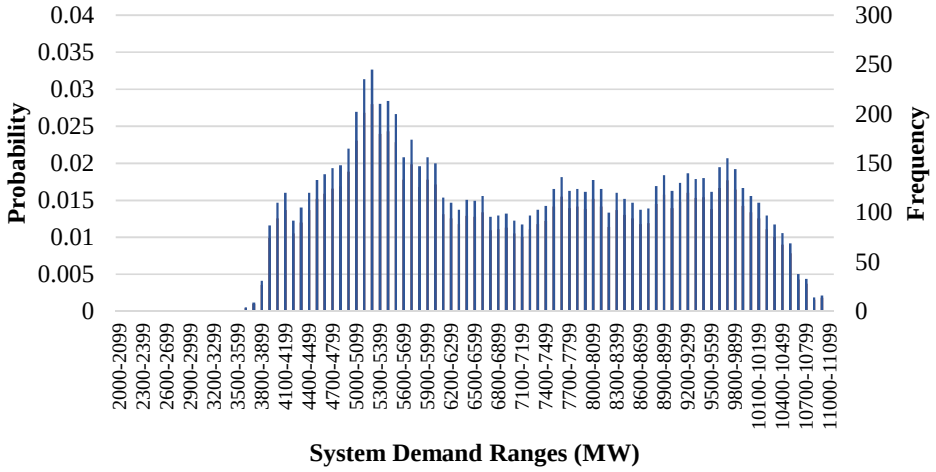

Figure 5.5: Frequency Distribution and PDF for system demand for the 'stressed' year of 2021

5.3 Reliability data for Dubai transmission power system

Reliability data of failure and their duration were obtained from Dubai Electricity and Water Authority (DEWA). Single and double components failures on the transmission system for 2004 to 2011 are shown in Table 5.2 for both 400 kV and 132 kV levels [5]. As can be seen,

2009 was the worst year for 400 kV single line failures, i.e., four individual 400 kV single lines failures occur

ed with an average duration for each failure of 65.78 hours; due to rectification time. In addition, it can be noted that simultaneous 400 kV double line outages didn't occur during the study period, although bus bar outages and one total blackout did occur due to technical failures. The 400 kV transmission system operated by DEWA had been faced with about eight single line outages, during eight years (i.e. once a year as average), with an average duration of nine hours for each outage. Using Equation 4.9, the probability of the 'N-1' contingency $Pc_{(N-1)}$ was calculated as

$$Pc_{(N-1)} = \frac{\lambda r}{T} = \frac{1*9}{8760} = 0.0001027397 .$$

As no contingency of second order line failures (i.e. 'N-2' contingency) occurred during the study period in Dubai, a failure frequency of double circuit outages was assumed to be 7.5 % of the 'N-1' [137]. The probability of an event in which two independent line outages overlap is very small. Hence,

$$Pc_{(N-2)} = Pc_{(N-1)} * 7.5\% = 0.0001027397 * 7.5\% = 0.00000770581$$

The simulations also determined the effect of planned maintenance line outages on the LORI. Statistics of maintenance outages of 400 kV lines were collected for the years 2010, 2011, and 2012. The average frequency of occurrence of planned maintenance outages for each 400 kV line was derived along with the corresponding average duration, as tabulated in Table 5.3. The probability of maintenance outage was found to be (2.2 x 70.8)/8760 = 156 / 8760. However, for the simplicity purpose, no more results will be shown for maintenance outages.

Table 5.2: Failure statistics for Dubai transmission system

Component		400 kV				132kV		
		Single circuit	**Double circuit**	**Busbar**	**400/132 transformer**	**Single circuit**	**Double circuit**	**Bus bar**
2004	**Freq**	1	0	0	1	5	1	0
	Duration (hrs)	4.38	0	0	42	5.75	1	0
2005	**Freq**	0	0	0	0	6	0	0
	Duration (hrs)	0	0	0	0	2.8	0	0
2006	**Freq**	0	0	0	4	9	0	0
	Duration (hrs)	0	0	0	30.67	37.77	0	0
2007	**Freq**	0	0	0	1	11	1	0
	Duration (hrs)	0	0	0	9.8	23.53	2.45	0
2008	**Freq**	2	0	1	0	4	1	0
	Duration (hrs)	1.01	0	483.3	0	1.12	0.4	0
2009	**Freq**	4	0	1	0	10	0	2
	Duration (hrs)	65.78	0	1.77	0	30.44	0	4.72
2010	**Freq**	0	0	0	0	12	1	0
	Duration (hrs)	0	0	0	0	16.96	5.67	0
2011	**Freq**	1	0	0	0	13	0	1
	Duration (hrs)	0.72	0	0	0	29.82	0	2.03
Average	**Freq**	1	0	0	1	9	1	0
	Duration (hrs)	9	0	61	10	19	1	1

Table 5.3: The average frequency of planned maintenance outages along with the average duration for 400 kV lines.

Year	Average Frequency	Average Duration (hours)
2010	2.2	42.66
2011	2.1	59.07
2012	2.3	110.58
Average	2.2	70.8

5.4 Thermal rating calculation for transmission overhead lines of the Dubai power system

Hourly steady state thermal ratings for 400 kV lines were calculated using IEEE Std. 738. The weather data set used in this study was obtained from the Dubai Metrology Office [139], and corresponds to a location at Dubai international airport within the area of study and representative of the whole area. The data set contains historical hourly values of measured meteorological data. Each set of hourly weather data contains three weather elements: ambient

air temperature, wind speed, and wind direction for the calendar year 2013. Given that year-on-year changes are small and no drastic changes in climate has been observed, it has been assumed that data are representative for application to the 2011 and 'stressed' year 2021 study. The Dubai area contains very similar geographic and climate characteristics (i.e. desert and a coastal area). Therefore, this study assumed and used a single area which has common geographic and weather features. Figure 5.6 shows hourly weather data for ambient temperature and wind speed. As can be seen, the ambient temperature appears to be the least variable parameter, in comparison to wind speed. Frequency distributions were used to represent the weather parameters of ambient temperature, wind speed, and wind direction, as shown in Figure 5.7. As can be seen from Figure 5.7(a), ambient temperatures in Dubai city range from 47 to 12 ^{o}C, and the most frequent range for the ambient temperature is 30 – 34 ^{o}C, which occurred for 2,369 hours during 2013. DEWA used 45 ^{o}C , 38 ^{o}C and 32 ^{o}C for summer, spring/autumn and winter, respectively. Figure 5.7(b) illustrates that wind speeds in Dubai city range from 14.4 to 0 m/s, and the most frequent range of wind speed is 2 – 3 m/s; which occurred for 4,201 hours [5, 132, 133, 138]. DEWA utilized wind speed of 1 m/s for all seasons. Finally, Figure 5.7(c) indicates that the wind direction range of 300^{o} – 329^{o} (dominant 'Shamal' wind) occurs more frequently in comparison with other wind direction ranges, i.e., it occurred for 1,121 hours [5, 132, 133, 138]. DEWA used wind angle of 20 ^{o} for all seasons. For DEWA to calculate their thermal rating, especially for summer season, values of 45 ^{o}C, 1 m/s and 20^{o} were used for ambient temperature, wind speed and wind angle respectively [5].

The wind angle is the direction of the movement of the wind relative to the conductor axis. When the wind angle is zero, the wind is blowing parallel to the conductor axis. When the wind angle is 90°, the wind is blowing perpendicular to the conductor axis. [5]. For application to

the IEEE equations [131], and due to the similarity of wind hitting effects, it was necessary to convert meteorological wind directions in the range from 91° to 360° into an equivalent range of 0° to 90°, according to Table 5.4.

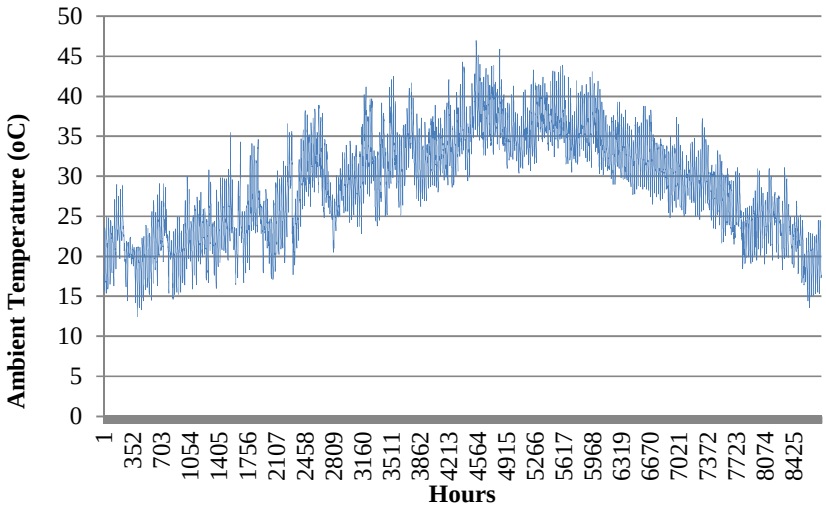

(a) Ambient temperature

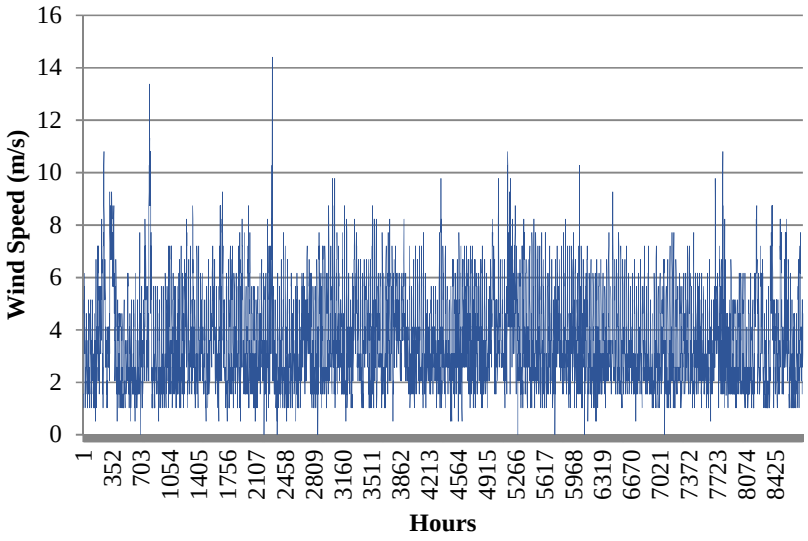

(b) Wind speed

Figure 5.6: hourly weather for Dubai during 2013

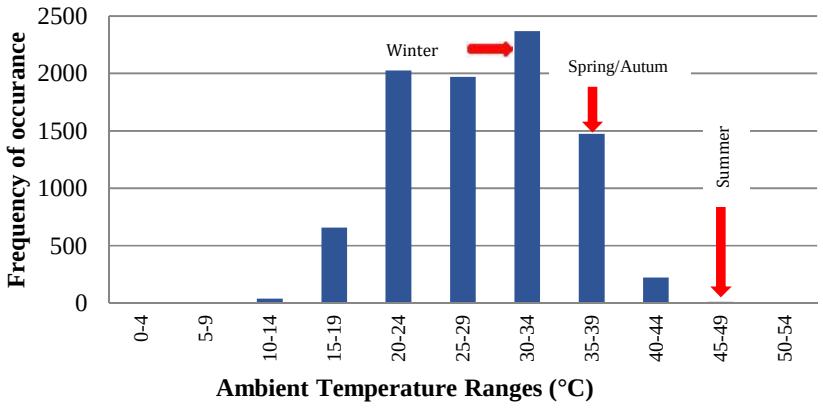

(a) Ambient temperature

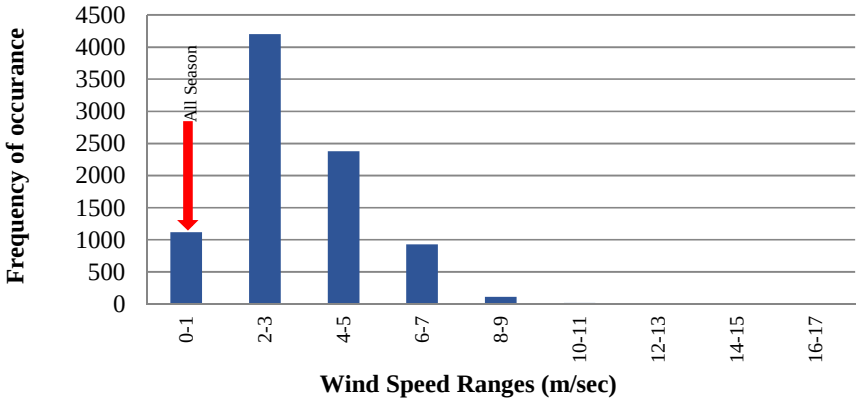

(b) Wind speed

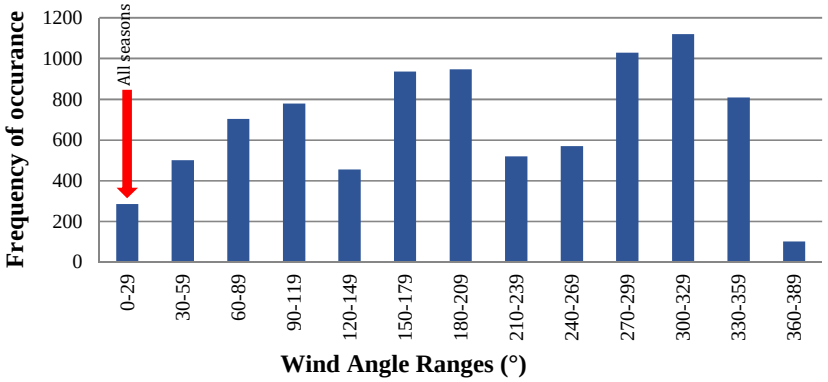

(a) Wind angle

Figure 5.7: Frequency distributions for weather parameters for Dubai during 2013 and DEWA selected values

AAAC ‘Yew’ and ACSR ‘Zebra’ quad conductors are used in all 400 kV transmission overhead lines in the Dubai transmission network and the thermal rating calculations are based only on these two types of conductors. Table 5.5 shows the specifications for these conductors [5].

Table 5.4: Conversion of 91° to 360° wind angles into ‘0° to 90°’ angles

Wind Direction	Conversion to cope with IEEE calculation
0 - 90°	0 → 90°
90° - 180°	90° → 0°
180° - 270°	0 → 90°
270° - 360°	90° → 0°

Table 5.5: Engineering parameters for 400 kV transmission line conductors

	Yew AAAC	Zebra ACSR
Conductor Outer Diameter (mm)	28.42	28.62
Conductor DC Resistance at 20 °C (Ω/km)	6.908×10^{-5}	6.74×10^{-5}
Maximum allowable temperature (°C)	95	100
Conductor surface absorptivity	0.9	
Conductor surface emissivity	0.7	

Conductor DC resistance is given in Table 5.5 at a temperature of 20 °C. Equations 5.1 and 5.2 [140] were used to convert the conductor DC resistance at a temperature of 20°C into AC resistances at 25 °C and 75 °C.

$$R_{DC(2)} = R_{DC(1)}\left(1 + \alpha_1 (T_2 - T_2)\right)$$ Equation 5.1, where

$R_{DC(1)}$: resistance at temperature T_1
$R_{DC(2)}$: resistance at temperature T_2
α_1: temperature coefficient of resistance at T_1

$R_{AC} = R_{DC}.S$ Equation 5.2, where

S : skin effect factor for the conductor. As [5], a value of 1.03354 was used for ACSR conductors, while 1.0123 was used for AAAC conductors.

The Maximum Operating Temperature (MOT) (generally between 50 °C and 100 °C) is the highest temperature at which a conductor can operate and still maintain minimum clearance requirements for the safe line operation considering line sags and annealing. Maximum allowable conductor temperatures of 95 ºC and 100 ºC for Yew AAAC and Zebra ACSR conductors, respectively, were used in this study to determine the steady-state thermal conductor rating.

The conductor elevation height was assumed to be 100 metres above sea level [5]. The latitude for Dubai city is 25 º.

Usually, coefficients of emissivity (ε) and absorption (α) of a new conductor are in the range of 0.2 to 0.3, and increase up to 1 with age as a function of the system voltage and the density of particulates in the air [127]. For our study, the coefficients of emissivity (ε) and absorption (α) were selected as 0.7 and 0.9, respectively, as used in DEWA [5].

The geographic locations (in degree angle) of transmission lines with respect to North pole, i.e. its azimuth, were found e.g. the azimuth for the 400 kV transmission line 'K-N' is 44º. For simplicity purpose, it was assume that wind will hit the line in an angle based on single calculated line azimuth angle, although it is well-known that line will not maintain single azimuth.

5.4.1 Sensitivity analysis of effect of weather parameters

There are various parameters that affect the thermal rating of overhead lines. These parameters may be characterized into conductor properties, geographical properties, and weather environmental conditions. A sensitivity analysis was carried out to assess the effect of wind speed, wind direction, and ambient temperature on the calculated thermal rating. The analysis was conducted such that one parameter at a time was varied while the other parameters were maintained constant. The effects of selected input of weather conditions on conductor thermal ratings, specific to Dubai are shown in Figures 5.8. From Figure 5.8(a), it can be seen that an increase in ambient temperature to the maximum experienced has a significant de-rating effect on the lines. The thermal rating decreases from 4,493 Amps at 10 ℃ to 3,190 Amps at 47.5 ℃. At 47.5 ℃, the de-rating is around 29% compared to operation at 10 ℃. Figure 5.8(b) shows that a relatively small initial increase in wind speed results in a very marked increase in the line rating, e.g. from 0 m/s to 2 m/s, there is nearly a four-fold increase in the rating. The thermal rating increases from 1,075 Amps at a wind speed of 1 m/s up to 6,167 Amps at a wind speed of 14 m/s. Figure 5.8(c) confirms that the maximum thermal rating occurs when the wind direction is perpendicular to the line, i.e., 4,055 Amps.

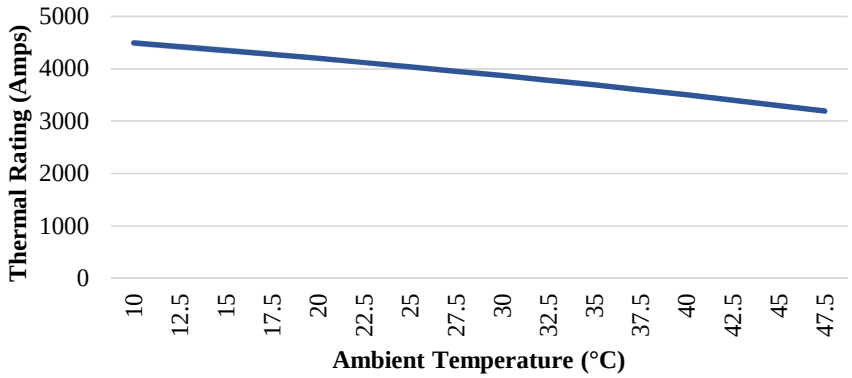

(a) Effect of ambient temperature (constant: wind speed 1 m/s and direction 20◦)

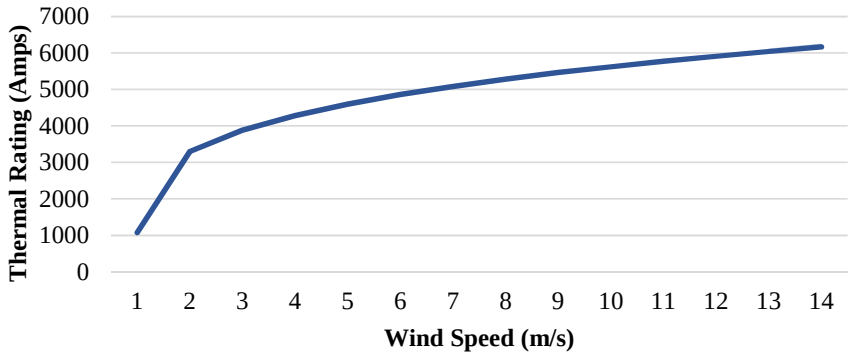

(b) Effect of wind speed (constant: ambient temperature at 45°C and wind direction 20°)

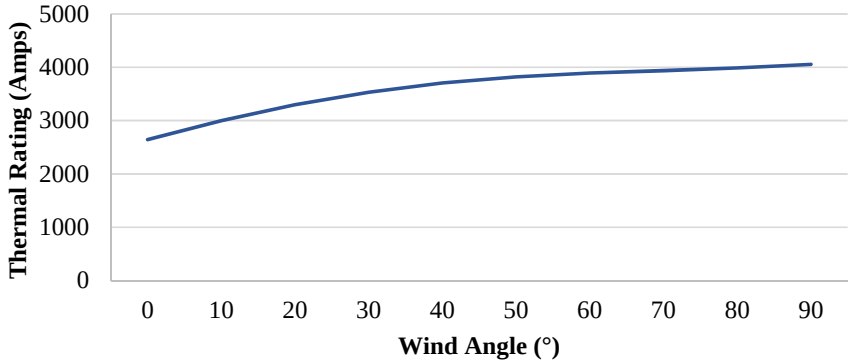

(c) Effect of wind direction (constant: ambient temperature at 45°C and wind speed 1 m/s)
Figure 5.8: Effect of weather changes on line thermal rating

A sensitivity analysis shows that different weather parameters have a different impact on line thermal ratings, and ranked from lowest to highest, these are ambient temperature, wind

direction, and wind speed. The maximum current-carrying capacity of the power transmission line is decreased by high temperatures or low wind speeds.

As future work, more studies could be elaborated on the correlation between effect of ambient temperature on both system demand and thermal rating.

5.4.2 Probabilistic Distribution Function (PDF) of thermal rating

As weather conditions change, the thermal rating of a transmission overhead line also changes. Figures 5.9 show the hourly thermal rating for 'Yew' and 'Zebra' conductor lines, respectively, calculated over a one-year period and based on the data set of ambient temperature, wind speed and wind direction for 2013. The calculations show that the line ratings range from 2,789 Amps to 9,785 Amps for 'Yew' conductor lines, and from 3,017 Amps up to 10,085 Amps for 'Zebra' conductor lines. The mimima of thermal ratings are more frequent during the summer period.

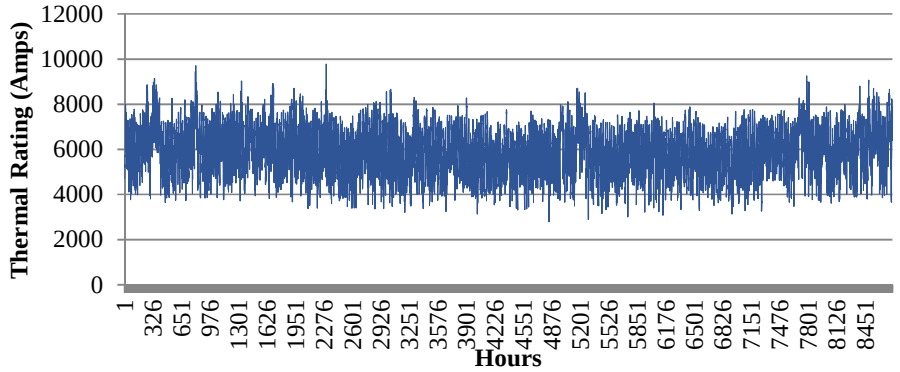

(a) Yew conductor lines

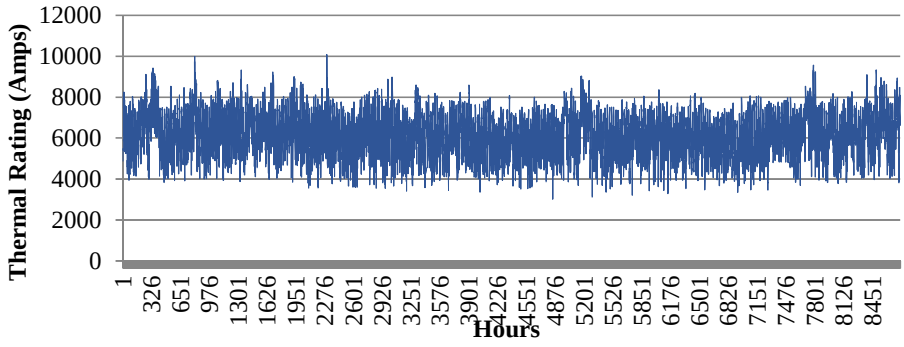

(b) Zebra conductor lines

Figure 5.9: Hourly thermal rating for transmission lines

Thermal ratings were represented by a time-varying thermal rating probabilistic model as illustrated in Figure 5.10. It can be seen that the most frequent range of thermal rating for a 'Yew' conductor is 5,340 - 5,369 Amps, which occurs for 104 hours during a year (probability of 0.0119). On the other hand, the most probable thermal rating for a 'Zebra' conductor is 6,570 - 6,599 Amps, occurs for 111 hours during a year (probability of 0.012671). In comparison with that used in DEWA, for 'Yew' the adopted thermal rating is 3,290 Amps, 3,590 Amps and 3,880 Amps for summer, spring/autumn and winter respectively. For 'Zebra', the used thermal rating is 3,550 Amps, 3,825 Amps and 4,100 Amps for summer, spring/autumn and winter respectively.

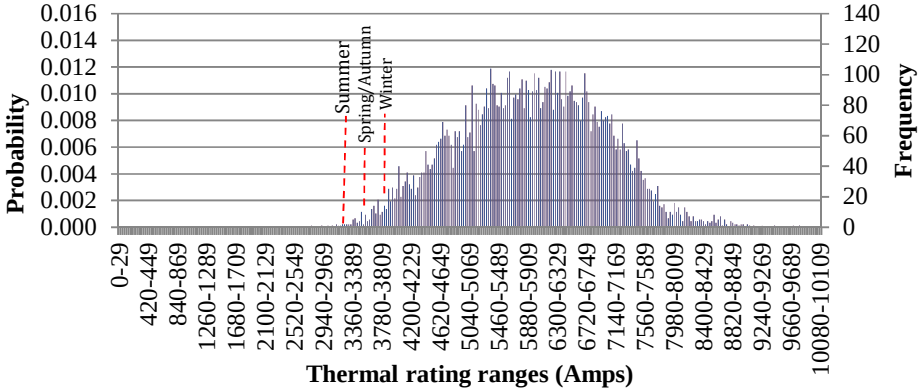

(a) Yew conductor lines

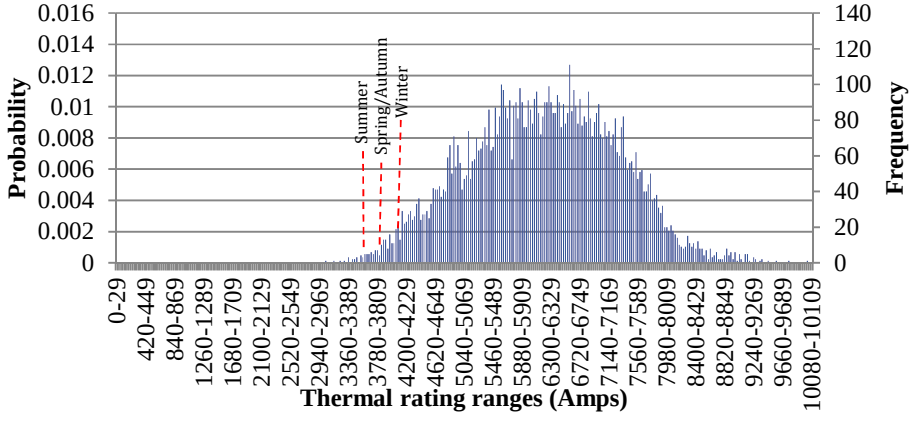

(b) Zebra conductor lines

Figure 5.10: Frequency and Probabilistic Distribution Functions for the resultant thermal ratings

5.5 Multiple load flow simulations

In the evaluation of the LORI proposed in this research, the controlled multiple study facility was conducted using the C++ programming code. NEPLAN Programming Library (NPL) was used to automate network modelling and contingency simulation.

Generating units that are assigned to supply base load are called on to operate at a continuous output level, while peaking generating units are called on to operate according to their priority ranking order if additional power is required for supplying system demand. To operate the system securely, the system needs to maintain an additional margin of flexibility (in terms of reserve) to be maintained. The amount of primary reserves to be maintained by DEWA as of year 2011 is 130 MW based on the size of largest generating unit present in interconnected system and interconnection codes. In the simulation for the DEWA system, the slack bus is maintained in at the location of one of the generators at B power station.

A programming code with around 55,000 lines, was developed to execute the flow charts shown in Figure 4.4 and Figure 4.5. For each of the modelled study cases, the system loads were adjusted to within the targeted range of system demand, and generators were connected based on their ranking order, while keeping the slack bus generation to within +/- 130 MW.

For a system with N_L lines and N_D system demand levels, the total required number of studies is $N_s = N_D N_L (N_L + 1)/2$. For the Dubai system for single year 2011, with an adopted 43 system demand levels and 301 lines, the total required number of simulations is therefore nearly 2 million. To expedite the simulation process, parallel computers were set up. The study states in each system demand level of a study of years 2011 and 2015, in Dubai system case studies with 301 transmission lines include (i) one normal state (no line failure), (ii) 'N-1' contingency states for all 132 kV and 400 kV lines, equivalent to N_l (i.e. 301), and (iii) 'N-2' contingencies

requiring a number of states equivalent to $\frac{(N-1)N}{2}$ (i.e. 45,150). For 2021, due to the installation of further planned power stations and network modifications, the study states increased to include, in addition to one normal state, 308 first-order states and 47,278 second-order states.

Using the NPL, each simulation set was carried out in approximately 650 hours; using parallel workstations. Table 5.6 shows the simulation numbers and duration for all cases.

Table 5.6: Computation burden for Dubai system

Year	No. Lines	No. system demand levels	Intact system		N-1 (i.e. [illegible])		N-2 (i.e. [illegible])		Overall (i.e. [illegible])	
			Simulation No.	Simulation Duration (hrs)	Simulation No.	Simulation Duration (hrs)	Simulation No.	Simulation Duration (hrs)	Simulation No.	Simulation Duration (hrs)
2011	304	43	1	0.1	304	2	46,056	475	1,993,523	477
2015	304	56	1	0.1	304	2	46,056	642	2,596,216	644
2021	308	65	1	0.1	308	2	47,278	810	3,093,155	812
2021 'stressed'	310	76	1	0.1	310	2	47,278	1115	3,616,764	1117

5.6 The Line Overload Risk Index (LORI) calculation for the Dubai transmission system

Four cases of actual and forecasted years have been studied to show the impact of uncertainties of system demand, line faults, maintenance outages, and variable thermal ratings on the reliability of transmission systems. These cases were defined for years 2011, 2015, and 2021 and the so-called 'stressed' system for the year 2021. However, to simplify the particular only, the results for 2011 and the 'stressed' 2021 systems, without maintenance results, are presented here.

5.6.1: The Line Overloading Risk Index (LORI) calculation for system study for 2011

Following the methodology outlined in the previous chapter, the loadings of all 400 kV lines were calculated for the year 2011. Results for selected lines connecting (i) power stations

(Figure 5.11), (ii) power stations to load stations (Figure 5.12), and (iii) load stations (Figure 5.13) are shown for (i) the intact system, (ii) all 'N-1' contingencies, and (iii) all 'N-2' contingencies for all 43 system demand levels. From Figure 5.11, it can be seen that the loadings on the 400 kV lines that interconnect power stations generally increases as the system demand increases, due to the effect of the generator output changes to maintain the slack bus within the required range. However for the 400 kV lines that connect power stations to load stations (Figure 5.12) or that connect load stations (Figure 5.13), it was observed that loadings increases following increase in the system demand. Furthermore, the rate of line loading increases progressively for 'N-1' and 'N-2' contingencies. The highest loading was found to be on line K-N with a maximum loading of 1,565 Amps in the intact system, 2,027 Amps in the 'N-1' contingencies, and 2,375 Amps in the 'N-2' contingencies.

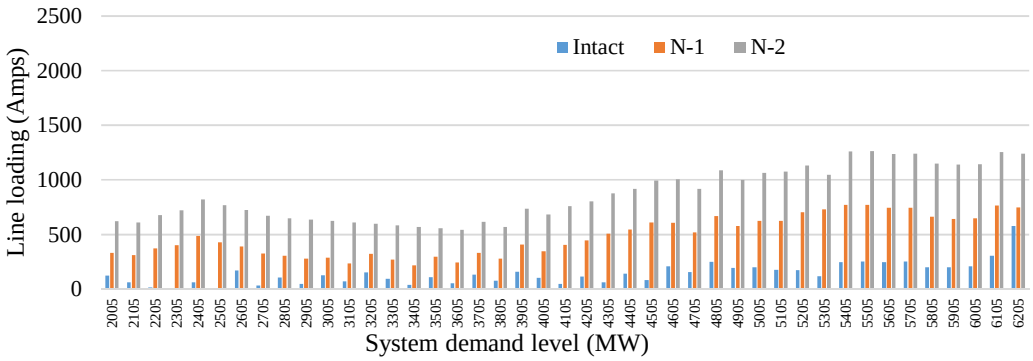

Figure 5.11: Loadings on 400 kV D - B line connecting power stations for different system demands and different system contingency for 2011

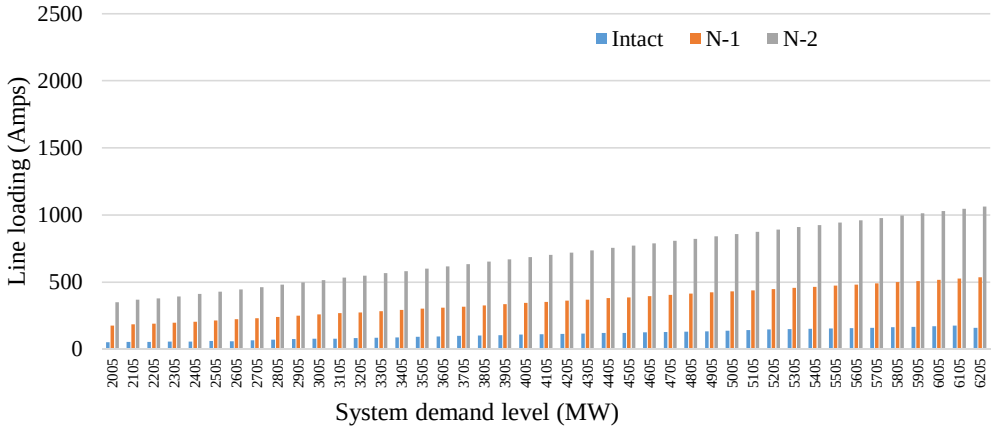

Figure 5.12: Loadings on 400 kV M - F line connecting power station to load stations for selected system demands and different system contingency for 2011

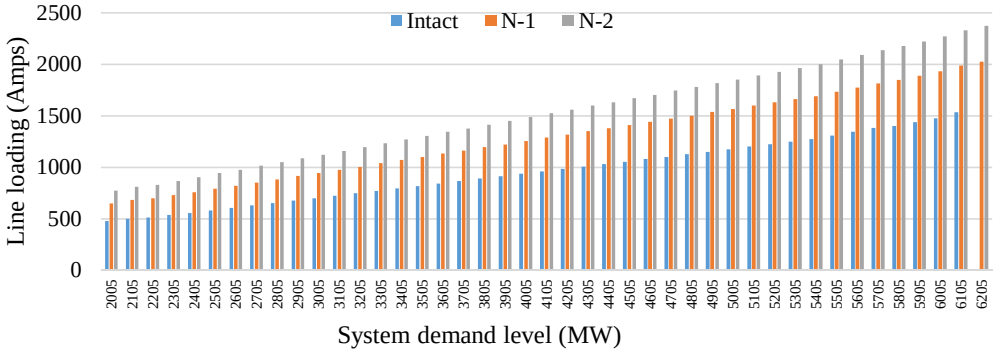

Figure 5.13: Loadings on 400 kV K – N line connecting load stations for selected system demands and different system contingency for 2011

From these results, the probability distributions of line loadings were calculated. The results for one sample line of three categories of lines i.e. the D - B generator-generator line, the M - F generator-load line and the K - N load-load line are shown in Figures 5.14, 5.15 and 5.16, respectively, for the intact system, ‘N-1’ contingencies, and ‘N-2’ contingencies. From the figures, it can be seen that the probability of line loadings due to ‘N-1’ contingency is lower than that in the intact system; and is significantly further lower than that due to ‘N-2’ contingency. This is as expected due to the different probability assigned to the contingencies. Also, it can be seen that line loadings significantly increasing due to contingencies.

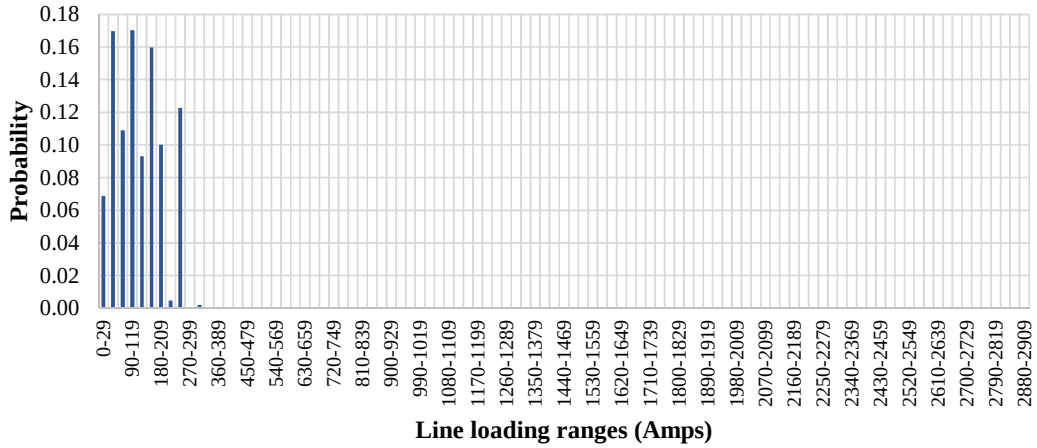

(a) During intact system

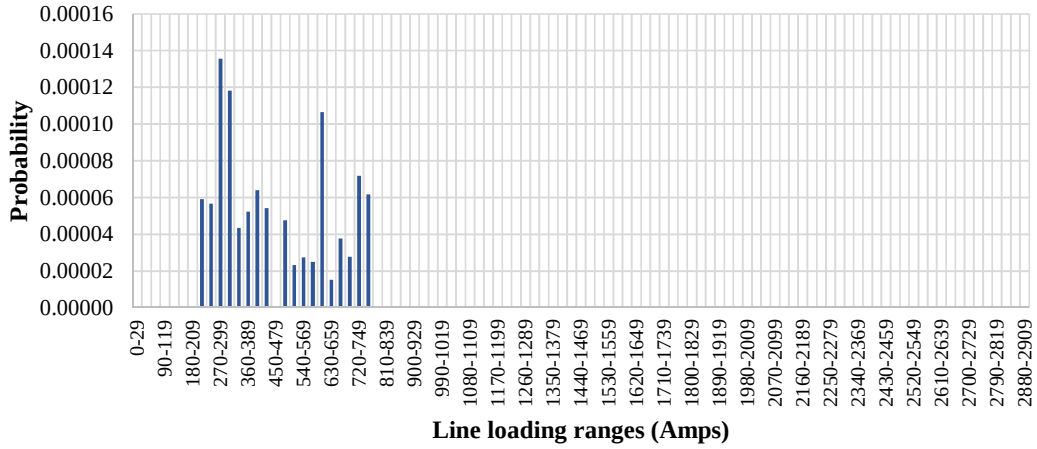

(b) During 'N-1'

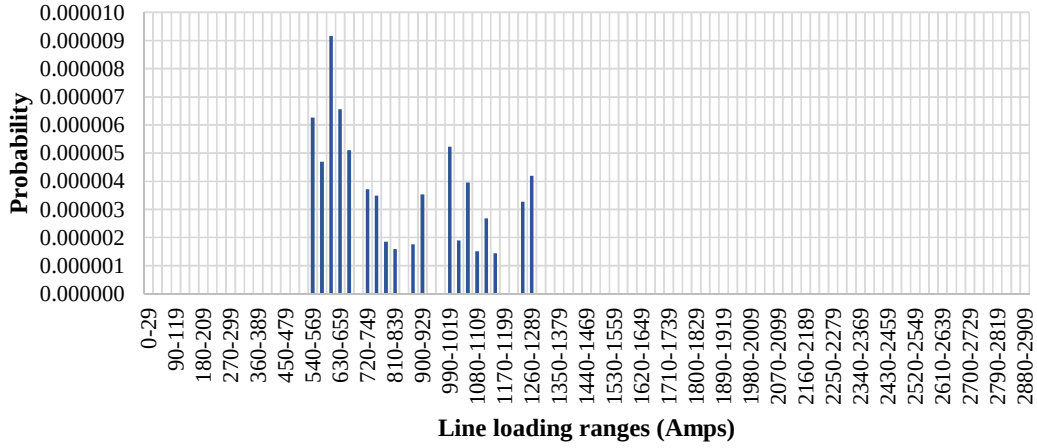

(c) During 'N-2'

Figure 5.14: Line loading PDFs for D - B Generator-Generator line for the year 2011

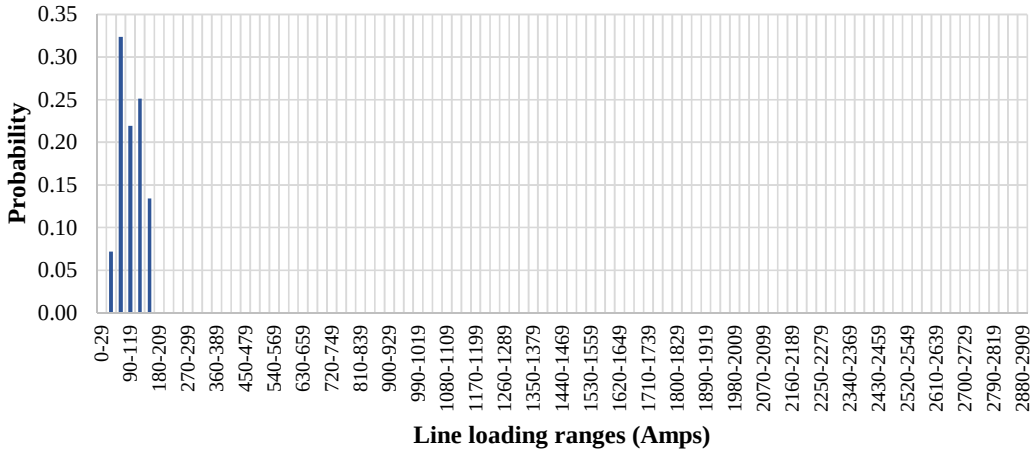

(a) During intact system

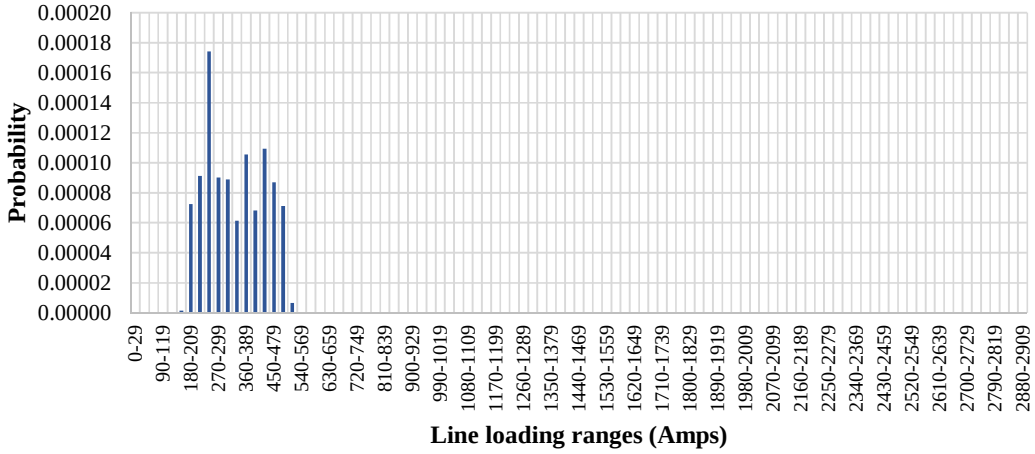

(b) During 'N-1'

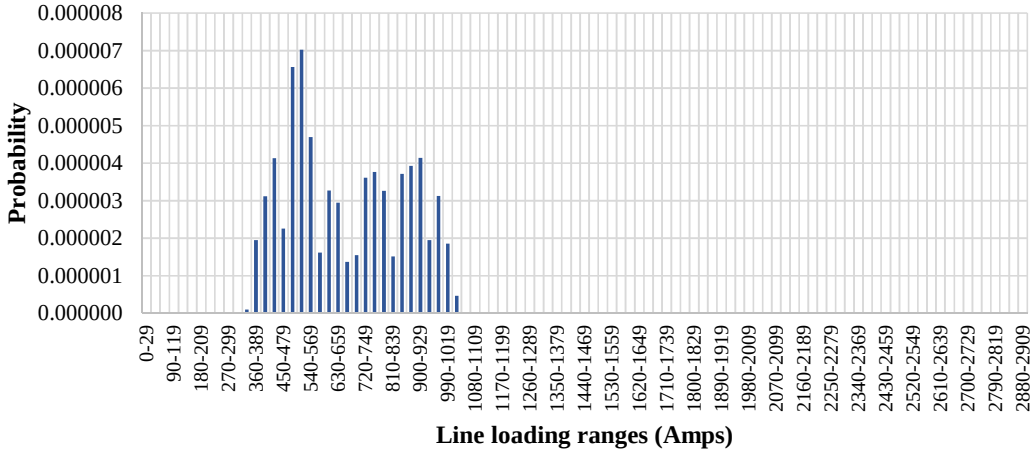

(c) During 'N-2'

Figure 5.15: Line loading PDFs for M - F Generator-load line for the year 2011

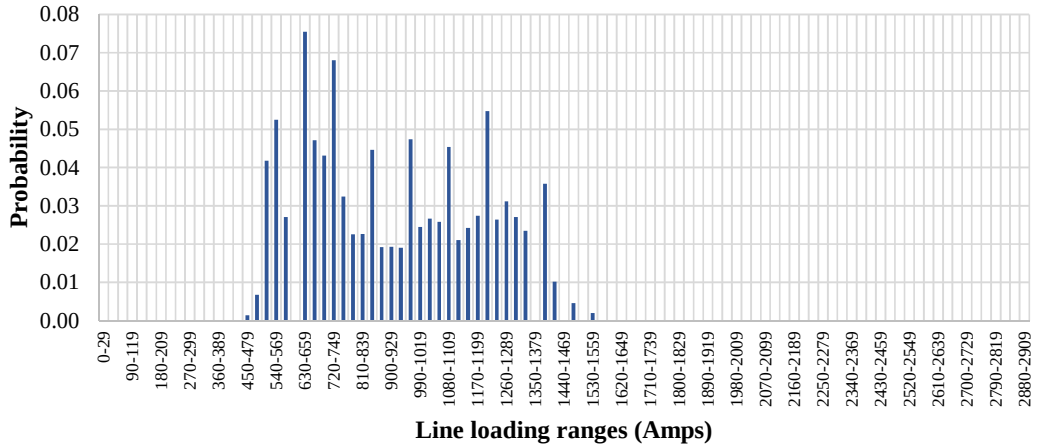

(a) During intact system

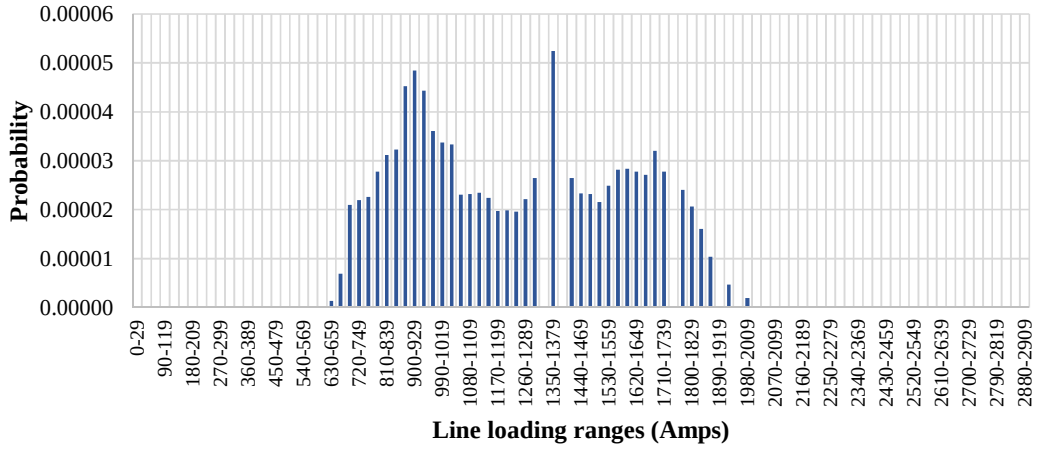

(b) During 'N-1'

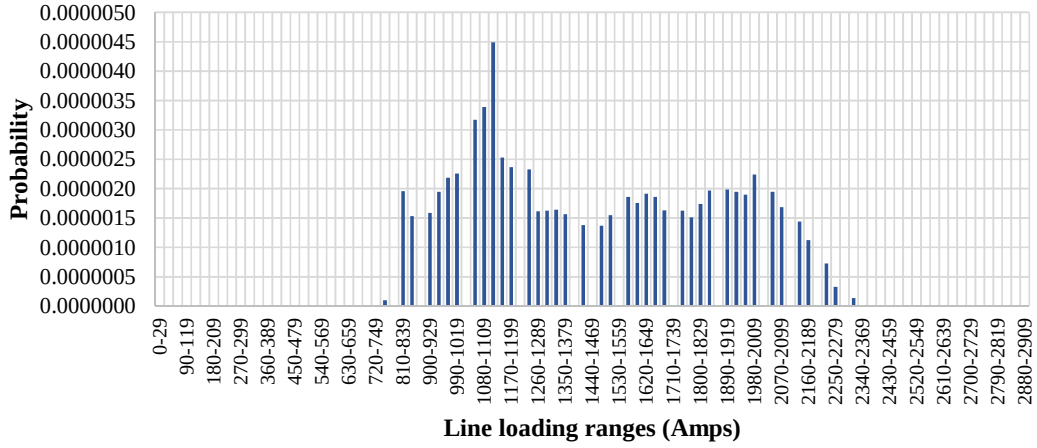

(c) During 'N-2'

Figure 5.16: Line loading PDFs for K – N load-load line for the year 2011

Figure 5.17, Figure 5.18, and Figure 5.19 show the combined PDFs for line loading and thermal rating (Yew type conductor) for three types of lines (i.e. with respect to connection to either generator or load buses), namely, the D - B generator-generator line, M - F generator-load line, and K - N load-load line, respectively for the intact system, 'N-1' contingencies, and 'N-2' contingencies. It can be seen in Figure 5.18 that under intact conditions, as expected, there is a considerable margin between the maximum line loading and the minimum thermal rating, which found to be at least 2,535 Amps. The line loading for all 'N-1' conditions increases, and it is noted that the maximum loading moves closer towards the minimum rating, that is, the margin was reduced considerably (i.e. to 2,046 Amps). For the 'N-2' contingencies, the margin was reduced further (i.e. 1,552 Amps). Also as expected, the period of minimum margin is approached during the hottest summer period. Similar behaviour is noticed for other transmission lines.

Hourly system demands and hourly thermal ratings were sorted, based on 'system demand' from largest to lowest, in order to find the equivalent thermal rating for each system demand level (previously discretised with 100 MW bins). The minimum thermal rating was selected here (instead of the maximum and average value) to take into account the worst case thermal rating for each system demand level, as shown in Table 5.7. This will be used later to find out the severity of the line loadings of the transmission lines in each system demand level to calculate the LORI.

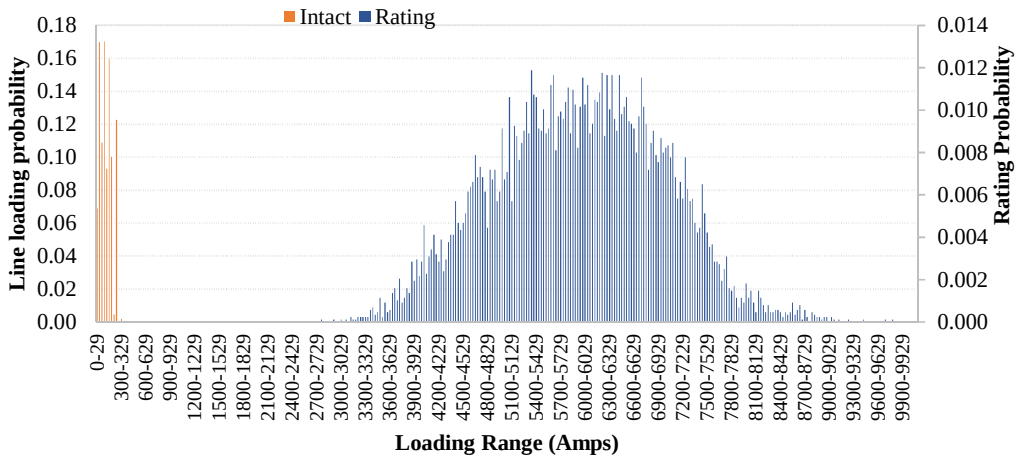

(a) During intact system

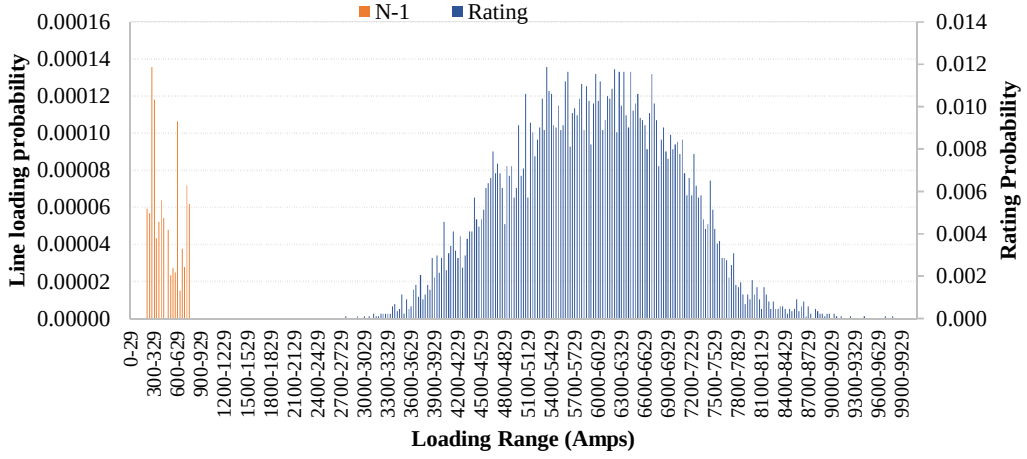

(b) During 'N-1'

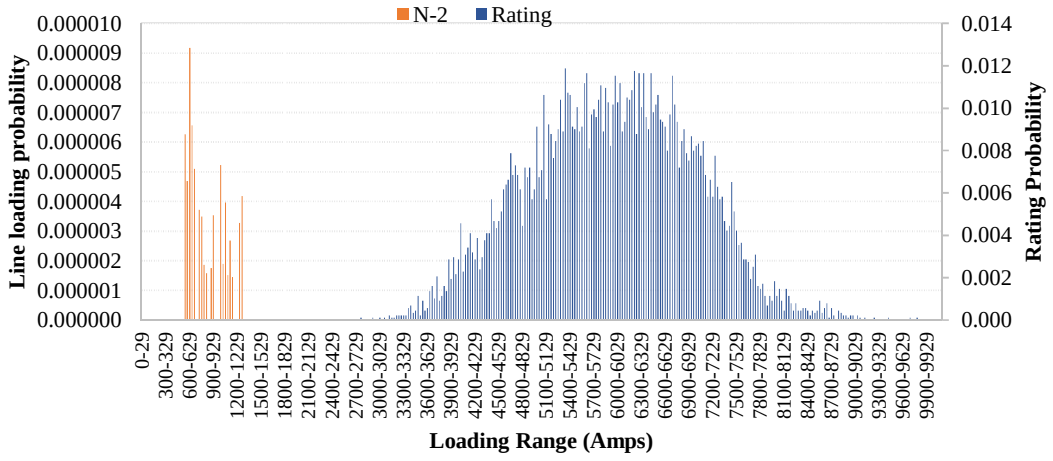

(c) During 'N-2'

Figure 5.17: Line loading and rating PDFs for D - B generator-generator line for the year 2011

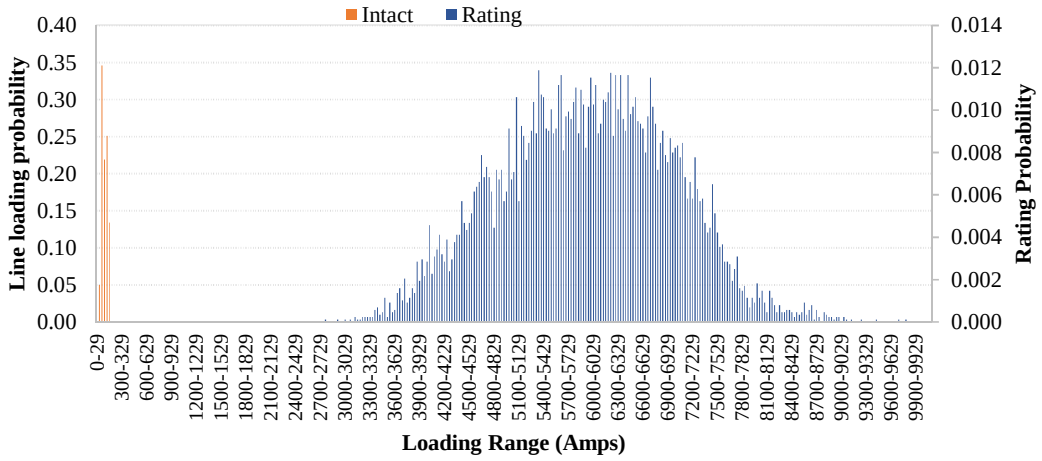

(a) During intact system

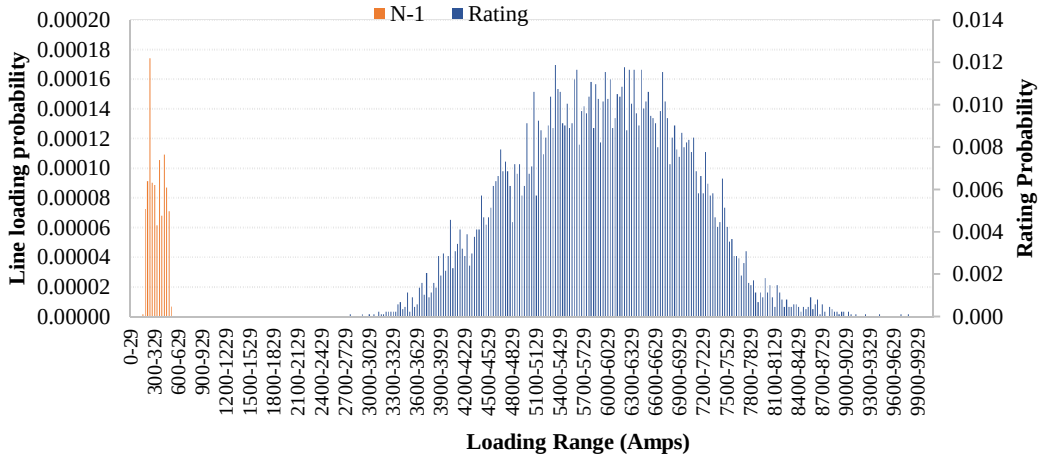

(b) During 'N-1'

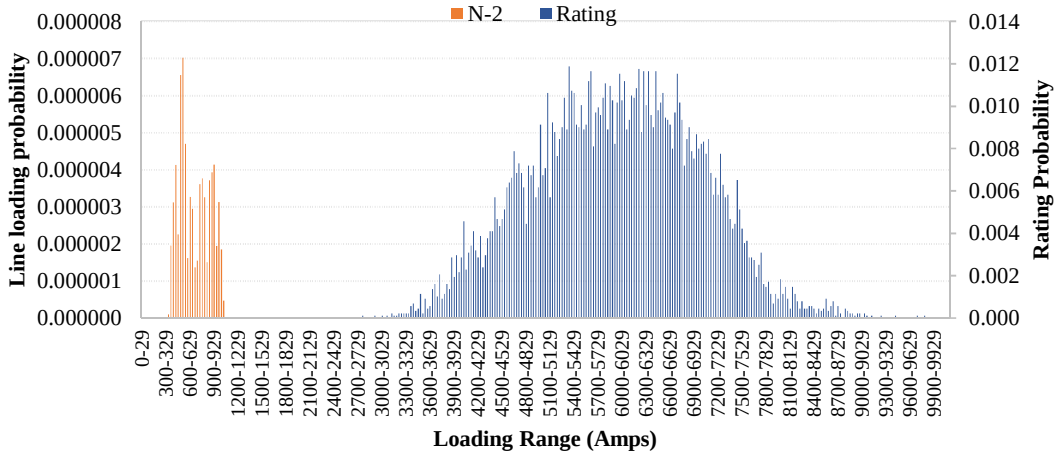

(c) During 'N-2'

Figure 5.18: Line loading and rating PDFs for M - F Generator-load line for the year 2011

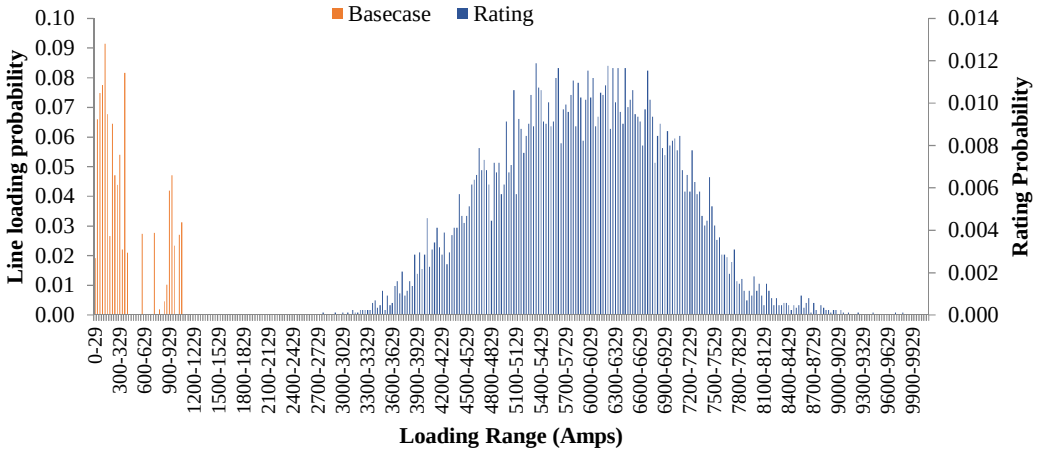

(a) During intact system

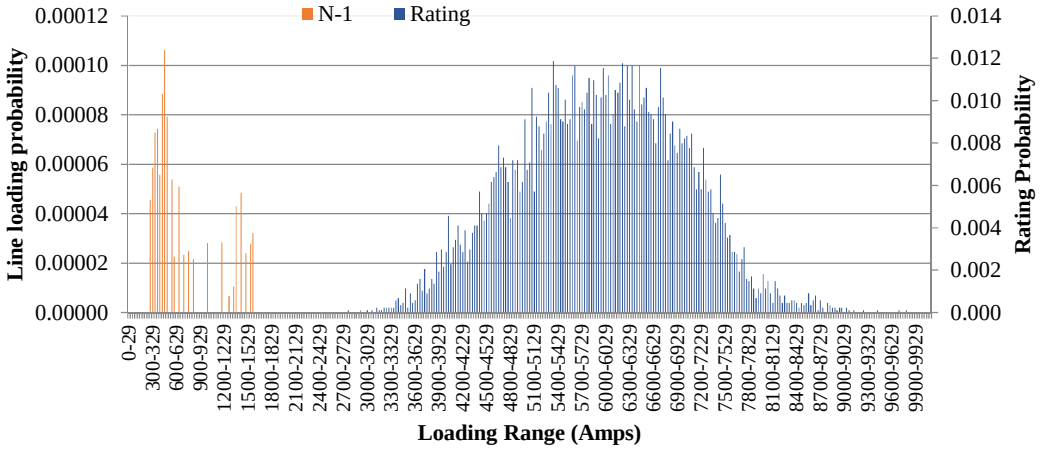

(b) During 'N-1'

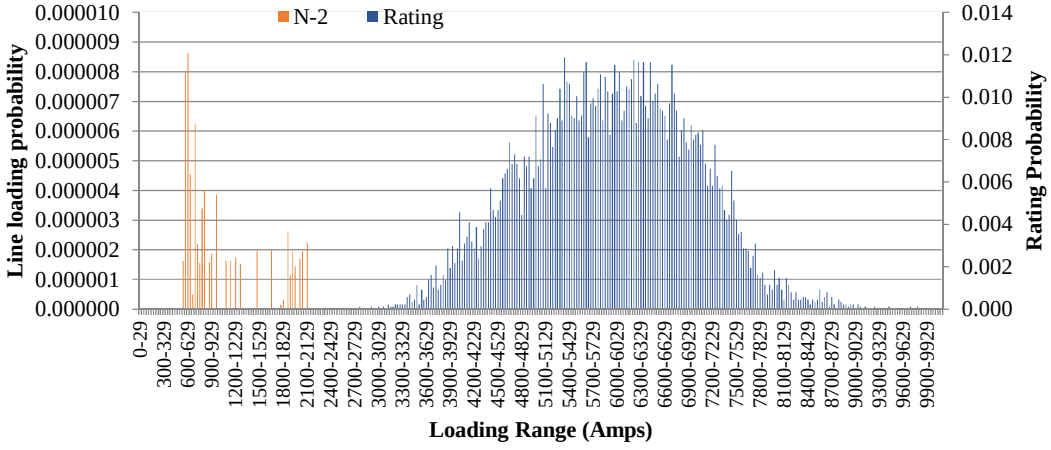

(c) During 'N-2'

Figure 5.19: Line loading and rating PDFs for K - N load-load line for the year 2011

Table 5.7: Thermal ratings for each of the system demand ranges

System Demand Ranges	Max	Min	Average	System Demand Ranges	Max	Min	Average
6205-6104	6873	4666	5845	**4005-3904**	8660	3559	5876
6105-6004	7743	3441	6110	**3905-3804**	8637	3636	5938
6005-5904	8115	3744	6104	**3805-3704**	9785	3669	6061
5905-5804	7699	3160	6053	**3705-3604**	7802	3365	5842
5805-5704	7660	3546	6126	**3605-3504**	8370	3410	5945
5705-5604	7974	2789	6058	**3505-3404**	8727	3201	6057
5605-5504	8148	3081	5947	**3405-3304**	8641	3374	6057
5505-5404	8507	3487	5943	**3305-3204**	8924	3506	5931
5405-5304	8096	2917	5914	**3205-3104**	9444	3662	6156
5305-5204	8299	3250	5933	**3105-3004**	9710	3613	6253
5205-5104	8160	3674	5838	**3005-2904**	9268	3406	6274
5105-5004	8547	3132	5836	**2905-2804**	8870	3492	6293
5005-4904	8701	3442	5757	**2805-2704**	9040	3724	6013
4905-4804	7956	3214	5629	**2705-2604**	8880	3732	6069
4805-4704	7912	3334	5662	**2605-2504**	8977	3377	5957
4705-4604	8022	3003	5551	**2505-2404**	8954	3911	5906
4605-4504	7938	3525	5693	**2405-2304**	8595	3820	5814
4505-4404	7984	3397	5681	**2305-2204**	9148	3650	5698
4405-4304	8705	3276	5726	**2205-2104**	8906	3737	5671
4305-4204	8681	3264	5808	**2105-2004**	8556	4643	6352
4205-4104	8135	3283	5549	**2005-1904**	5707	5707	5707
4105-4004	8565	3481	5576				

Figure 5.20 shows the hourly line loading for one of the load-load lines of K - N, and it can be seen clearly that no overloading occurs for the intact system, or for the ‘N-1’ and ‘N-2’ outages.

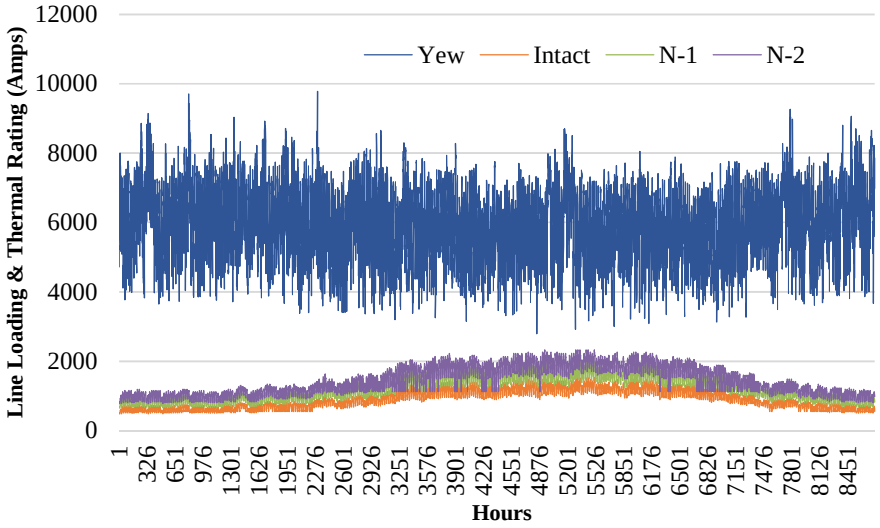

Figure 5.20: Hourly line loadings and thermal ratings for K-N load-load line for the year 2011

It can be noted as well that both line loading and its equivalent thermal rating are variable quantities, and depending on the extent of the overlap of these two distributions, associated risks occur. The selected risk index known as the LORI is calculated as the product of the probability of the loading of a line and the severity of the line loading, as shown previously in Chapter 4. The results of this extensive systematic study show that under all studied conditions, no line loading reaches 90% of its rating and the severity of line loading, $Sl_{(i,j)}$, is always zero for this case. Consequently, the LORI as expressed in Equation 4.12 for this study case is also zero.

By applying the developed methodology, the loadings of all 400 kV lines were calculated using NEPLAN for the years 2015 and 2021 for (i) the intact system, (ii) all 'N-1' contingencies, and (iii) all 'N-2' contingencies for all discretised system demand levels. It was found that no overloading occurred and thus the LORI was found to be zero. Hence, the system of 2021 was

required to be further stressed, by increasing the system demand level close to full generation capacity.

5.6.2: Evaluating the Line Overload Risk Index (LORI) for the 'stressed system' for 2021

The results of the simulations for the 'stressed' 2021 system show that some overloadings were resulted, specifically for lines of D – C, E – R, D – R and P – R due to 'N-1' contingencies. Further overloading values were observed on these lines due to 'N-2' contingency. Line P – R, as an example, was loaded to maximum of 2,856 Amps, 3,474 Amps and 3740 during intact condition, 'N-1' contingency and 'N-2' contingency, respectively. This line exceeded the relevant thermal rating. Figure 5.21 and Figure 5.22 shows probability of line loadings for two 400kV lines i.e. D – C and P – R, respectively.

Furthermore, probability of overloading of one of line, for example D – C, was calculated to occur 37 hours in a year (i.e. probability of 0.000004224) due to 'N-1' and 160 hour (i.e. probability of 0.00000018265) due to 'N-2' contingency.

Figure 5.23 and Figure 5.24 demonstrate the combined PDFs for the line loading and thermal rating for the same lines and contingency conditions. As can be seen in Figure 5.23, under intact conditions there is a margin between the maximum line loading and the minimum thermal rating, which was found to be 157 Amps. The line loading due to 'N-1' conditions increases, and the highest line loading moves further towards the minimum rating, and overlapping between the two PDFs occurs. Under 'N-2' contingencies, the margin is further reduced and more overlapping occurs.

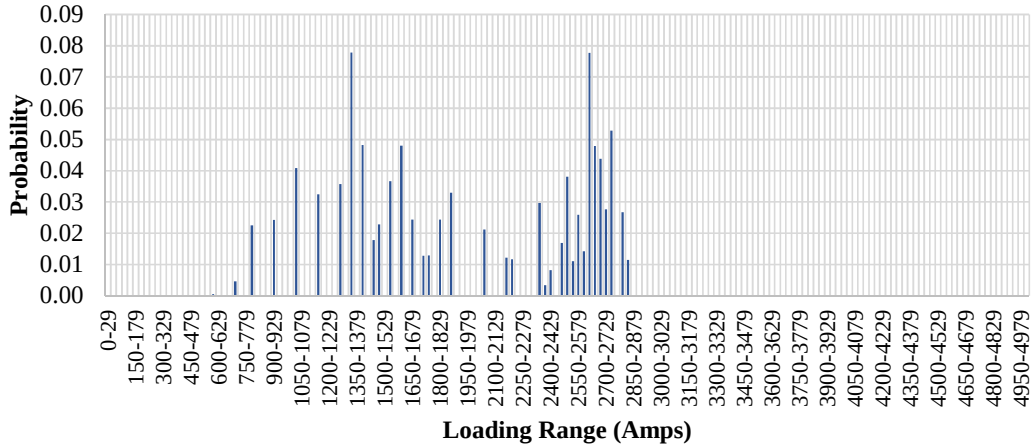

(a) During intact system

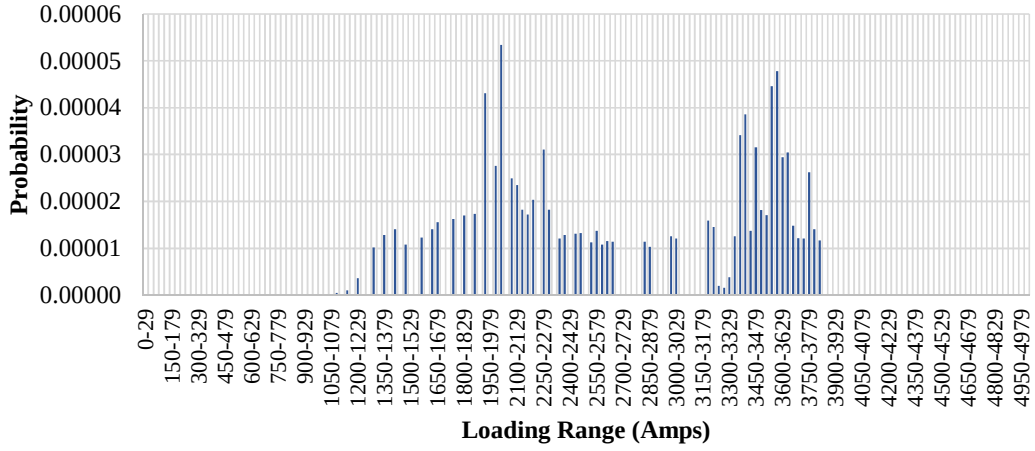

(b) During ‘N-1’

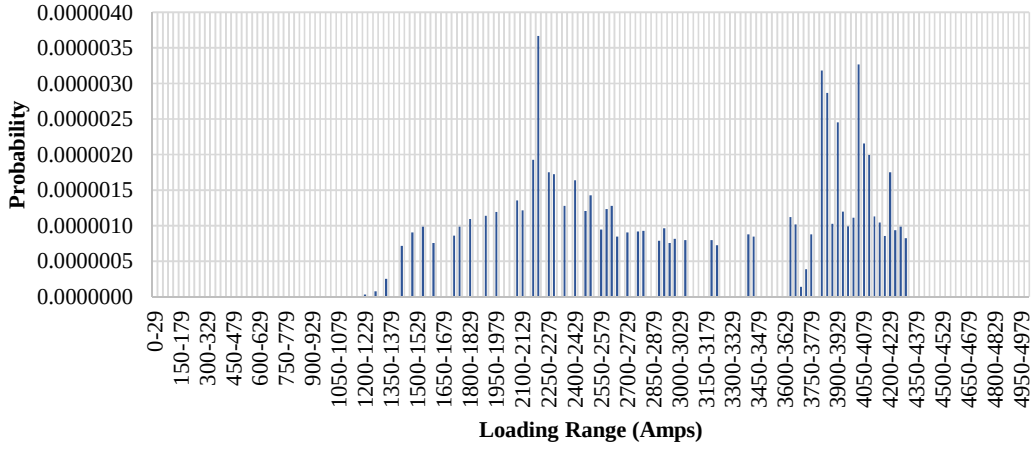

(c) During ‘N-2’

Figure 5.21: Line loading PDFs for D - C Generator-Generator line for the ‘stressed’ year 2021

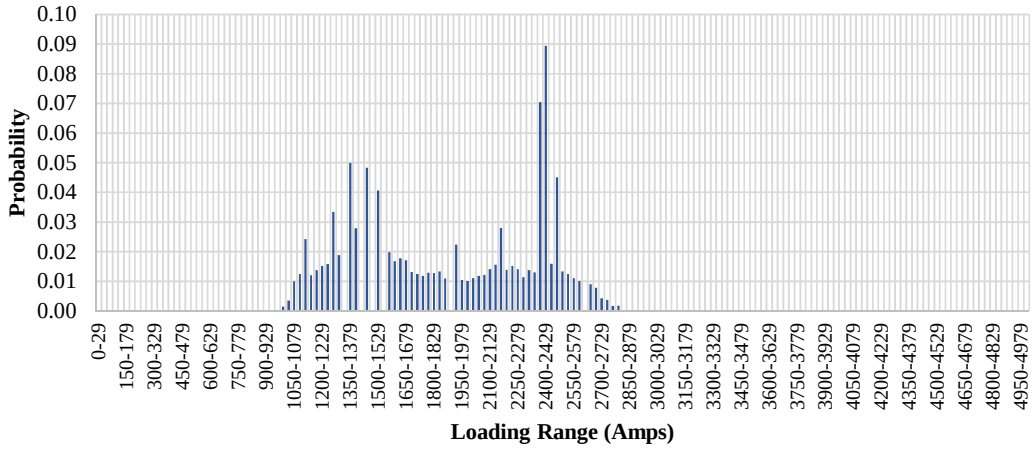

(a) During intact system

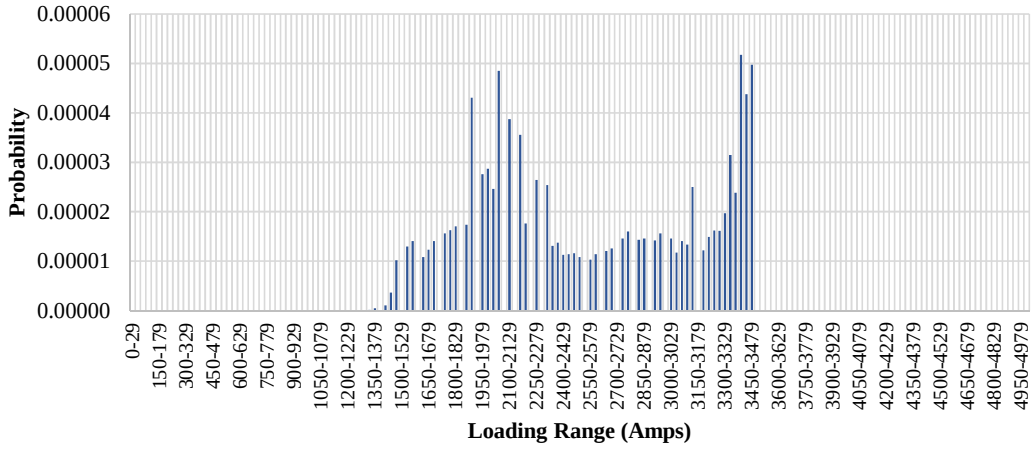

(b) During 'N-1'

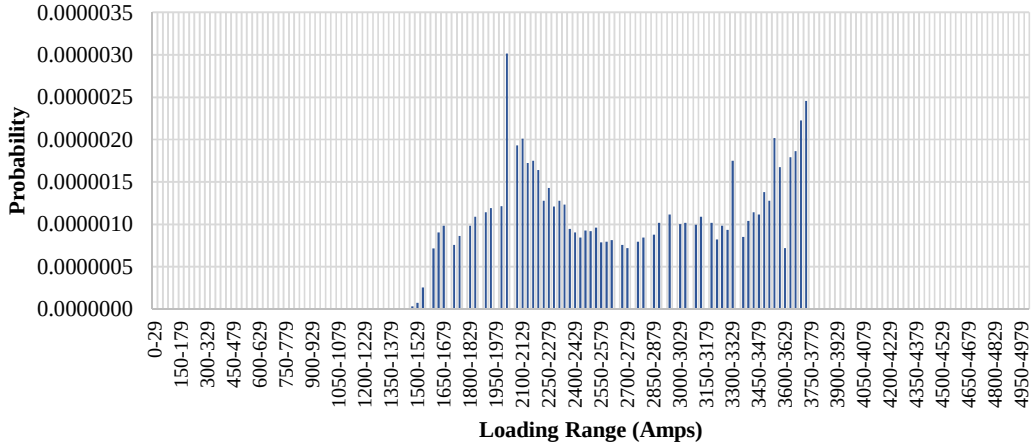

(c) During 'N-2'

Figure 5.22: Line loading PDFs for P - R load-load line for the 'stressed' year 2021

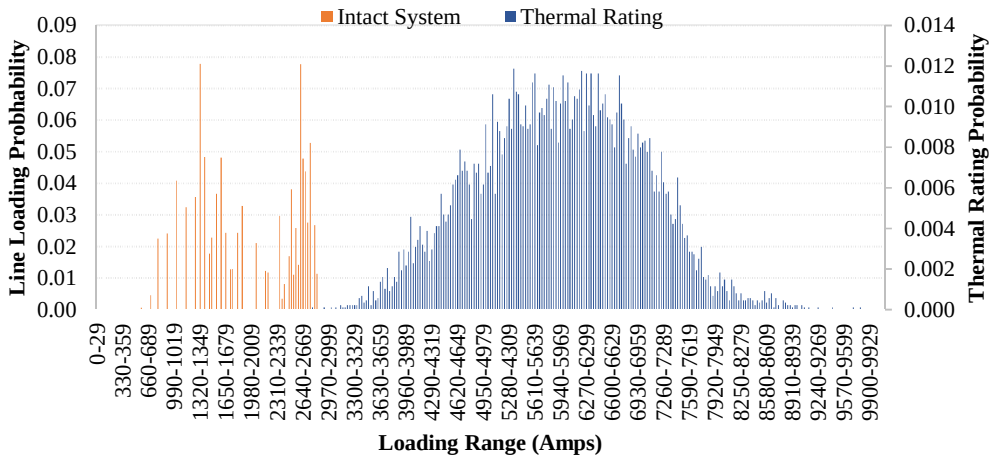

(a) During intact system

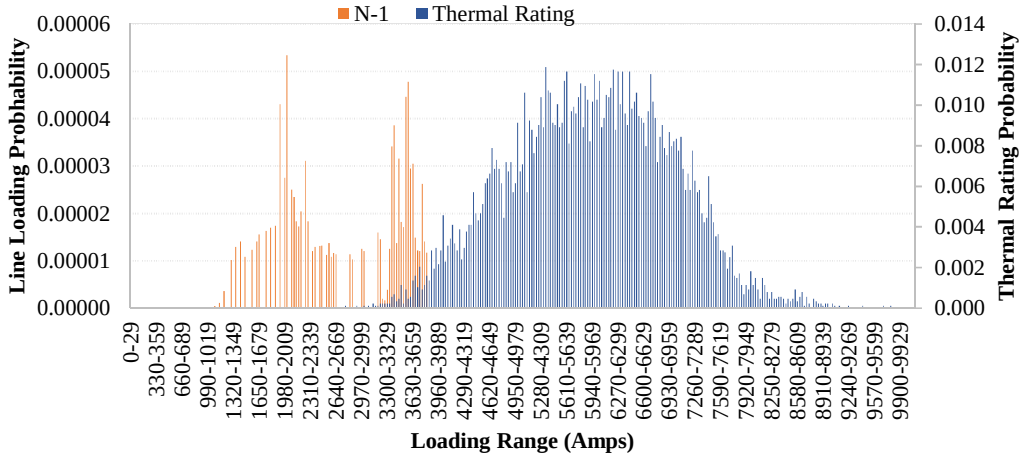

(b) During 'N-1'

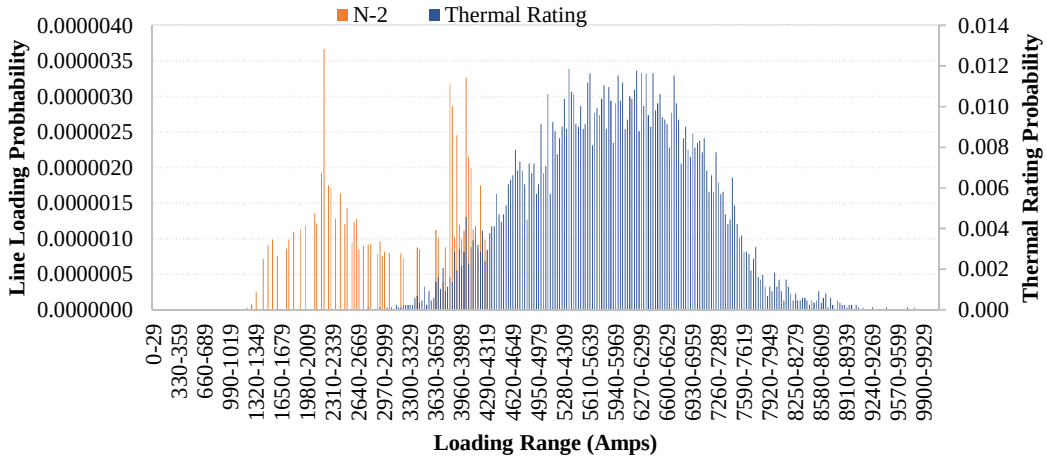

(c) During 'N-2'

Figure 5.23: Line loading and rating PDFs for D - C generator-generator line for the 'stressed' year 2021

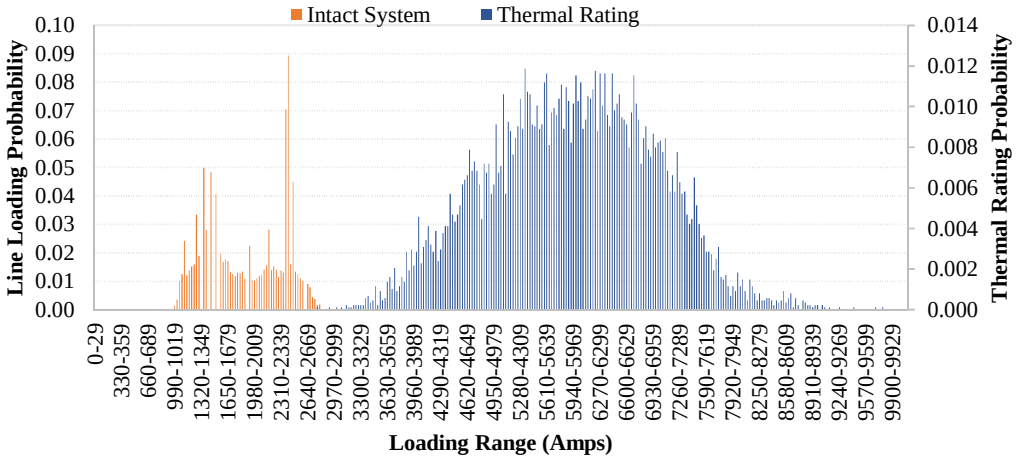

(a) During intact system

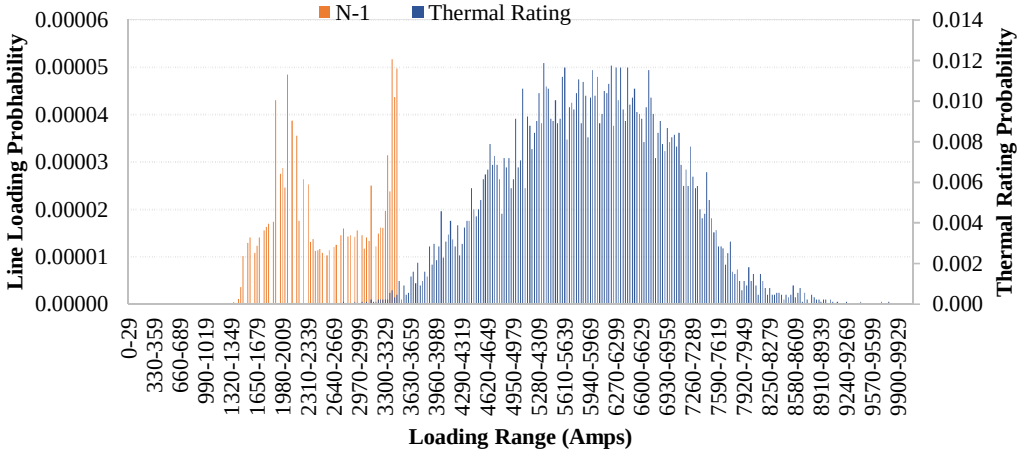

(b) During 'N-1'

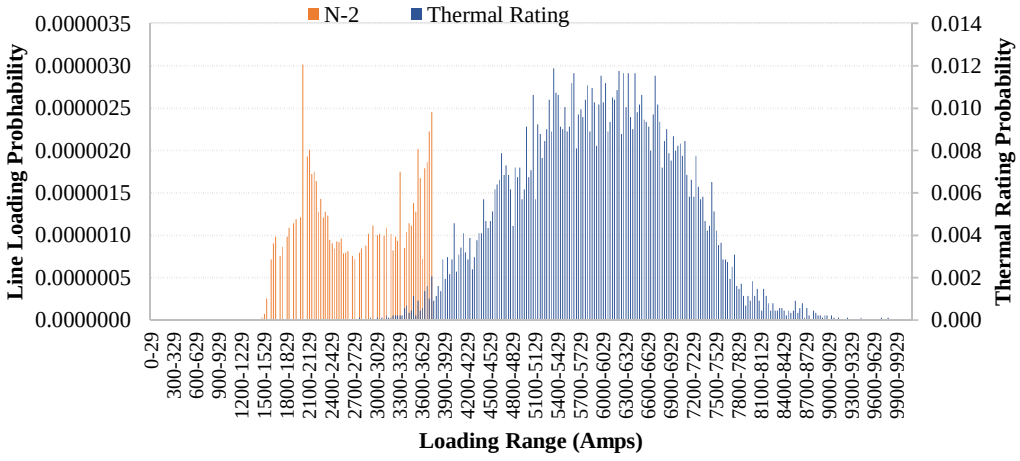

(c) During 'N-2'

Figure 5.24: Line loading and rating PDFs for P - R load-load line for the 'stressed' year 2021

Although it may be observed that some lines reveal an area of overlapping between the PDFs of line loading and of thermal rating; this in itself does not necessarily mean that overloading occurs because of the noncoincident pairing of line loading and line thermal rating rating events. For example, when 'zooming in' on the overlapping area for one of the lines (e.g. P – R) as shown in Figure 5.25, it can be seen that a loading range of 2,760 – 2,789 occurs for both line thermal rating and line loading, but with a different probability; i.e. it does not necessarily mean that the contradicting events occur at the same time. It was therefore necessary to confirm, manually, the overlapping of the same time series for both line loading and line thermal rating; in order to evaluate the LORI correctly.

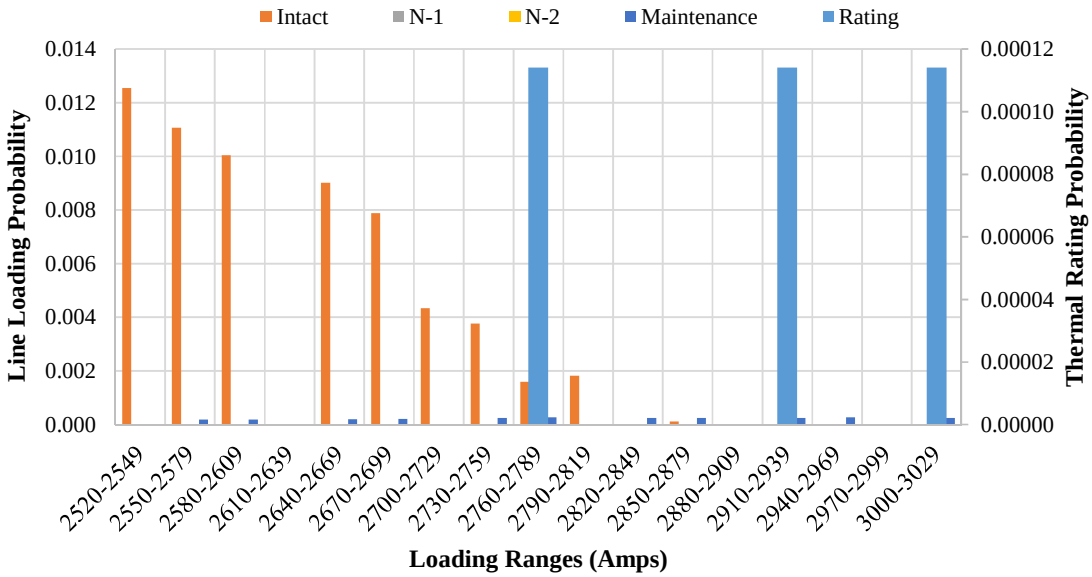

Figure 5.25: Zoomed in an overlapping area

The overloadings for the line P – R is demonstrated to occur and this is illustrated in Figure 5-26, which shows the combined time series for hourly line loading and line rating. From the same figure it can be seen clearly that overloading occurs for 'N-1' and 'N-2' outages. The

LORI was calculated accordingly for the cases where the line loading reaches to 90% of the thermal rating at the same time series.

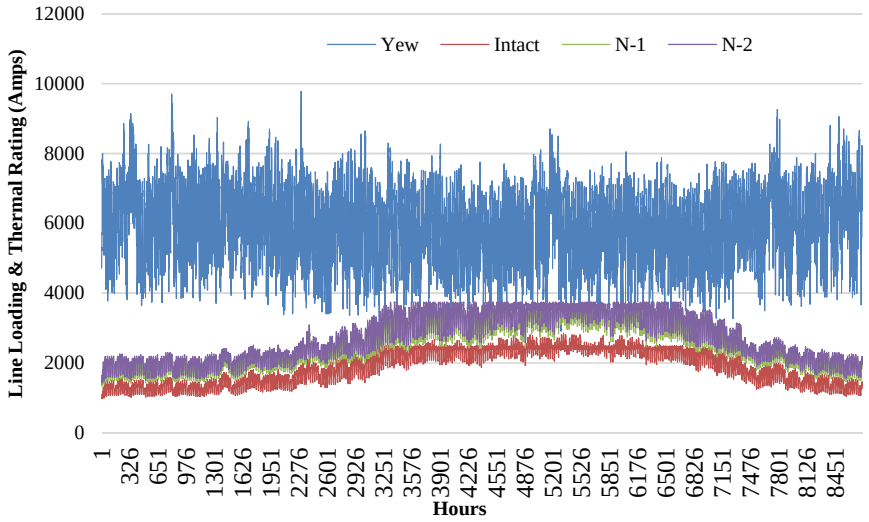

Figure 5-26: Hourly line loadings and thermal ratings for P-R load-load line

The results of this extensive systematic study show that under studied conditions, there were some overloadings on 400 kV lines, i.e., some of the line loading reached more than 90% of its rating and the severity of the line loading, $Sl_{(i,j)}$, is calculated based on the 'continuous' model. The calculated line overloading risk indices as expressed in Equation 4.12 for this case study system are shown in Figure 5-27. It can be seen that line D - C has the largest LORI index due to 'N-1; and 'N-2' contingencies, which would need to be considered during system design and operation. The LORI was used to rank the lines based on both probability and severity. When comparing the result with that obtained in Chapter 3, it can be seen that the LORI is calculated with respect to both probability and severity, while in Chapter 3, it is calculated with respect only to severity.

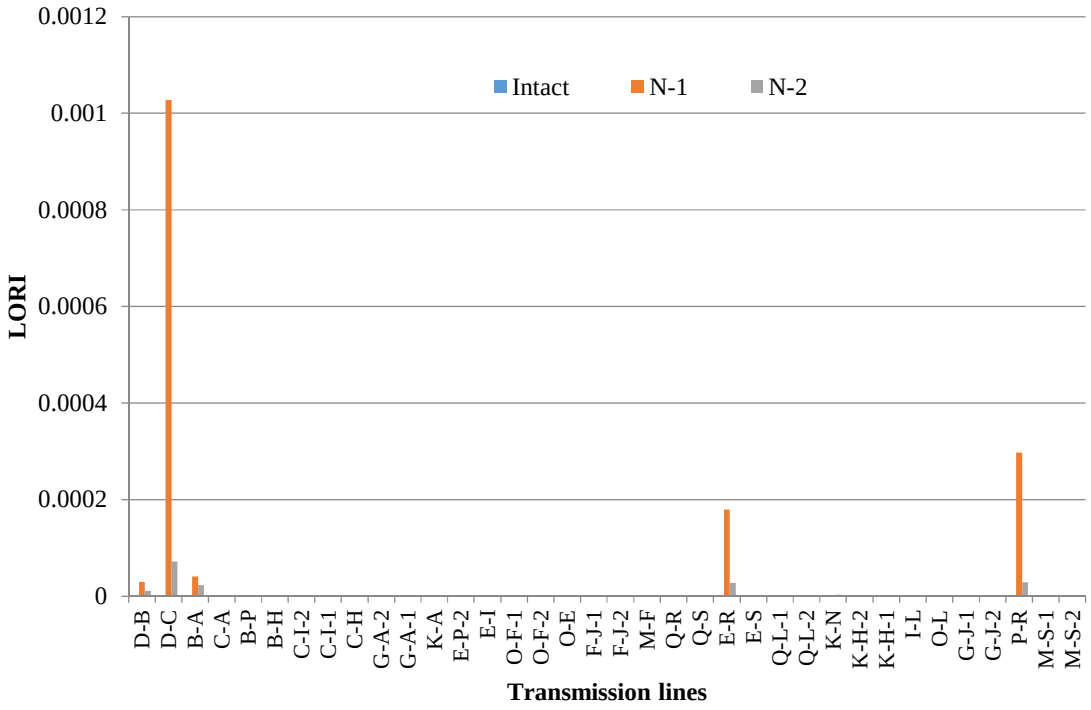

Figure 5-27: LORI calculated for 400 kV lines

5.7 Conclusions

The proposed LORI algorithm was applied to the Dubai transmission system over the period 2011 to 2021 through an extensive systematic evaluation of the steady-state probabilistic performance under hour-by-hour loading levels over a one-year period. The probabilistic performances of 400 kV overhead lines with respect to line loading were shown, where line flow and thermal rating vary. Risk of line overloading may arise from the following uncertainties: (i) hourly variations in system demand, (ii) maintenance outage, and (iii) 'N-x' line outages, taking into account respective variations in the thermal rating.

The hourly thermal rating was calculated for Dubai system transmission overhead lines and was based on an annual set of meteorological data. It is noted that this approach to line rating assessment provides much higher thermal ratings than those derived from the traditional

method as the latter method considers conservative values for wind speed, wind direction and ambient temperature. The probability distribution of the line thermal rating was also calculated and developed.

The power flow simulation results, using NEPLAN commercial load flow software, were utilized to determine the PDFs of loading for each line incorporating actual fault rates. The evaluation algorithm considered intact conditions, for maintenance outage, all ‘N-1’ contingencies, and every combination of ‘N-2’ contingencies. Systematic multiple study execution along with data handling was achieved using a developed C++ based programming code.

The PDFs for the resultant line loadings were compared with the PDFs for the thermal ratings of each line and the LORI was determined. A systematic evaluation algorithm of the LORI of all the lines of the transmission system over one complete annual cycle was calculated. The LORI was calculated based on the probabilistic method that determines the likelihood and severity of line overloading.

In the case study for the year 2011, the LORI was found to be zero as under all studied conditions no line loading reached 90% of its rating, and thus the severity of line loading is always zero. A similar observation was noted for the projected system in 2015 and 2021. Hence, system demand for year 2021 was increased hypothetically to reach its maximum generation capacity, hence stressing the system. In this case overloadings on some cases were observed i.e. some of the line loading reached more than 90% of its rating. The severity of the line loading was calculated based on the continuous theory and the respective LORIs were calculated and plotted. It was noticed that line D - C has the largest LORI index due to ‘N-1’ and ‘N-2’ contingencies.

CHAPTER 6. PROBABILISTIC RELIABILITY ASSESSMENT AND ITS APPLICATION TO THE GB TRANSMISSION SYSTEM

6.1 Introduction

This chapter presents the calculation of the LORI (as explained in Chapter 4) for the GB transmission system (specifically for Zone 8) over a one-year period, considering uncertainties of (i) hourly variations in system demand, (ii) different contingencies, and (iv) respective variations in the line thermal rating. Initially, the Probabilistic Distribution Function (PDF) of the system demand will be developed using the hourly system demand for one year, in order to identify the system demand levels to be studied. Then, using NEPLAN and C++ programming code, load flows are conducted for an intact system and different contingencies in order to find the line loadings and develop the PDF. Moreover, for each hour of a year, the relative line thermal ratings were evaluated based on local weather data, and an equivalent PDF was developed.

6.2 GB transmission system

National Grid is requested to publish into the public domain via the GB Ten Year Statement [141] technical data for the 400 kV and 275 kV levels, including network topologies, half hourly system demands, network capability and future requirements. The GB transmission system includes the systems owned and operated by National Grid (SYS), Scottish Power Transmission (SPTL), and Scottish Hydro Electric Transmission (SHETL). In this work, only the England and Wales part of the GB transmission system is considered, specifically Zone 8. The NEPLAN readily-available model of the GB transmission system for 2009 was adopted from a previous project [124]. A simplified block diagram of the GB system divided into 11

zones is illustrated in Figure 6.1. Figure 6.2 shows a geographic representation of the 400 kV and 275 kV system and the main interconnection boundaries. Figure 6.3 shows the implemented NEPLAN load flow model. It should be noted that the network is undergoing a programme of continuous expansion and reinforcement and that the current network in this study represents one configuration approximating to the 2009 timeline.

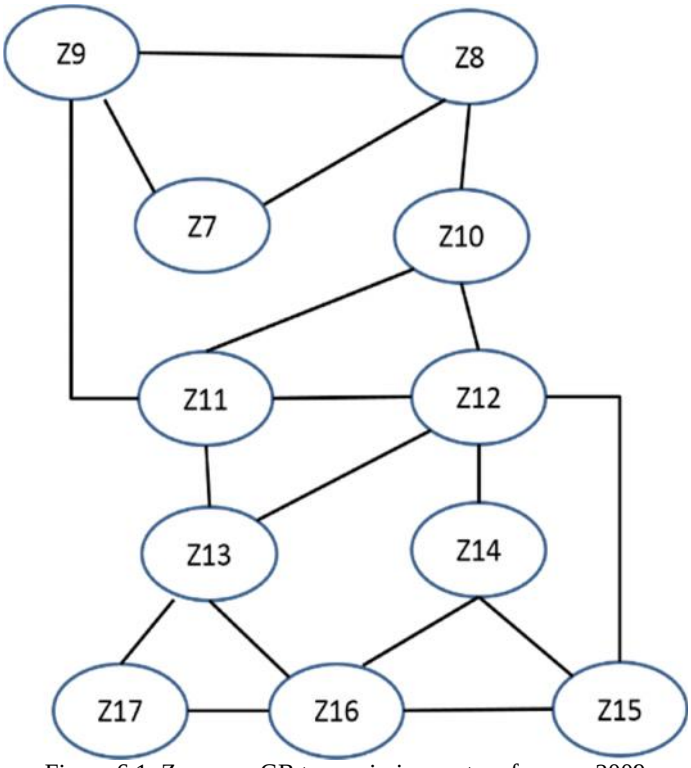

Figure 6.1: Zones on GB transmission system for year 2009

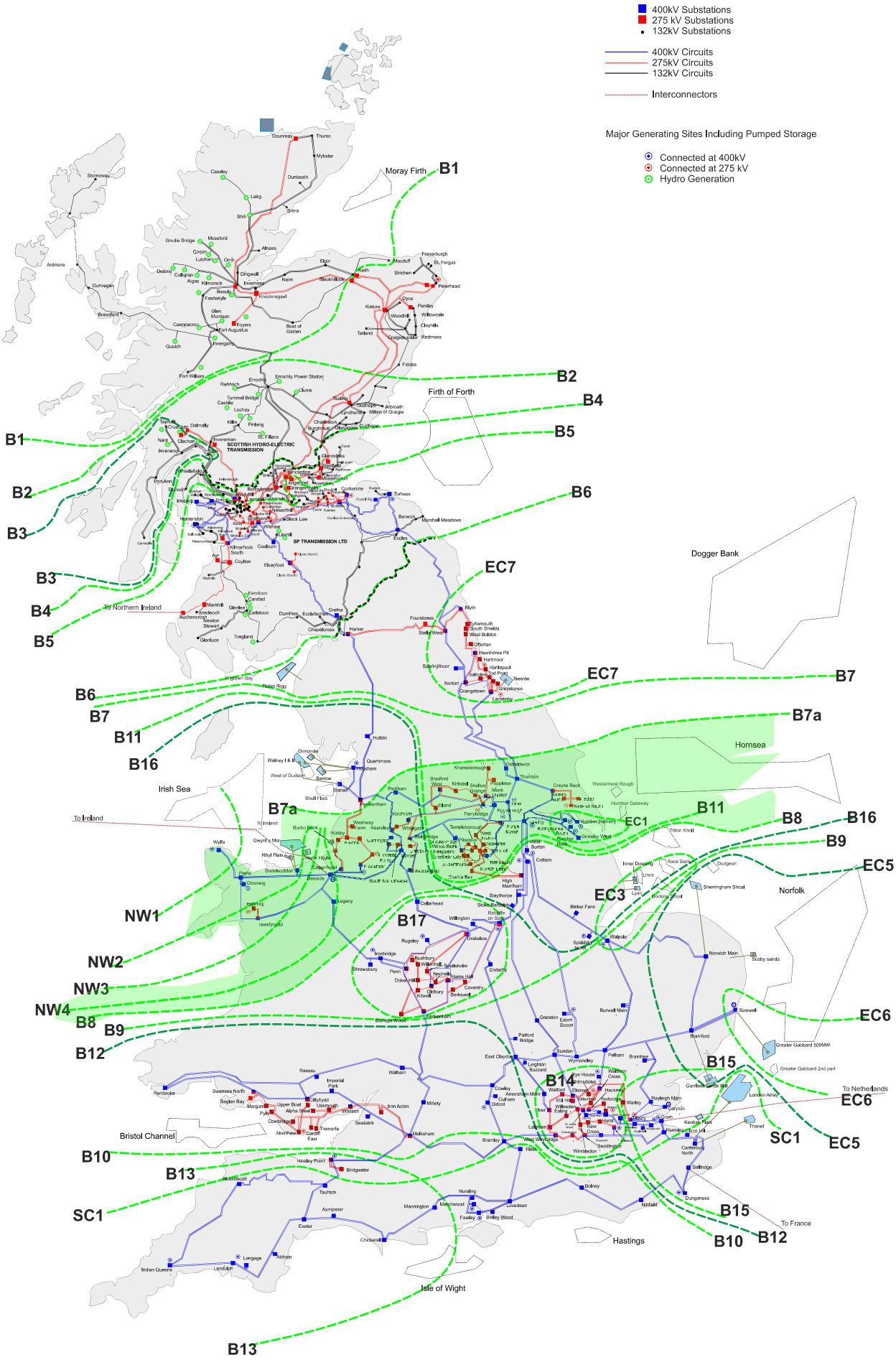

Figure 6.2: Detailed geographic GB Transmission system for year 2013 / 2014 [141]

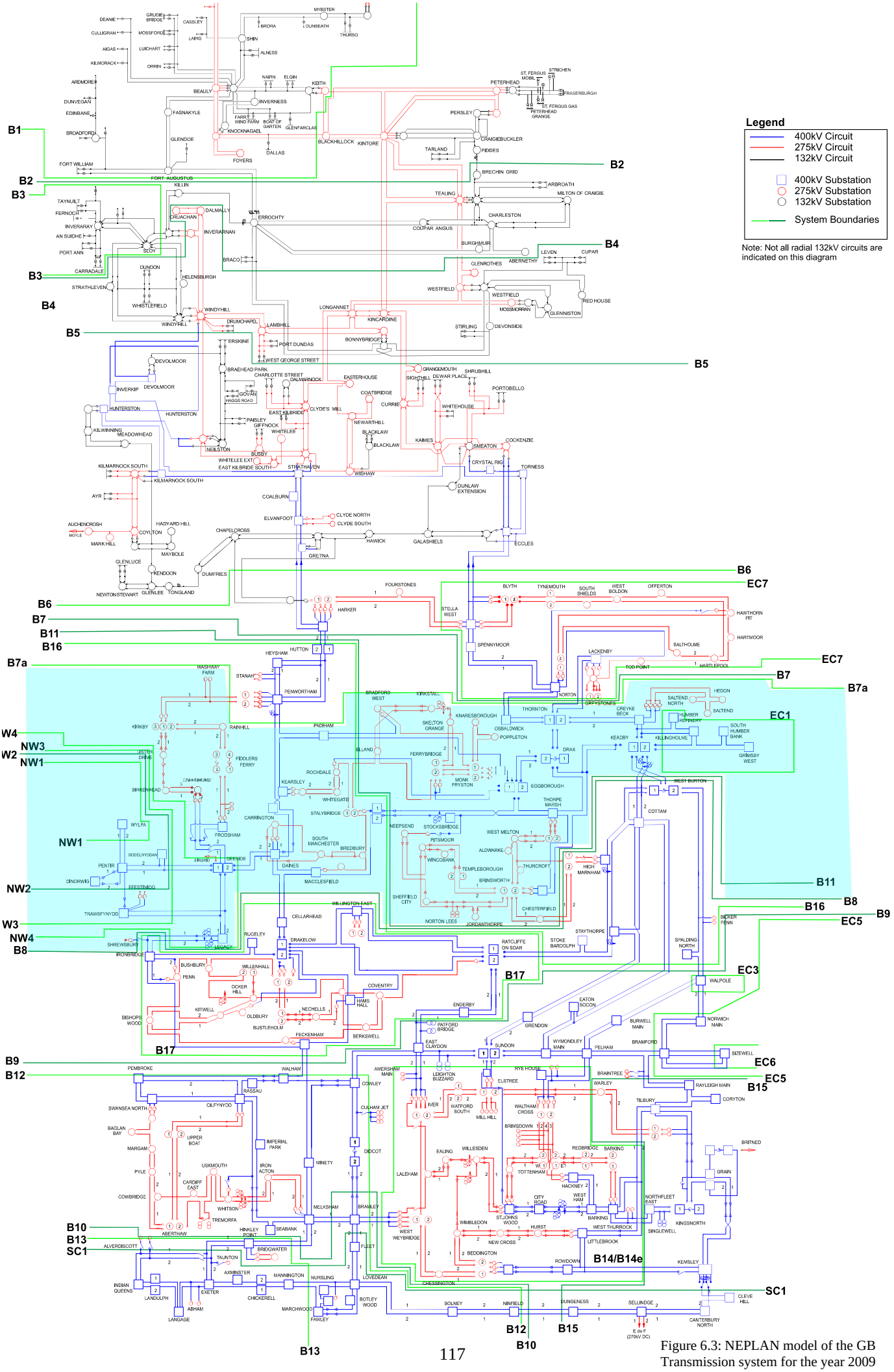

Figure 6.3: NEPLAN model of the GB Transmission system for the year 2009

In the 2009 model, there are 409 substations, 496 transmission lines, and 83 generators. The generating sources include gas, coal, wind, hydro, and nuclear power. The installed generation capacity in the 2009 model is 60,300 MW. GB transmission system consisted of two hundred and six 400 kV substations and two hundred and eighty-nine 400 kV lines, with a total length of about 10,854 km. The 400 kV circuits are mainly of an overhead tower line construction employing ACSR 2x400, ACSR 4x400, AAAC 2x500, AAAC 2x700, or ACAR 2x500 conductors. Table 6.1 gives a summary of the GB transmission system as of 2009.

Table 6.1: Summary of the GB transmission system as of 2009

Number of 400 kV substations	206
Number of 275 substations	203
Number of 400 kV lines	289
Number of 275 kV lines	209
Installed Generation Capacity	60,300 MW

It should be noted that the GB transmission networks are interconnected to continental Europe power networks, that is, Northern Ireland, France, and now also to the Netherlands.

For the network under study, an hourly peak system demand of 60,100 MW was considered as of year 2010 which is the nearest year to 2009 for which system demand data was availed as on hourly basis [141].

In applying the developed algorithm, Zone 8 of the system was selected as the study area which is found to be comparable with Dubai system and in order to simplify the study. In Zone 8, forty-six 400 kV circuits are in parallel operation. This area has thirty-three 400 kV substations and thirty-six 275 kV substations. The 275 kV transmission circuits are constructed from overhead lines and underground cables. Table 6.2 gives a summary of Zone 8 of GB transmission system as of 2009. Figure 6.4 shows the topology for Zone 8 of the GB transmission system. To the north and east of Zone 8 are the power-exporting regions of Scotland, Yorkshire, and the Humber.

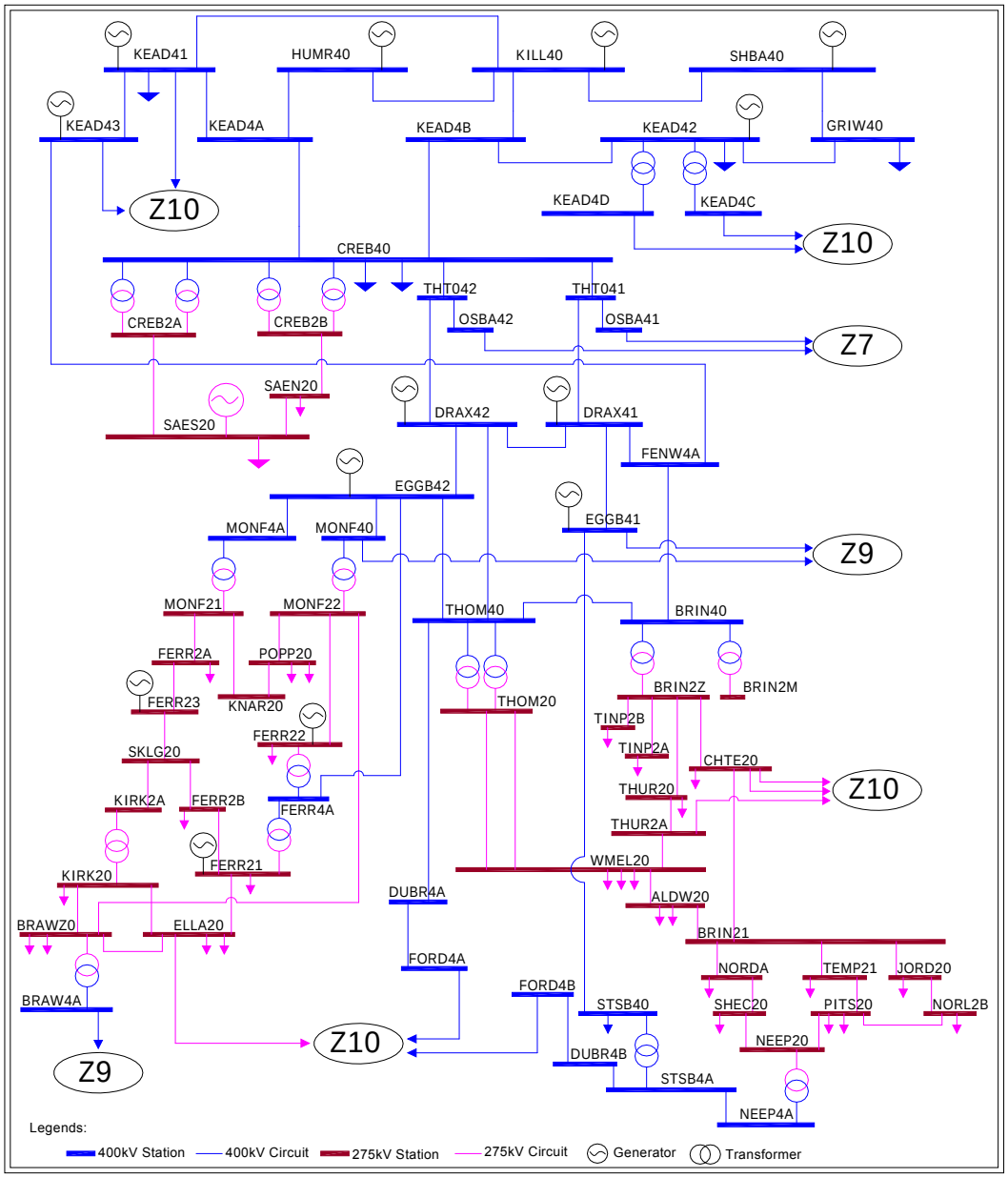

Figure 6.4: Interconnections of Zone 8 (of GB Transmission System) with other zones [124]

Generation from Scotland is transported south, leading to high power transfer levels across Zone 8. Zone 8 has traditionally been heavily loaded at the time of the winter peak due to high north to south power flows, and Zone 8 is dominated by thermal generation. Currently, the zone has a bulk power transfer capability of 12,254 MW. [141].

Table 6.2: Statistics for Zone 8 of the GB transmission system as of 2009

Number of 400 kV substations	33
Number of 275 substations	36
Number of 400 kV circuits	46
Number of 275 kV circuits	41

The GB transmission network data, which were obtained from the National Grid 10 Year Statement, however, do not include data for the following

• Capacity and ranking order for the generator units

• Component reliability data (i.e. fault rate and maintenance rate)

• Overhead line conductor types.

These data in this work have been either assumed or collected from other sources e.g. [22] in order to obtain a full transmission system model.

6.3 System demand for GB power system

Actual hourly system demand data for a power system over a one-year period were found in the National Grid 10 Year Statement. The hourly system demand for the year 2010 is shown in Figure 6.5. It is noted that the highest system demands (e.g. 60,216 MW at 17:00 hrs on 20 December 2010) occur during the winter period (start and end of graphs), while the minimum system demands (e.g. 21,951 MW at 04:00 hrs on 04 July 2010) are located in the summer season (middle of graph).

The system demand levels were divided into 500 units (bins), each with a bin size of 500 MW. The resultant system demand levels showing their frequencies and probabilities, is illustrated in Figure 6.6. The system demands in the GB ranged from 60,216 MW to 21,951 MW. The most frequent range of the system demand was between 40,300 - 40,799 MW, which occurred for 289 hours in the year (i.e. probability of 0.033), while the least frequent range of system

demand was 59,800 – 60,299 MW which occurred for 2 hours in a year (i.e. probability of 0.0002).

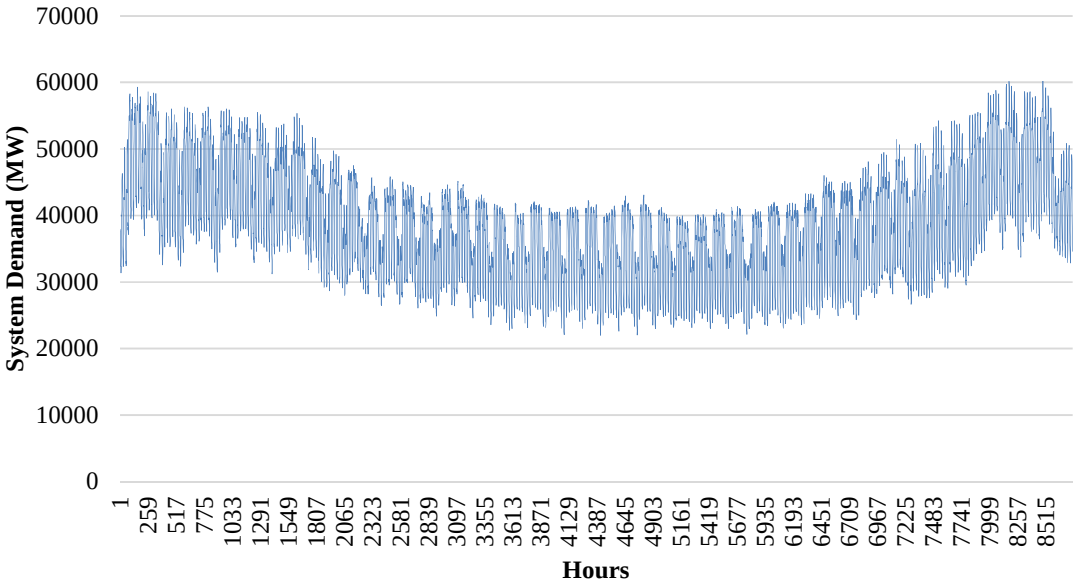

Figure 6.5: Hourly system demand variation along a year of 2010 for GB power system

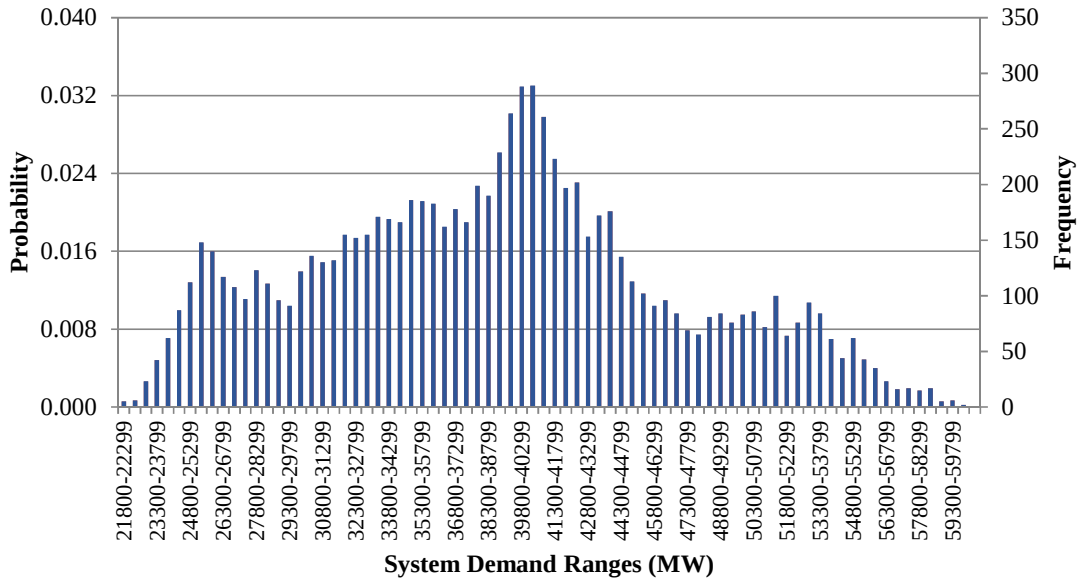

Figure 6.6: Frequency Distribution and PDF for system demand for the year of 2010

6.4 Reliability data for GB transmission power system

Historical failure records were not found in 10 year statement for the GB transmission system. Consequently, reliability data of failure and duration were taken from [22]. Table 6.3 shows the component reliability data (per km) for the GB transmission system at 400 kV and 275 kV, and this has been used in this study. Based on this data, a single 400 kV line failure may occur for 0.0007+0.0043 in a year with an average duration of 24.68+0.11 hours. Then, as of Equation 4.9, the probability of the 'N-1' contingencies is calculated as the following:

$$Pc_{(N-1)} \text{ is } \frac{(0.0007*24.68)+(0.0043*0.11)}{8760} = 0.000002026.$$

Table 6.3: Assumed failure statistics for GB transmission system

Component	275 kV		400 kV	
	Probability	**Duration (hrs)**	**Probability**	**Duration (hrs)**
Line (long outages)	0.0013	14.59	0.0007	24.68
Line (Short outages)	0.0109	0.14	0.0043	0.11
Busbar	0.0173	1.47	0.0269	3.42
Power Transformer	0.0222	0.11	0.0222	0.11

The failure of double circuit outages was assumed to be 7.5 % of that of 'N-1' [137].

$$P_{c(N-2)} = P_{c(N-1)} * 7.5\% = 0.000002026 * 7.5\% = 0.000000151$$

6.5 Thermal rating calculation for transmission overhead line for the GB transmission system

The historical hourly weather data, used in this study to calculate thermal ratings, are given by the GB Meteorology Office corresponding to the Church Fenton measurement point (which represents Zone 8), for the year 2004. It was assumed that year-on-year changes are small, and that the weather data is representative for application to this study. Figure 6.7 illustrates the hourly ambient temperature and wind speed recorded for year 2004. Ambient temperature

ranges from -5.6 to 28.2 ºC, which is much lower than Dubai. Moreover, Zone 8, located on the North

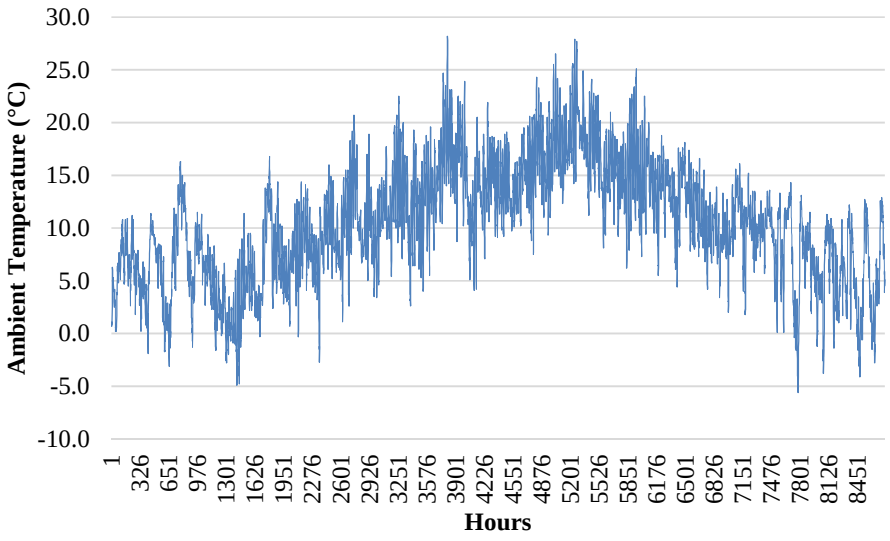

(a) Ambient Temperature

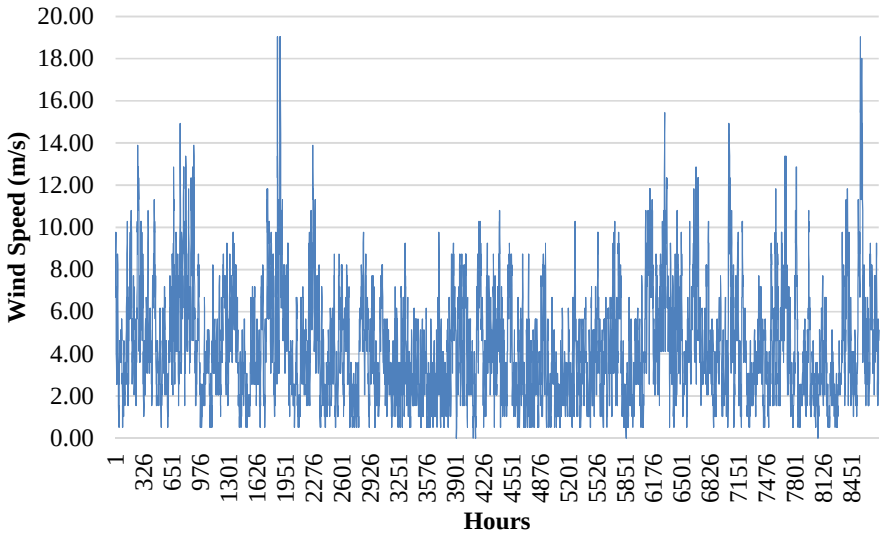

(b) Wind Speed

Figure 6.7: Hourly weather for Zone 8 during 2004

sea coast, is a quite windy area with wind speed values ranging between 0 – 19 m/s, which is quite higher than Dubai. Frequency distributions for the ambient temperature, wind speed, and wind direction, are shown in Figure 6.8. As can be seen from Figure 6.8(a), the most frequent

range of ambient temperature is 10 – 15 ºC, which occurred for 2,785 hours during 2004. Figure 6.8(b) illustrates that the most frequent range of wind speed is 2 – 4 m/s; which happened for 3,123 hours, which is comparable with that in Dubai. Figure 6.8(c) indicates that the wind direction range of 270 - 299º has the highest frequency, occurring for 1,696 hours.

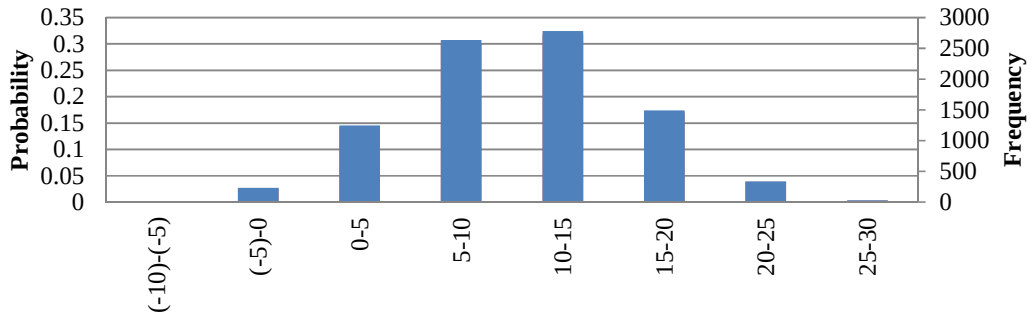

(a) Ambient Temperature

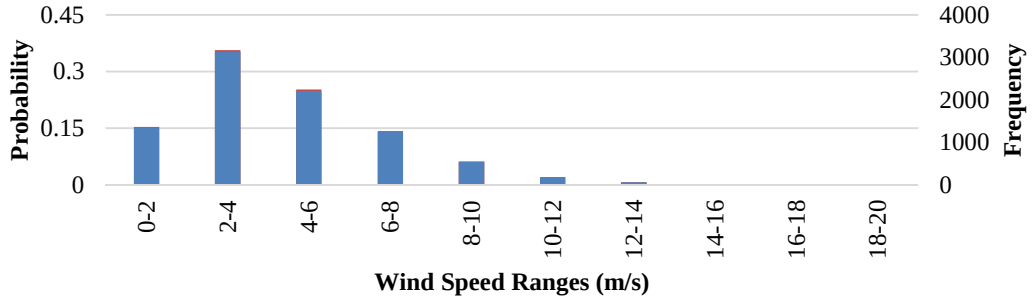

(b) Wind Speed

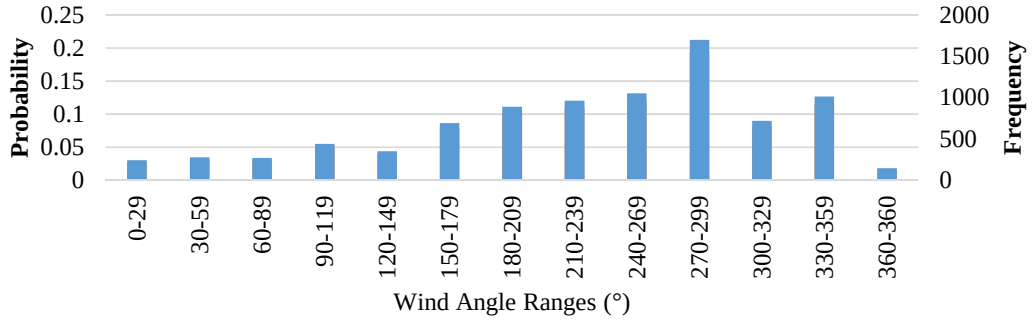

(c) Wind Angle

Figure 6.8: Frequency distributions for weather parameters for Zone 8 during 2004

400 kV overhead transmission lines in the GB use different types of conductors as shown in Table 6.4. Three operating temperatures are as given by the manufacturer for different types of conductors. Conductor with 50 ◦C of Zebra was used so that it results in the worst thermal rating value.

Table 6.4: Types of conductors used in the GB overhead transmission system

Type	No. of Conductors and Aluminium Area	Maximum Operating Temperature (◦C)
ACSR	2x400	50, 65, 75
	4x400	50, 65, 75
AAAC	2x500	75
	2x700	75
ACAR	2x500	75

ACSR Zebra conductor was chosen for the study because this type of conductor is found to be widely used in 400 kV transmission overhead lines in Zone 8 of the GB transmission network. Typically, this conductor is used in formation as a $4x400\,mm^2$ conductor bundle. Table 6.5 shows the specifications for this conductor. The conductor elevation height for Zone 8 was assumed to be 100 metres above sea level while the latitude was found to be 53.7º [142]. For the current study, the coefficients of emissivity (ε) and absorption (α) were selected as 0.5 and 0.5, respectively.

Table 6.5: Engineering parameters for 400 kV transmission ACSR line conductors

	Zebra ACSR
Conductor outer diameter (mm)	28.6
Conductor DC resistance at 20°C (Ω/km)	$6.74*10^{-5}$
Maximum allowable temperature (°C)	50
Conductor surface absorptivity	0.5
Conductor surface emissivity	0.5

The geographic locations of the start and end points of the line were used to evaluate its azimuth with respect to the North Pole. For a 400 kV transmission line of DRAX - EGG, it was found that the azimuth is 106.5º with respect to the North Pole.

The calculated hourly thermal rating values for Zebra conductor lines are illustrated in Figure 6.9. Line thermal ratings range from 1,849 Amps up to 9,327 Amps.

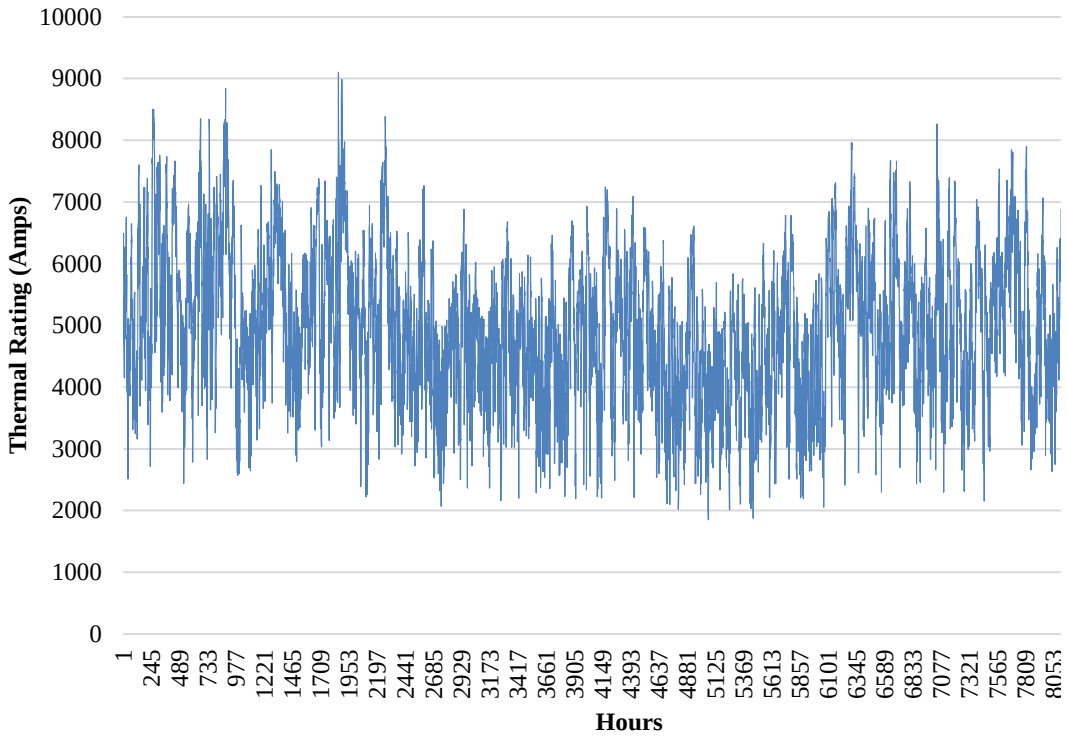

Figure 6.9: Hourly thermal rating for Zebra ACSR transmission lines

Moreover, thermal ratings are shown as probabilistic distribution in Figure 6.10. The most frequent thermal rating is 4,620 - 6,449 Amps, which occurs for 100 hours during a year.

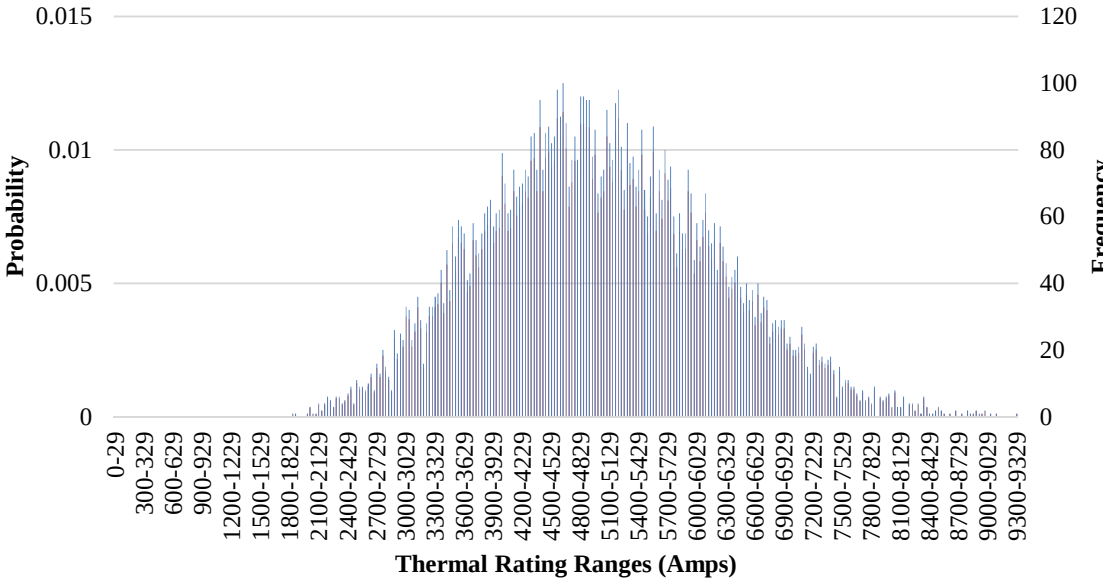

Figure 6.10: Frequency and Probabilistic Distribution Functions for the resultant thermal ratings

6.6 Multiple load flow simulations

The available GB model of year 2009 (in a NEPLAN format) with the system demand corresponding to 2010 was used for the power flow study, with seventy-seven different discretized system demand scenarios.

The scheduled generation and ranking order of the generators are not stated in National Grid Ten Year Statement [141]. The generators are listed in Table 6.6, and ordered from highest to lowest to capacity. Ranking is assumed to follow generator capacity (i.e. a lower generator capacity, lower ranking order). For each modelled system demand, generators were committed based on the assumed ranking order maintaining the slack bus generation to within an assumed reserve of +/-1,000 MW. Of course, the load flow will change based on different unit commitment.

Table 6.6 Scheduled generation and ranking order of the generators

Name	Ranking		Name	Ranking		Name	Ranking	
	Order	P Gen		Order	P Gen		Order	P Gen
WBUR40G	1	2415	EGGB41G	29	970	FIDF21G	57	485
HEYS40G	2	2405	EGGB42G	30	970	FIDF22G	58	485
COTT40G	3	2000	GRST22G	31	963	FIDF23G	59	485
SIZE40G	4	1700	GRST21G	32	963	FIDF24G	60	485
ABTH20gen	5	1641	LANG40G	33	905	FFES21G	61	485
BAGB20gen	6	1641	MAWO40G	34	900	FFES22G	62	485
DRAX42G	7	1620	KILL40G	35	900	USKM2AG	63	425
DRAX41G	8	1620	SPLN40G	36	880	NORW40G	64	420
DEES41G	9	1540	ROCK40G	37	810	GREN40G	65	401
HUMR40	10	1320	DAMC40G	38	805	KEAD42G	66	367.5
SHBA40G	11	1285	COSO40G	39	800	KEAD41G	67	367.5
HINP40G	12	1261	WALP40G	40	800	KEAD43G	68	260
SEAB40G	13	1234	DIDC41G	41	775	CARE20G	69	245
INDQ40G	14	1200	ECCLES(1)	42	773	HUTT4BG	70	229
BOLNEYG	15	900	ECCLES(2)	43	767	WILL20G	71	228
SELL40G	16	800	STRATHAVEN	44	750	OLDS20G	72	228
EASO40G	17	800	GRETNA	45	737	DEES42G	73	210
GRAI40G	18	540	RYEH40G	46	715	BARK21G	74	197
HATL20G	19	1208	LITT40G	47	665	BARK22G	75	197
SAES20G	20	1101	TILB22G	48	552	WISD20G	76	197
DIDC42G	21	1054	TILB21G	49	552	BRIM2G	77	197
RATS42G	22	1000	DINO40G	50	548	FAWL40G	78	158
RATS41G	23	1000	DUNG40G	51	540	HUTT4AG	79	155
PEMB40G	24	1000	DUNG20G	52	540	USKM2CG	80	121
IRON40G	25	1000	FERR20G	53	491	USKM2DG	81	121
RUGE40G	26	996	FERR22G	54	491	BLYT22G	82	50
WYLF40G	27	980	FERR23G	55	491	BLYT21G	Slack	
KINO42G	28	970	KINO41G	56	485			

The study cases include one intact state, first-order contingency for 275 kV and 400 kV lines, and the corresponding second-order contingency. With $N_s = N_D N_L (N_L + 1)/2$, for 77 system demand levels and 496 lines in the GB system, the total number of simulations is 9.5 million.

Using the automated NPL code and running on parallel computers, the simulations were carried out in 465 hours, as shown in Table 6.7.

Table 6.8: Computation burden

	Simulation No.	Simulation Duration (hrs)
Intact system	77	0.1
'N-1'	38269	4
N-2	9,490,712	460
Overall	9,529,058	465

Figure 6.11 shows the hourly resulted line loading for a sample 400 kV line of KEAD42 - KEAD4B along with its thermal rating, during intact system, N-1 and N-2 contingencies.

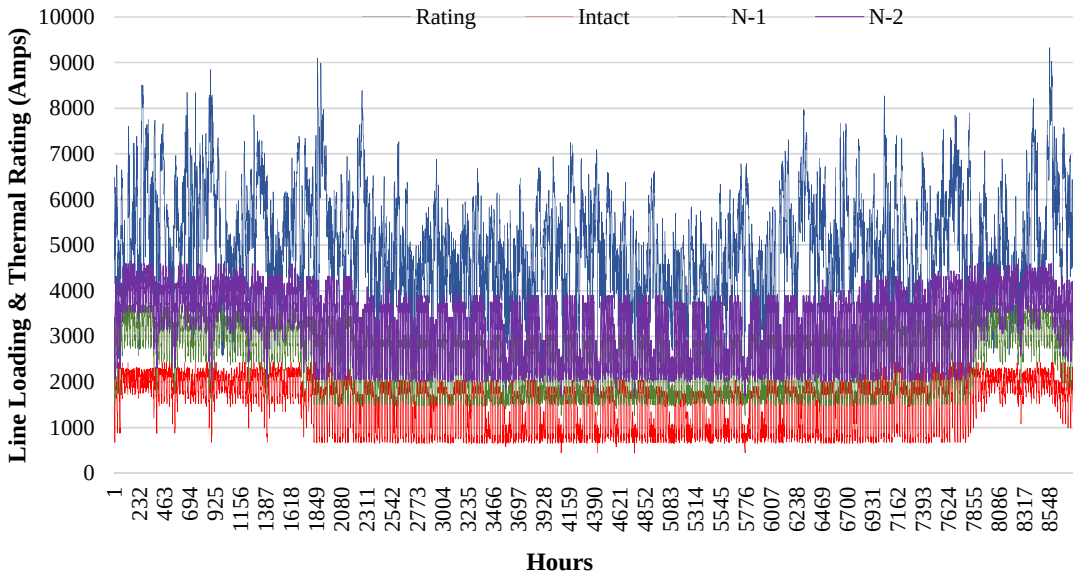

Figure 6.11: Hourly line loading and thermal rating for a sample line

6.7 Line Overload Risk Index (LORI) calculation for GB Transmission System of year 2010

The results of the simulations for GB system, considering only Zone 8 revealed that out of 41 400 kV lines, 16 lines overloaded due to 'N-1' contingencies and 26 lines due to 'N-2'

contingencies. The probability distributions of the resultant lines loading were developed. The results for one sample circuit with the highest line loading of KEAD42 - KEAD4B are shown in Figure 6-12, for an intact system, ‘N-1’ contingencies, and ‘N-2’ contingencies.

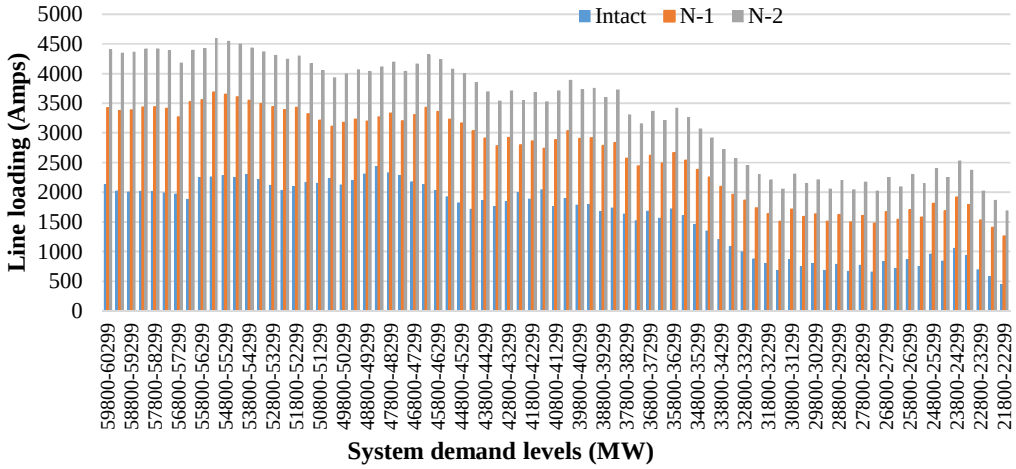

Figure 6.12: Line loadings on 400 kV lines of Zone 8 for system demands

Figure 6.13 shows probability of line loadings for same example line of KEAD42 - KEAD4B. The probability of overloading of this line is 0.000000565 (occurs 307 hours in a year) due to ‘N-1’ and 0.00000018 (occurs 1334 hours in a year) due to ‘N-2’ contingency.

Figure 6-14 shows the overall PDFs of the line loading and thermal rating for the line of KEAD42 - KEAD4B and contingency conditions. Under intact system, there is a very small margin (i.e. 9 Amps) between the highest line loading (2,434 Amps) and the lowest thermal rating (2,443 Amps). The line loading due to ‘N-1’ conditions increases, and the highest line loading (e.g. 3,361 Amps) moves towards the minimum thermal rating (e.g. 2,223 Amps), that is, overlapping occurs between two PDFs for some lines in different system demand levels but not necessarily at the same time series. Due to ‘N-2’ contingencies, the margin if further reduced and more overlapping occurs between the maximum line loading (e.g. 4,236 Amps) and the lowest thermal rating (e.g. 2,223 Amps).

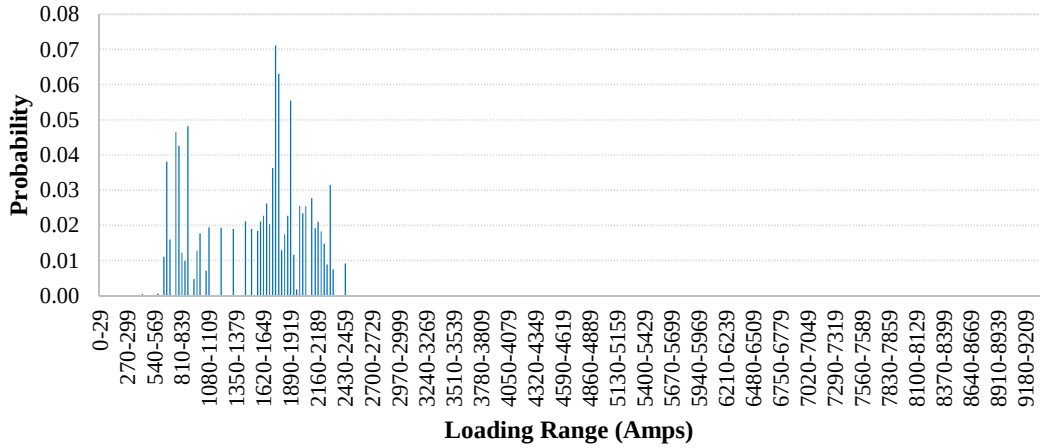

(a) During intact system

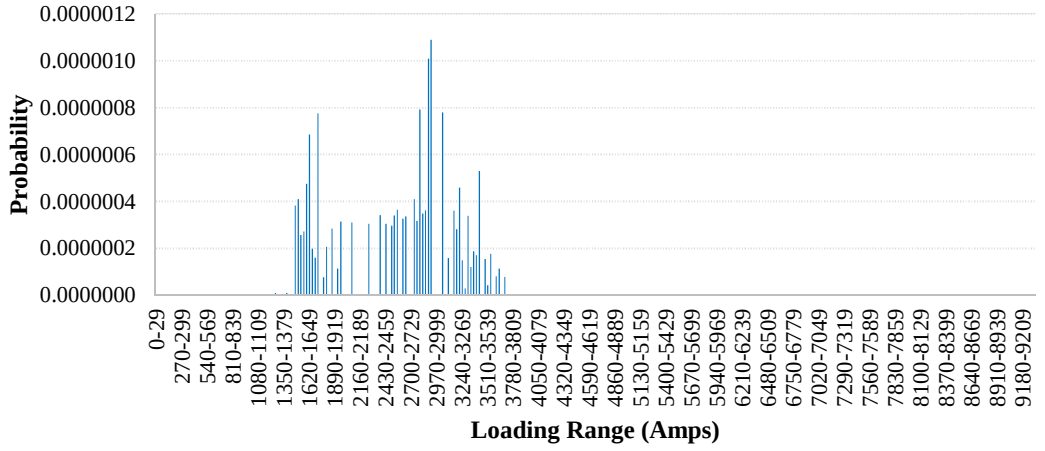

(b) During 'N-1'

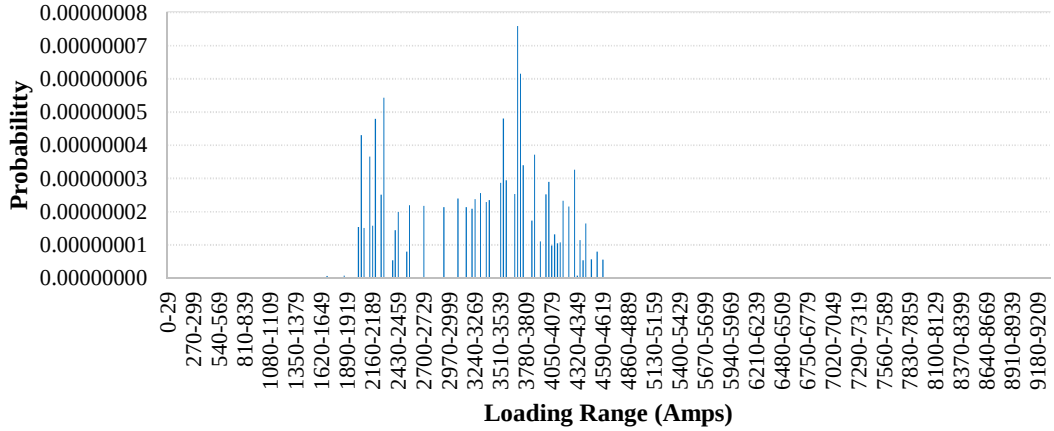

(c) During 'N-2'

Figure 6-13: Lines loading PDFs for KEAD42-KEAD4B 400 kV line

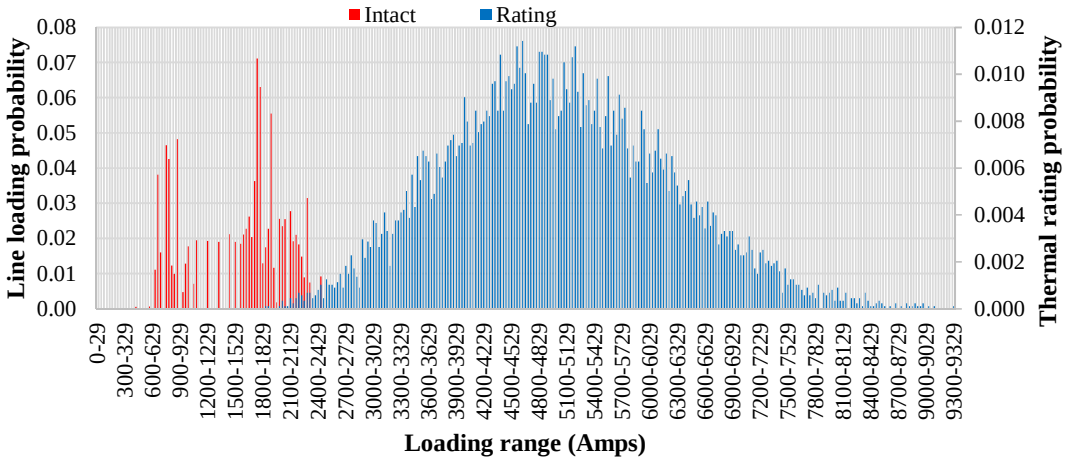

(a) During intact system

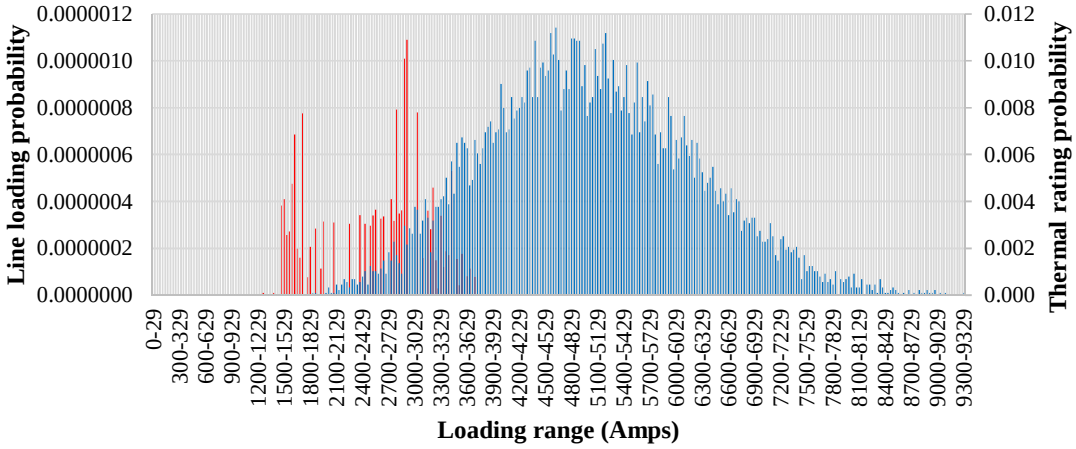

(b) During 'N-1'

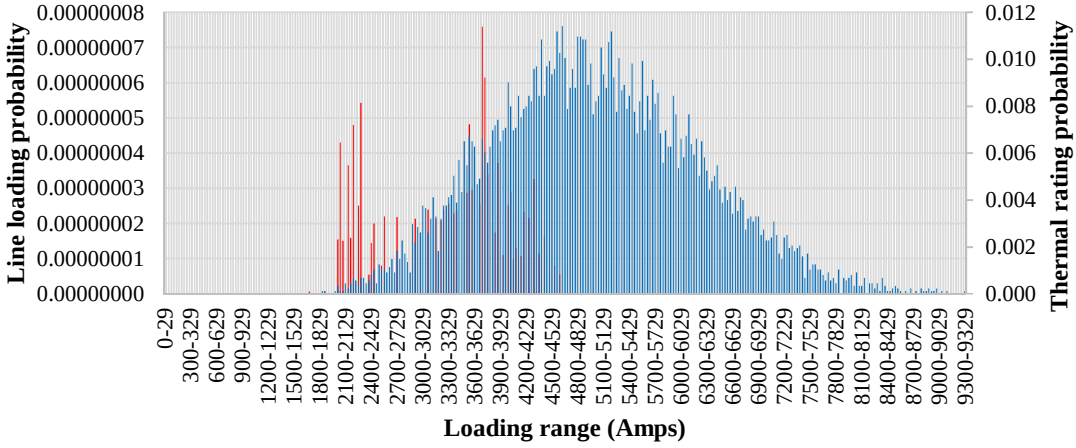

(c) During 'N-2'

Figure 6-14: Line loading and rating PDFs for KEAD42 - KEAD4B 400 kV line

The LORIs were calculated and graphed in Figure 6-15. It can be seen that the line DRAX42 - THOM40 has the highest LORI index due to 'N-1' and KEAD4B-KILL40 due to 'N-2' contingency and need to be considered while system designing and operating. In contrast with the LORIs found for the Dubai system, GB lines have the greater risk. UK system is different in the sense that maximum system demand is greater in winter but the line thermal rating is also greater, while in Dubai it is different because when there is maximum demand in summer there is minimum thermal rating.

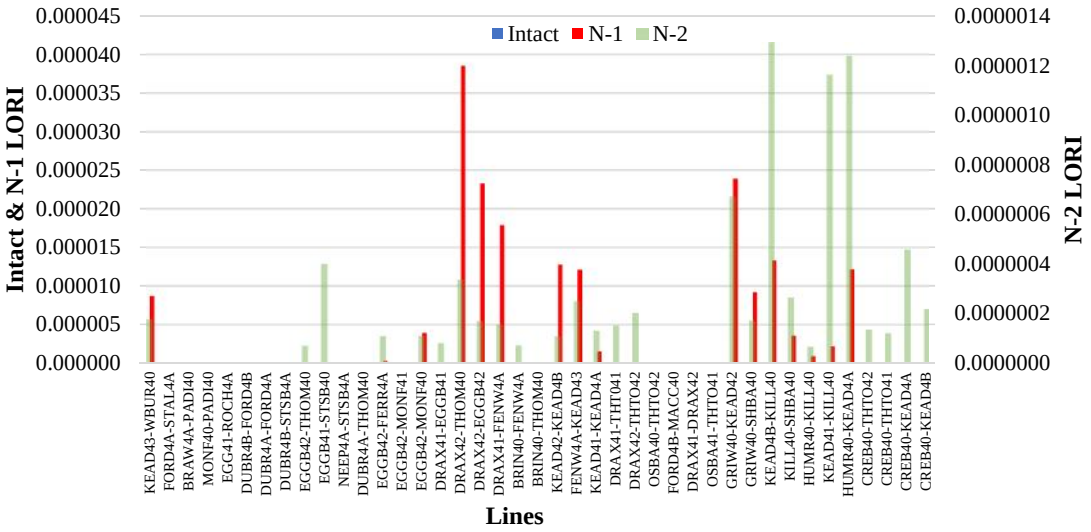

Figure 6-15: LORI calculated for all 400 kV lines

6.8 Conclusions

LORI index was analysed for 400kV transmission lines of Zone 8 of GB hourly system demand of year 2010 and network of year 2009. Risk of line overloading was studied systematically taking into account uncertainties of (i) hourly variations in system demand, (ii) maintenance

outage, and (iii) ‘N-x’ line outages, considering variations in the thermal rating. Based on an annual set of meteorological data, the hourly thermal rating and relative PDF were calculated and developed for Zone 8 of the GB transmission overhead lines. The simulation results were used to determine the PDFs of loading for each line incorporating actual fault rates. The PDFs for the resultant line loadings were compared with the PDFs for the thermal ratings of each line and the LORI is determined.

The overloading risk index was calculated based on the overloadings observed under some conditions i.e. some of the line loading reached more than 90% of its rating and hence the severity of the line loading was evaluated according to the continuous theory. It was noticed that line DRAX42 - EGGB42 has the largest LORI index, i.e. is the line with greatest risk.

CHAPTER 7. CONCLUSIONS

In this investigation, existing risk assessment for transmission power systems has been examined closely and new algorithm was developed and applied. The new developed algorithm incorporates probabilities of some important uncertainties and the severity with respect to the line overloading. Hourly thermal rating was also calculated based on given weather conditions. The new method is automated in the form of a programming code.

An extensive literature review was conducted primarily with the aim of describing the existing deterministic and probabilistic approaches for conducting the risk assessment process in order to measure the reliability of the transmission system. An extensive review revealed a range of different processes, techniques, tools, and indices, some of which have been adopted on various transmission test systems for different applications. It was shown that probabilistic approach could be more superior to deterministic approach.

To date, there is not enough confidence in the probabilistic risk assessment for power systems to be used effectively for decision making, and it is sometimes employed as a next step assessment after the use of the deterministic approach. This is may be due to a lack of historical data or the complexity of the procedure. The industry always looks for a more efficient, simple, and realistic procedure to carry out the risk assessment of power systems.

A deterministic approach was applied to the Dubai transmission system; this was studied in detail, which ensured the necessity of the development of a new modified approach of the probabilistic risk assessment.

Many indices have been used in the probabilistic approach, but the author found that the LORI is the most suitable for use for transmission system that could quantify the security of the transmission system.

Based on the latest findings of investigations on the effect of uncertainties on the transmission system, a process that considers their effect was developed. An appraisal of the existing probabilistic and deterministic approaches and indices has shown that, for transmission systems, the probability of uncertainties of hourly system demand variation and variable thermal rating (in addition to maintenance and contingency) was not given enough attention when calculating the LORI. Some recent research has focused on the assessment of the LORI; however, such research has been limited to a small number of system demand levels and a single line thermal rating.

The new proposed method aimed to extend the evaluation of the LORI through an extensive evaluation of the transmission system performance under hour-by-hour system demand levels for a one-year period, for an intact system, 'N-1' contingencies, 'N-2' contingencies, and maintenance outage. In addition, hourly line thermal ratings have also been evaluated and considered over an annual cycle, based on detailed meteorological data. The new method is further developed and automated in the form of a software routine. A detailed analysis of reliability was conducted in this work using engineering, historical line fault, and maintenance data. The PDFs for line loading, line thermal rating, and system demand were developed, considering coincidence time of line loading and thermal rating. In this work, the methodology was applied on the real transmission systems of Dubai (for the years 2011 and 'stressed' 2021) and GB (for the year 2010).

For the year of 2011 on Dubai system, there were no overloadings, hence the severity for the lines was zero, and LORIs were equated to be zero. Same results were observed for the year 2015 and 2021. After stressing the network of year 2021, some lines were overloaded, and respective severity, probability and LORI were calculated. For GB system of year 2010, some

overloadings were also observed and LORIs were evaluated. Based on LORIs, transmission lines were ranked and the most risky lines were identified. It was found that line loadings on GB system is much higher than that on Dubai system, and were more risky. UK system differs in the aspect that maximum system demand and maximum thermal rating occur in winter, while in Dubai it is different since when there is maximum demand in summer there is minimum thermal rating.

LORI of each line can be calculated and used as a benchmark for the comparison of different system operations and designs. Use of this methodology allows systems to be designed and operated to an acceptable level of risk. Knowing this could help system operators and designers make the best decisions to prevent damage to conductors or a potential cascading failure. It is important to specify the LORI tolerance (i.e. acceptable LORI). As, currently, there is no standard in power industry for specifying it, this is a decision that should be taken by individual utilities. Some of the foreseen advantage for adopting LORI algorithm could be better use of the existing assets and reduction in future assets infrastructure based on adopted tolerance. In the Dubai system, when there is a lot of system demand growth, a lot of new Transmission investment could be put off. However, In GB, the main challenge is with change in generation distribution rather than system demand growth i.e. Directive to get rid of coal and with more renewable energy.

Overall, the research in this thesis offers an improved algorithm of the probabilistic reliability assessment for transmission systems. The improved index, along with the developed algorithm, can be used to rank the transmission lines based on the line overloading risk, thus assisting the power engineers and decision makers to manage and control potential risks.

During the research programme, the following contributions were accomplished:

- Development of an advanced probabilistic procedure for the reliability assessment of transmission systems which opened a path for considering line overloading risk based on some important uncertainties.
- Hourly calculation and analysis of thermal ratings for a transmission line for a period of one year, according to on actual given weather condition and engineering parameters.
- Development of sets of PDFs for system demand, line thermal ratings, and resultant line loading.
- Evaluation of LORI for real systems of Dubai and GB transmission systems.
- Development of a C++ programming code in order to automate modelling and multi-contingency analysis, thus evaluating the severity of the transmission lines.

This work could be extended in future to include the following areas:

- Further studies on the LORI that could incorporate other uncertainties, e.g., generator outputs, load shedding, etc.
- Utilizing the same algorithm but with other indices, e.g., voltage and system frequency.
- Reducing further the number of cases to be studied, while maintaining high level of accuracy.
- Fully automating the process (to include calculations of probability, severity, and LORI) using an advanced programming code.
- Enabling utilities to specify the suitable tolerance for the LORI.
- LORI algorithm could be adopted in real-time and offline software tool.
- LORI algorithm could be adopted in distribution system.

REFERENCES

[1] R. Billinton R. and R. N. Allan, *Reliability Evaluation of Power Systems*, 2nd Edition, New York, Plenum Press, 1996.

[2] M. El-Hawary, *Introduction to Electrical Power Systems*, A John Wiley & Sons, 2008.

[3] *Modern Power Station Practice*, Incorporating Modern Power System Practice, EHV Transmission, Volume K, British Electricity International, Third ed., London, Pergamon Press, 1991.

[4] H. Griffiths and N. Pilling, *Earthing Systems* in A. Haddad and D. Warne, (Eds.): *Advances in high voltage engineering*. Ed, IEE, 2004.

[5] Dubai Electricity and Water Authority, (2011), [online], Available: www.dewa.gov.ae [confidential data].

[6] D. S. Kirschen, "Power System Security," *Power Engineering Journal*, vol. 16, no.5, pp. 241-248, Oct, 2002.

[7] D. Alali, H. Griffiths, L. Cipcigan and A. Haddad, "Assessment of Line Overloading Risk for Transmission Networks," *in 11th IET International Conference on AC and DC Power Transmission*, Birmingham, 2015, pp. 1-6.

[8] R. Billinton and R. N. Allan, *Reliability Evaluation of Engineering Systems*, 2nd ed, New York, Springer Science Business Media, 1992.

[9] H. R. Stuart, "Discussion on Time-Limit Relays and Duplication of Electrical Apparatus to Secure Reliability of Service," *American Institute of Electrical Engineers Transactions*, vol. XXIV, pp. 281-282, Pittsburg, June, 1905.

[10] V. M. Cook, M. J. Steinberg, C. D. Galloway and A. J. Wood, “Determination or Reserve Requirements or Two Interconnected Systems,” *Power Apparatus and Systems, IEEE Transactions*, vol. 82, no. 65, pp. 18-33, April, 1963.

[11] D. Alali, H. Griffiths, L. Cipcigan and A. Haddad, “Steady-State Security Assessment for Transmission Systems and its Application to the Dubai Network,” in *47th International Universities Power Engineering Conference (UPEC)*, London, 2012, pp. 1-6.

[12] Y. Gao, M. Zhou and G. Li, “Sequential Monte Carlo Simulation Based Available Transfer Capability Calculation,” in *Power System Technology (PowerCon)*, 2006, pp. 1-6.

[13] M. Rosero and M. Rios, “Characterization of the Maximum Loadability in Power Systems Due to Contingencies in the Operative Planning Scenario,” in *IEEE Power Tech*, Lausanne, 2007, pp. 1272-1277.

[14] T. Bi, X. Qin and Q. Yang, “Risk Theory based On-line Power System Security Assessment,” in *DRPT*, Nanjing China, 2008

[15] G. Papaefthymiou, J. Verboomen, P. Schavemaker and V. Sluis, “Impact of Stochastic Generation in Power Systems Contingency Analysis,” in *Probabilistic Methods Applied to Power Systems (PMAPS)*, June, 2006, pp. 1-6.

[16] R. Billinton and W. Wangdee, “Delivery PointRreliability Indices of a Bulk Electric System using Sequential Monte Carlo Simulation,” *IEEE Trans. Power Del.*, vol. 21, no. 1, pp. 345-352, Jan., 2006.

[17] A. Sankarakrishnan and R. Billinton, “Sequential Monte Carlo Simulation for Composite Power System Reliability Analysis with Time Varying Loads,” *IEEE Trans. Power Syst.*, vol. 10, no. 3, pp. 1540-1545, Aug., 1995.

[18] Y. Dai, J. D. McCalley J. D., N. Abi-Samra and V. Vittal, "Annual Risk Assessment for Overload Security," *IEEE Trans. Power Syst.*, vol. 16, no.4, PP. 616-623, Nov. 2001.

[19] C. Agreira, C. Ferreira, J. Pinto, F. Barbosa, "The Performance Indices to Contingencies Screening," in *9th International Conference on Probabilistic Methods Applied to Power Systems (PMAPS)*, Stockholm, 2006, pp. 1-8.

[20] J. Hazra and A. K. Sinha, "A Risk Based Contingency Analysis Method Incorporating Load and Generation Characteristics," *Elsevier Ltd Electrical Power and Energy Systems*, pp. 433-442, 2010.

[21] G. Papaefthymiou, J. Verboomen, P. H. Schavemaker and L. van der Sluis, "Impact of Stochastic Generation in Power Systems Contingency Analysis," in *International Conference on Probabilistic Methods Applied to Power Systems (PMAPS)*, Stockholm, 2006, pp. 1-6.

[22] J. Setreus, P. Hilber, S. Arnborg and N. Taylor, "Identifying Critical Components for Transmission System Reliability," *IEEE Trans. Power Syst.*, vol. 27, no. 4, pp. 2106-2115, Nov., 2012.

[23] L. Guo, C. X. Guo, W. H. Tang and Q. H. Wu, "Evidence-based Approach to Power Transmission Risk Assessment with Component Failure Risk analysis, Generation," in *Transmission & Distribution, IET*, vol.6, no.7, pp. 665-672, Jul., 2012.

[24] P. Kongmany, S. Premrudeepreechacharn and K. Charoenpatcharakij, "Transmission System Reliability Evaluation in the Central-1 and Northern Regions of the Lao PDR in Corresponding to Transmission System Development Plan," in *Power and Energy Engineering Conference (APPEEC)*, Asia-Pacific, 2009, pp. 1-4.

[25] R. Fischl and J. Chow, “On the Probabilistic Evaluation of Indices for Power System Security Assessment,” in *IEEE International Conference on Systems*, 1992, pp. 768-773, vol.1.

[26] P. Zhang, Y. Hou and G. Liu, “Coordination of System Planning and Operation using Probabilistic Risk Assessment Method,” in *IEEE Power and Energy Society General Meeting (PES)*, Jul., 2013, pp. 1-5.

[27] J. Nahman, I. Skokljev, “Probabilistic Steady-State Power System Security Indices,” *Elsevier Ltd Electrical Power and Energy Systems*, pp. 515-522, 1999.

[28] M. Ramezani, H. Falaghi and C. Singh, “A Deterministic Approach for Probabilistic TTC Evaluation of Power Systems Including Wind Farm Based on Data Clustering,”, *IEEE Transactions on Sustainable Energy*, vol.4, no.3, pp. 643-651, Jul., 2013.

[29] M. Perninge and L. Soder, “Analysis of Transfer-Limit Induced Power System Security by Markov Chain Monte Carlo Simulation,” *European transactions on electrical power*, pp. 140-151, 2012.

[30] J. Wei, G. Li, M. Zhou and K. L. Lo, “Monte Carlo Simulation Based Assessment of Available Transfer Capability in AC-DC Hybrid Systems,” in *5th International Conference on Critical Infrastructure (CRIS)*, pp. 1-6, Sept., 2010.

[31] C. Wang, X. Wang and P. Zhang, “Fast Calculation of Probabilistic TTC with Static Voltage Stability Constraint,” in *IEEE Power Engineering Society General Meeting*, pp. 1-7, Jun., 2007.

[32] J. W. Stahlhut and G. T. Heydt, “Stochastic-Algebraic Calculation of Available Transfer Capability,” *IEEE Trans. Power Syst.*, vol. 22, no. 2, pp. 616-623, May, 2007.

[33] X. Yu and C. Singh, “Probabilistic Analysis of Total Transfer Capability Considering Security Constraints,” in *International Conference on Probabilistic Methods Applied to Power Systems*, pp. 242-247, Sept., 2004.

[34] K. Audomvongseree and A. Yokoyama, “Consideration of an Appropriate TTC by Probabilistic Approach,” *IEEE Trans. Power Syst.*, vol. 19, no. 1, pp. 375-383, Feb., 2004.

[35] Y. Ou and C. Singh, “Assessment of Available Transfer Capability and Margins,” *IEEE Trans. Power Syst.*, vol. 17, no. 2, pp. 463-468, May, 2002.

[36] Y. Cui, Z. Bie and Wang X., “Study, on Calculation of Probabilistic Available Transfer Capability,” in *International Conference on Power System Technology (PowerCon)*, vol.4, pp. 2052-2056, 2002.

[37] A. S. C. Kumari, “Calculation of Available Transmission Capability Based on Monte Carlo Simulation,” *International Journal of Engineering Research and Applications (IJERA)*, vol. 2, pp. 1254-1260, 2012.

[38] F. Aboytes, “Stochastic Contingency Analysis,” *IEEE Trans. Power Syst.*, vol. PAS-97, no. 2, pp. 335-341, Mar., 1978.

[39] P. L. P. Henneaux and J. Maun, “A Level-1 Probabilistic Risk Assessment to Blackout Hazard in Transmission Power Systems," *Elsevier Ltd, Reliability Engineering and System Safety*, pp. 41-52, 2012.

[40] Q. Chen and L. Mili, “Risk-based Composite Power System Vulnerability Evaluation to Cascading Failures using Importance Sampling,” *IEEE Power and Energy Society General Meeting*, pp. 1-6, Jul., 2011.

[41] O. A. Mousavi, G. B. Gharehpetian and M. S. Naderi, "Estimating Risk of Cascading Blackout using Probabilistic Methods," in *International Conference on Electric Power and Energy Conversion Systems (EPECS)*, pp. 1-4, Nov., 2009.

[42] D. M. Greenwood and P. C. Taylor, "Investigating the Impact of Real-Time Thermal Ratings on Power Network Reliability," *IEEE Trans. Power Syst.*, vol.29, no.5, pp. 2460-2468, Sept., 2014.

[43] W. Wangdee and R. Billinton, "Reliability-Performance-Index Probability Distribution Analysis of Bulk Electricity Systems," *Canadian Journal of Electrical and Computer Engineering*, vol.30, no.4, pp. 189-193, Fall 2005.

[44] R. Billinton and W. Wangdee, "Predicting Bulk Electricity System Reliability Performance Indices using Sequential Monte Carlo Simulation," *IEEE Trans. Power Del.*, vol.21, no.2, pp. 909-917, Apr., 2006.

[45] J. Rossmaier and B. Chowdhury, "Development of a New System Vulnerability Index — The Overload Risk Index," in *40th North American Power Symposium (NAPS)*, pp. 1-8, Sept., 2008.

[46] J. Rossmaier and B. Chowdhury, "Further Development of the Overload Risk Index, an Indicator of System Vulnerability," in *North American Power Symposium (NAPS)*, pp. 1-6, Oct., 2009.

[47] C. Barbulescu and S. Kilyeni, "Congestion and ATC Driven Transmission Network Expansion Planning," in *16th IEEE Mediterranean Electrotechnical Conference (MELECON)*, pp. 967-970, Mar., 2012.

[48] M. Rahnamay-Naeini, Z. Wang, A. Mammoli and M. M. Hayat, “A Probabilistic Model for the Dynamics of Cascading Failures and Blackouts in Power Grids,” in *IEEE Power and Energy Society General Meeting*, pp. 1-8, Jul., 2012.

[49] D. M. J. Setrus, P. Hilber and S. Arnborg, “Component Ranking in Great Britain Transmission System based on Either Equipment Failures or Sabotage,” *Proceedings of the Institution of Mechanical Engineers, Part O: Journal of Risk and Reliability*, vol. 226, pp. 96-108, 2012.

[50] J. Setreus, S. Arnborg, R. Eriksson and L. Bertling, “Components' Impact on Critical Transfer Section for Risk based Transmission System Planning,” in *IEEE PowerTech*, Bucharest, pp. 1-8, Jun., 2009.

[51] A. M. M. Marsadek and Z. Norpiah, “Risk Assessment of Line Overload in a Practical Power System Considering Different Types of Severity Functions,” In *Proceedings of the 9th WSEAS International Conference on Applications of Electrical Engineering*, Houston, USA, 2009.

[52] G. A. Hamoud, “Assessment of Transmission System Component Criticality in the De-Regulated Electricity Market,” in *Proceedings of the 10th International Conference on Probabilistic Methods Applied to Power Systems (PMAPS)*, pp. 1-8, May, 2008.

[53] J. Kwon, S. Jeong, B. Shi, T. Tran, J. Choi, J. Cha, Y. Yoon, H. Choi and D. Jeon, “Probabilistic Reliability Evaluation of Korea Power System in Operation Mode,” in *IEEE Power Engineering Society General Meeting*, pp. 1-5, Jun., 2007.

[54] J. C. O. Mello, A. C. G. Melo, S. P. Romero, G. C. Oliveira, S. H. F. Cunha, M. Morozowski, M. V. F. Pereira and R. N. Fontoura, “Development of a Composite System Reliability Program for Large Hydrothermal Power Systems-Issues and

Solutions," in *Third International Conference on Probabilistic Methods Applied to Electric Power Systems*, pp. 64-69, Jul., 1991.

[55] L. Arya, L. Titare and D. Kothari, "Determination Of Probabilistic Risk Of Voltage Collapse Using Radial Basis Function (RBS) Network," *Elsevier Electric Power Systems Research*, pp. 426–434, 2006.

[56] J. Yu, W. Li, W. Yan, X. Zhao and Z. Ren, "Evaluating Risk Indices of Weak Lines and Buses causing Static Voltage Instability," in *IEEE Power and Energy Society General Meeting*, pp.1-7, Jul., 2011.

[57] C. Agreira, S. Jesus, S. Figueiredo, C. Ferreira, J. Pinto and F. Barbosa, "Probabilistic Steady-State Security Assessment of an Electric Power System Using A Monte Carlo Approach," in Proceedings of the *41st International Universities Power Engineering Conference (UPEC)*, vol. 2, pp. 408-411, Sept., 2006.

[58] J. McCalley, S. Asgarpoor, L. Bertling, R. Billinion, H. Chao, J. Chen, J. Endrenyi, R. Fletcher, A. Ford, C. Grigg, G. Hamoud, D. Logan, A. P. Meliopoulos, M. Ni, N. Rau, L. Salvaderi, M. Schilling, Y. Schlumberger, A. Schneider, C. Singh, "Probabilistic Security Assessment for Power System Operations," in *IEEE Power Engineering Society General Meeting*, pp. 212-220, Vol. 1, Jun., 2004.

[59] L. Dong, W. Cheng, H. Bao and Y. Yang, "A Probabilistic Load Flow Method with Consideration of Random Branch Outages and Its Application," in *2010 Asia-Pacific Power and Energy Engineering Conference (APPEEC)*, pp. 1-4, Mar., 2010.

[60] J. Ubeda and R. Allan, "Sequential Simulation Applied to Composite System Reliability Evaluation," in *Proceedings on Transmission and Distribution*, vol.139, no.2, pp. 81-86, Mar., 1992.

[61] H. Ren, I. Dobson and B. A. Carreras, “Long-Term Effect of the N-1 Criterion on Cascading Line Outages in an Evolving Power Transmission Grid,” *IEEE Trans. Power Syst.*, vol.23, no.3, pp. 1217-1225, Aug., 2008.

[62] X. Luo, C. Singh and Q. Zhao, “Loss-Of-Load Probability Calculation Using Learning Vector Quantization,” in Proceedings on *International Conference of Power System Technology (PowerCon)*, vol.3, pp. 1707-1712, 2000.

[63] T. A. M. Sharaf and G. J. Berg, “Loadability in Composite Generation/Transmission Power-System Reliability Evaluation,” *IEEE Trans. Reliab.*, vol. 42, no. 3, pp. 393-400, Sep., 1993.

[64] P. Jirutitijaroen and C. Singh, “Comparison of Simulation Methods for Power System Reliability Indexes and Their Distributions,” *IEEE Trans. Power Syst.*, vol. 23, no. 2, pp. 486-493, May, 2008.

[65] S. E. El-Arab and H. Zarzoura, “Reliability Evaluation for the Egyptian Transmission and Sub-Transmission Networks,” in *IEEE Power Tech*, Lausanne, pp. 1723-1725, Jul., 2007.

[66] J. Choi, T. Tran, A. A. El-Keib, R. Thomas, O. HyungSeon and R. Billinton, “A Method for Transmission System Expansion Planning Considering Probabilistic Reliability Criteria,” *IEEE Trans. Power Syst.*, vol. 20, no. 3, pp. 1606-1615, Aug., 2005.

[67] S. Kumar and R. Billinton, “Adequacy Equivalents in Composite Power System Evaluation,” *IEEE Trans. Power Syst.*, vol. 3, no. 3, pp. 1167-1173, Aug., 1988.

[68] D. S. Kirschen, D. Jayaweera, D. P. Nedic and R. N. Allan, “A Probabilistic Indicator of System Stress,” *IEEE Trans. Power Syst.*, vol. 19, no. 3, pp. 1650-1657, Aug., 2004.

[69] K. B. D. Kirschen, D. Nedic, D. Jayaweera, R. Allan, “Computing the Value of Security,” *IEE Proceedings*, vol. 150, pp. 673-678, 2003.

[70] A. A. Chowdhury and S. M. Islam, “Development and Application of Probabilistic Criteria in Value-based Transmission System Adequacy Assessment,” *Australasian Universities Power Engineering Conference (AUPEC)*, pp. 1-9, Dec., 2007.

[71] J. Aghaei, N. Amjady, A. Baharvandi, M. A. Akbari, “Generation and Transmission Expansion Planning: MILP–Based Probabilistic Model,”, *IEEE Trans. Power Syst.*, vol. 29, no. 4, pp. 1592-1601, Jul., 2014.

[72] C. G. O. Dzobo and R. Herman, “Investigating the Use of Probability Distribution Functions in Reliability-Worth Analysis of Electric Power Systems,” *Elsevier Ltd Electrical Power and Energy Systems*, pp. 110-116, 2012.

[73] J. He, L. Cheng, D. S. Kirschen and Y. Sun, “Optimising the Balance Between Security and Economy on a Probabilistic Basis,” in *IET Generation, Transmission & Distribution*, vol. 4, no. 12, pp. 1275-1287, Dec., 2010.

[74] S. M. G. Gross, R. Schuler and C. Singh, “Reliability Assessment Incorporating Operational Considerations and Economic Aspects for Large Interconnected Grids,” in *Power Systems Engineering Research Center (PSER)*, USA, 2007.

[75] M. Xin, Y. Jingyan, X. Xiaochun and Z. HuiRu, “Reliability Worth Assessment of Composite System for Operational Purposes,” in Proceedings *International Conference on Power System Technology (PowerCon)*, vol. 2, pp. 1249-1253, 2002.

[76] T. Akbari, “Towards Integrated Planning: Simultaneous Transmission and Substation Expansion Planning,” *ScienceDirect Electric Power Systems Research*, Vo. 86, pp. 131-139, May, 2012.

[77] G. Strbac, R. Moreno, D. Pudjianto and M. Castro, "Towards a Risk-based Network Operation and Design Standards," in *IEEE Power and Energy Society General Meeting*, pp.1-4, Jul., 2011.

[78] G. Blanco, F. Olsina and F. Garces, "Transmission Investments Under Uncertainty: The Impact of Flexibility on Decision-Making," in *IEEE Power and Energy Society General Meeting*, pp.1-8, Jul., 2012.

[79] C. Wan, Z. Xu, Z. Y. Dong and K. P. Wong, "Probabilistic Load Flow Computation Using First-Order Second-Moment Method," in *IEEE Power and Energy Society General Meeting*, pp. 1-6, Jul., 2012.

[80] W. Li, P. Wang, Z. Guo, "Determination of Optimal Total Transfer Capability Using a Probabilistic Approach," *IEEE Trans. Power Syst.*, vol. 21, no. 2, pp. 862-868, May, 2006.

[81] A. P. S. Meliopoulos, S. W. Kang and G. J. Cokkinides, "Probabilistic Transfer Capability Assessment in a Deregulated Environment," in Proceedings of the *33rd Annual Hawaii International Conference on System Sciences*, Jan., 2000.

[82] J. C. O. Mello, A. C. G. Melo and S. Granville, "Simultaneous Transfer Capability Assessment by Combining Interior Point Methods and Monte Carlo Simulation," *IEEE Trans. Power Syst.*, vol. 12, no. 2, pp. 736-742, May, 1997.

[83] I. Dobson, K. R. Wierzbicki, J. Kim and H. Ren, "Towards Quantifying Cascading Blackout Risk," In *Bulk Power System Dynamics and Control – VII*, Charleston, South Carolina, pp. 1-12, Aug., 2007.

[84] I. D. K. Wierzbicki, “An Approach to Statistical Estimation of Cascading Failure Propagation in Blackouts,” In *Third International Conference on Critical Infrastructures*, Alexandria, VA, 2006.

[85] R. F. Chang, C. Y. Tsai, C. L. Su and C. N. Lu, “Method for Computing Probability Distributions of Available Transfer Capability,” in *IEE Proceedings-Generation, Transmission and Distribution*, vol. 149, no. 4, pp. 427-431, Jul., 2002.

[86] E. De Tuglie, M. Dicorato, M. La Scala and A. Bose, “Multiple Criteria Decision Making Methodology Based on a Probabilistic Evaluation of ATC for Congestion Management,” *22nd IEEE Power Engineering Society International Conference on Power Industry Computer Applications (PICA)*, pp. 362-367, 2001.

[87] M. Vaiman, K. Bell, Y. Chen, B. Chowdhury, I. Dobson, P. Hines, M. Papic, S. Miller and P. Zhang, “Risk Assessment of Cascading Outages: Methodologies and Challenges,” *IEEE Trans. Power Syst.*, vol. 27, no. 2, pp. 631-641, May, 2012.

[88] H. Ren and I. Dobson, “Using Transmission Line Outage Data to Estimate Cascading Failure Propagation in an Electric Power System,” *IEEE Trans. Circuits Syst II. Exp. Briefs*, vol. 55, no. 9, pp. 927-931, Sept., 2008.

[89] I. Dobson, B. A. Carreras and D. E. Newman, “Branching Process Models for the Exponentially Increasing Portions of Cascading Failure Blackouts,” in Proceedings of the *38th Annual Hawaii International Conference on System Sciences (HICSS)*, pp. 64a-64a, Jan., 2005.

[90] I. Dobson, B. A. Carreras, V. E. Lynch, B. Nkei and D. E. Newman, “Estimating Failure Propagation in Models of Cascading Blackouts,” in *2004 International Conference on Probabilistic Methods Applied to Power Systems*, pp. 641-646, Sept., 2004.

[91] I. Dobson, B. A. Carreras and D. E. Newman, "A Branching Process Approximation to Cascading Load-Dpendent System Failure," in *Proceedings of the 37th Annual Hawaii International Conference on System Sciences*, Jan., 2004.

[92] J. Zhang, J. A. Bucklew and F. L. Alvarado, "Search Strategies for Failure Cascade Paths in Power System Graphs," in *International Conference on Probabilistic Methods Applied to Power Systems*, pp. 651-656, Sept., 2004.

[93] Q. Chen, C. Jiang, W. Qiu and J. D. McCalley, "Probability Models for Estimating the Probabilities of Cascading Outages in High-Voltage Transmission Network," *IEEE Trans. Power Syst.*, vol. 21, no. 3, pp. 1423-1431, Aug., 2006.

[94] R. N. Allan, B. Borkowska and C. H. Grigg, "Probabilistic Analysis of Power Flows," *Proceedings of the Institution of Electrical Engineers*, vol. 121, no. 12, pp. 1551-1556, Dec., 1974.

[95] J. Usaola, "Probabilistic Load Flow in Systems with Wind Generation," *IET Generation, Transmission & Distribution*, vol. 3, no. 12, pp. 1031-1041, Dec. 2009.

[96] Z. Hu and X. Wang, "A Probabilistic Load Flow Method Considering Branch Outages," *IEEE Trans. Power Syst.*, vol. 21, no. 2, pp. 507-514, May, 2006.

[97] D. Lei, Z. Chuan-cheng, Y. Yi-han and Z. Pei, "Improvement of Probabilistic Load Flow to Consider Network Configuration Uncertainties," in *Asia-Pacific Power and Energy Engineering Conference (APPEEC)*, pp. 1-5, Mar., 2009.

[98] A. M. L. da Silva, R. N. Allan, S. M. Soares and V. L. Arienti, "Probabilistic Load Flow Considering Network Outages," *IEE Proceedings, Generation, Transmission and Distribution*, vol. 132, no. 3, pp. 139-145, May, 1985.

[99] R. N. Allan and A. M. L. da Silva, "Probabilistic Load Flow Using Multilinearisations," *IEE Proceedings Generation, Transmission and Distribution*, vol. 128, no. 5, pp. 280-287, Sept., 1981.

[100] B. Borkowska, "Probabilistic Load Flow," *IEEE Trans. Power App. Systems (PAS)*, no. 3, pp. 752-759, May, 1974.

[101] G. Valverde, A. T. Saric, V. Terzija, "Probabilistic Load Flow with Non-Gaussian correlated Random Variables using Gaussian Mixture Models," *IET Generation, Transmission & Distribution*, vol. 6, no. 7, pp. 701-709, Jul., 2012.

[102] S. Patra and R. B. Misra, "Probabilistic Load Flow Solution Using Method of Moments," in *2nd International Conference on Advances in Power System Control, Operation and Management (APSCOM)*, pp. 922-934, vol. 2, Dec., 1993.

[103] D. Cai, J. Chen, D. Shi, X. Duan, H. Li and M. Yao, "Enhancements to the Cumulant Method for Probabilistic Load Flow studies," in *IEEE Power and Energy Society General Meeting*, pp. 1-8, Jul., 2012.

[104] F. Coroiu, D. Dondera, C. Velicescu and G. Vuc, "Power Systems Reliability Evaluation Using Probabilistic Load Flows Methods," in *45th International Universities Power Engineering Conference (UPEC)*, pp. 1-5, Aug., 2010.

[105] J. Schwippe, O. Krause and C. Rehtanz, "Extension of a Probabilistic Load Flow Calculation based on an Enhanced Convolution Technique," in *IEEE PES/IAS Conference on Sustainable Alternative Energy (SAE)*, pp. 1-6, Sept., 2009.

[106] R. N. Allan, A. M. L. da Silva and R. C. Burchett, "Evaluation Methods and Accuracy in Probabilistic Load Flow Solutions," *IEEE Trans. Power App. Syst.*, no. 5, pp. 2539-2546, May, 1981.

[107] C. Su, “Probabilistic Load-Flow Computation Using Point Estimate Method,” *IEEE Trans. Power Syst.*, vol. 20, no. 4, pp. 1843-1851, Nov., 2005.

[108] K. Audomvongseree and B. Eua-arporn, “Composite System Reliability Evaluation Using AC Equivalent Network,” in Proceedings on *International Conference on Power System Technology (PowerCon)*, vol. 2, pp. 751-756, 2000.

[109] A. M. L. da Silva and V. L. Arienti, “Probabilistic Load Flow by a Multilinear Simulation Algorithm,” *IEE Proceedings Generation, Transmission and Distribution*, vol. 137, no. 4, pp. 276-282, Jul., 1990.

[110] A. P. S. Meliopoulos, G. J. Cokkinides, X. Y. Chao, “A New Probabilistic Power Flow Analysis Method,” *IEEE Trans. Power Syst.*, vol. 5, no. 1, pp. 182-190, Feb 1990.

[111] A. M. L. da Silva, S. M. P. Ribeiro, V. L. Arienti, R. N. Allan and M. B. Do Coutto Filho, “Probabilistic Load Flow Techniques Applied to Power System Expansion Planning,” *IEEE Trans. Power Syst.*, vol. 5, no. 4, pp. 1047-1053, Nov., 1990.

[112] A. M. L. da Silva, V. L. Arienti and R. N. Allan, “Probabilistic Load Flow Considering Dependence Between Input Nodal Powers,” *IEEE Trans. Power App. Syst. (PAS)*, vol. PAS-103, no. 6, pp. 1524-1530, Jun., 1984.

[113] R. N. Allan and M. R. G. Al-Shakarchi, “Linear Dependence Between Nodal Powers in Probabilistic a.c. Load Flow,” in *Proceedings of the Institution of Electrical Engineers*, vol. 124, no. 6, pp. 529-534, Jun., 1977.

[114] P. T. A. Michiorri, S. Jupe and C. Berry, “Investigation into the Influence of Environmental Conditions on Power System Ratings,” *Institution of Mechanical Engineers*, Part A, Journal of Power and Energy, pp. 223-743, 2009.

[115] F. R. McElvain and S. S. Mulnix, "Statistically Determined Static Thermal Ratings of Overhead High Voltage Transmission Lines in the Rocky Mountain Region," *IEEE Trans. Power Syst.*, vol.15, no.2, pp. 899, 902, May 2000.

[116] J. L. Reding, "A Method for Determining Probability based Allowable Current Ratings for BPA's Transmission Lines," *IEEE Trans. Power Del.*, vol. 9, no. 1, pp. 153-161, Jan., 1994.

[117] H. Wan, J. D. McCalley and V. Vittal, *"Increasing Thermal Rating by Risk Analysis," IEEE Trans. Power Syst.*, vol. 14, no. 3, pp .815-828, Aug., 1999.

[118] J. F. Hall and A. K. Deb, "Prediction of Overhead Transmission Line Ampacity by Stochastic and Deterministic Models," *IEEE Trans. Power Del.*, vol. 3, no. 2, pp. 789-800, Apr., 1988.

[119] K. K. A. Kapetanaki, "MOPSO using Probabilistic and Deterministic Criteria Based on OHL's Thermal Ratings," in *18th Power Systems Computation Conference*, Wroclaw, Poland, 2014.

[120] D. O. Koval and R. Billinton, "Determination of Transmission Line Ampacities by Probability and Numerical Methods," *IEEE Trans. Power App. Syst.*, vol. PAS-89, no. 7, pp. 1485-1492, Sept., 1970.

[121] *Security and Quality of Supply Standard*, National Electricity Transmission System, Version 2.0, June 24, 2009, [online], Available: http://www.nationalgrid.com/NR/rdonlyres/149DEAE1-46B0-4B20-BF9C-66BDCB805955/35218/NETSSQSS_GoActive_240609.pdf.

[122] J. J. Grainger and W. D. Stevenson, *Power System Analysis*, McGraw-Hill, 1994.

[123] BCP Busarello+Cott+Partner, *NEPLAN Planning and optimization system for electrical network*, [online], Available: http://www.neplan.ch.

[124] A. Amin, G. Chaffey, J. Lawthom and D. Milman, "Evaluation and Enhancement of Potential Severn Barrage Schemes," MSc/MA Dissertation, Cardiff University, 2012.

[125] M. A. Laughton and D. J. Warne, *Electrical Engineer's Reference Book*, Newnes, 2003.

[126] *Thermal Behaviour of Overhead Conductors*, CIGRE, Working Group 12, 2002.

[127] *IEEE Standard for Calculating the Current-Temperature of Bare Overhead Conductors*, IEEE Power Engineering Society, IEEE Std 738, 2006.

[128] J. Heckenbergerovi, P. Musilek, and K. Filimonenkov, "Quantification of Gains and Risks of Static Thermal Rating Based on Typical Meteorological Year," *Proceedings of the ELSEVIER*, 2013.

[129] M. Siller, J. Heckenbergerova, P. Musilek, and J. Rodway, "Sensitivity Analysis of Conductor Current-Temperature Calculations," *26th IEEE Canadian Conference of Electrical and Computer Engineering (CCECE)*, 2013.

[130] P. Zhang, M. Shao, A. Leoni, D. Ramsay, and M. Graham, "Determination of Static Thermal Conductor Rating using Statistical Analysis Method," In *DRPT*, Apr., 2008.

[131] N. Yenumula and R. Adapa, "Probabilistic Transmission Line Ratings," in *8th International Conference on Probabilistic Methods Applied to Power Systems*, Ames, Iawa, Sept., 2004.

[132] R. Eager, S. Raman, A. Wootten, D. Westphal, J. Reid, and A. Mandoos, "A Climatological Study of the Sea and Land Breezes in the Arabian Gulf Region," *Journal of Geophysical Research*, vol. 113, 2008.

[133] T. Quarda, C. Charron, J. Shin, P. Marpu, A. Mandoos, and M. Tamimi, “Probability Distributions of Wind Speed in the UAE,” *Elsevier*, pp. 414 – 434, 2015.

[134] M. Bockarjova and G. Andersson, “Transmission Line Conductor Temperature Impact on State Estimation Accuracy,” *IEEE Power Tech*, Lausanne, pp. 701-708, 2007,

[135] M. Schlapfer and P. Mancarella, “Probabilistic Modeling and Simulation of Transmission Line Temperatures under Fluctuating Power Flows,” *IEEE Trans. Power Del.*, vol. 26, no. 4, Oct., 2011.

[136] R. Allan and R. Billinton, “Probabilistic Assessment of Power Systems,” *Proceedings of the IEEE*, vol. 88, no. 2, Feb., 2000.

[137] C. Grigg, P. Wong, P. Albrecht, R. Allan, M. Bhavaraju, R. Billinton, Q. Chen, C. Fong, S. Haddad, S. Kuruganty, W. Li, R. Mukerji, D. Patton, N. Rau, D. Reppen, A. Schneider, M. Shahidehpour, C. Singh, “The IEEE Reliability Test System-1996,” A report prepared by the Reliability Test System Task Force of the Application of Probability Methods Subcommittee, *IEEE Trans. Power Syst.*, vol. 14, no. 3, pp. 1010-1020, Aug., 1999.

[138] M. Ni, J. McCalley, V. Vittal and T. Tayyib, “Online Risk-Based Security Assessment,” *IEEE Trans. Power Syst.*, vol. 18, no. 1, Feb., 2003.

[139] Dubai Met Office, https://services.dubaiairports.ae/dubaimet/MET/Climate.aspx

[140] *Aluminum Electrical Conductor Handbook*, 3rd edition, the Aluminum Association, 1989.

[141] National Grid, *Electricity Ten Year Statement*, UK electricity transmission, Nov., 2012, Available at http://www.nationalgrid.com/ [online].

[142] “Distances From”, (2015), [online], Avilable: http://www.distancesfrom.com/Latitude-Longitude.aspx [online].

Appendix A: Engineering parameters for the Dubai transmission system

Table A.1: DEWA power plants and their adopted ranking order for year 2011

Generator	Ranking Order (Priority to switch-on)	6081MW (Summer)			1997MW (Winter)		
		Status	Capacity @ 50° C Ambient Temp. (MW)	Power Generated (MW)	Status	Capacity @ 15° C Ambient Temp. (MW)	Power Generated (MW)
T-ST-1	**46**	OFF	68	0	OFF	68	0
T-ST-2	**47**	OFF	68	0	OFF	68	0
T-ST-3	**48**	ON	68	50	OFF	68	0
T-ST-4	**49**	OFF	68	0	OFF	68	0
T-ST-5	**50**	OFF	68	0	OFF	68	0
T-ST-6	**38**	ON	70	50	OFF	70	0
T-ST-7	**40**	OFF	70	0	ON	70	70
T-ST-8	**42**	OFF	70	0	OFF	70	0
B-GT-1	**37**	ON	132.33	132	OFF	159	0
B-GT-2 (Slack Bus)	**39**	ON	132.33		ON	159	
B-GT-3	**41**	OFF	132.33	0	OFF	159	0
U-GT-1	**33**	ON	84	80	ON	110	100
U-GT-2	**35**	OFF	84	0	OFF	110	
U-GT-3	**36**	ON	84	80	OFF	110	
U-GT-4	**43**	ON	87	80	OFF	116	
U-GT-5	**45**	ON	87	80	OFF	116	
U-ST-6	**44**	ON	105	105	OFF	105	
U-BPST-7	**34**	ON	58	58	ON	58	58
D-GT-1	**11**	ON	114.25	110	ON	150	100
D-GT-2	**15**	OFF	114.25	0	OFF	150	
D-GT-3	**16**	ON	114.25	110	OFF	150	
D-GT-4	**17**	OFF	114.25	120	OFF	150	
D-GT-5	**13**	ON	121	120	OFF	155	
D-BPST-6	**12**	ON	70	70	ON	70	70
D-BPST-7	**14**	ON	70	70	ON	70	70
E-GT-1	**55**	OFF	101.14	0	OFF	130	0
E-GT-2	**56**	OFF	101.14	0	OFF	130	0
E-GT-3	**57**	OFF	101.14	0	OFF	130	0
E-GT-4	**58**	OFF	101.14	0	OFF	130	0
E-GT-5	**59**	OFF	101.14	0	OFF	130	0
E-GT-6	**60**	OFF	101.14	0	OFF	130	0
E-GT-41	**61**	OFF	136.34	0	OFF	160	0
E-GT-42	**62**	OFF	136.34	0	OFF	160	0
E-GT-43	**63**	OFF	136.34	0	OFF	160	0
V-GT-1	**6**	ON	186.88	180	ON	241	200
V-GT-2	**8**	ON	186.88	180	OFF	241	0
V-GT-3	**10**	ON	186.88	180	OFF	241	0
V-BPST-4	**7**	ON	135	135	ON	135	135
V-BPST-5	**9**	ON	135	135	ON	135	135
C-GT-11	**1**	ON	183	180	ON	226	160
C-GT-12	**3**	ON	183	180	OFF	226	0

C-GT-13	**5**	ON	183	180	OFF	226	0
C-BPST-4	**2**	ON	156	156	ON	156	156
C-BPST-5	**4**	ON	156	156	ON	156	156
C-GT-21	**27**	ON	235.4	200	ON	270	160
C-GT-22	**29**	ON	235.4	200	OFF	270	0
C-GT-23	**31**	ON	235.4	200	OFF	270	0
C-GT-24	**32**	ON	235.4	200	OFF	270	0
C-BPST-25	**28**	ON	195.8	195	ON	195.8	196
C-BPST-26	**30**	ON	195.8	195	ON	195.8	196
F-GT-51	**51**	OFF	204.6	0	OFF	270	0
F-GT-52	**52**	OFF	204.6	0	OFF	270	0
F-GT-53	**53**	OFF	204.6	0	OFF	270	0
F-GT-54	**54**	OFF	204.6	0	OFF	270	0
A-GT-11	**18**	ON	234.1	230	OFF	270	0
A-GT-12	**20**	ON	234.1	230	OFF	270	0
A-GT-21	**21**	ON	234.1	230	OFF	270	0
A-GT-22	**23**	ON	234.1	230	OFF	270	0
A-GT-31	**24**	ON	234.1	230	OFF	270	0
A-GT-32	**26**	ON	234.1	230	OFF	270	0
A-BPST-10	**19**	ON	218.4	218	OFF	218	0
A-BPST-20	**22**	ON	218.4	218	OFF	218	0
A-BPST-30	**25**	ON	218.4	218	OFF	218	0
Total			**9544.89**	**6201**		**10865.6**	**1926**

Table A.2: Active and reactive powers derived for each load point for year 2011

Load Point #	**3273 MW**		**1997 MW**		**6081 MW**	
	P	**Q**	**P**	**Q**	**P**	**Q**
1	30	10	18	6	56	19
2	1	1	1	1	2	2
3	58	20	35	12	108	37
4	26	11	16	7	48	20
5	15	10	9	6	28	19
6	12	4	7	2	22	7
7	11	3	7	2	20	6
8	13	0	8	0	24	0
9	9	2	5	1	17	4
10	11	3	7	2	20	6
11	20	4	12	2	37	7
12	13	4	8	2	24	7
13	1	1	1	1	2	2
14	34	8	21	5	63	15
15	31	10	19	6	58	19
16	2	0	1	0	4	0
17	2	0	1	0	4	0
18	1	0	1	0	2	0
19	13	9	8	5	24	17

20	27	3	16	2	50	6
21	1	1	1	1	2	2
22	35	2	21	1	65	4
23	1	1	1	1	2	2
24	48	22	29	13	89	41
25	30	17	18	10	56	32
26	38	10	23	6	71	19
27	13	5	8	3	24	9
28	24	12	15	7	45	22
29	35	25	21	15	65	46
30	24	11	15	7	45	20
31	23	4	14	2	43	7
32	21	10	13	6	39	19
33	37	11	23	7	69	20
34	13	3	8	2	24	6
35	29	12	18	7	54	22
36	8	1	5	1	15	2
37	25	0	15	0	46	0
38	1	1	1	1	2	2
39	25	10	15	6	46	19
40	59	2	36	1	110	4
41	17	7	10	4	32	13
42	18	6	11	4	33	11
43	36	10	22	6	67	19
44	21	5	13	3	39	9
45	1	1	1	1	2	2
46	35	8	21	5	65	15
47	1	1	1	1	2	2
48	33	16	20	10	61	30
49	1	1	1	1	2	2
50	39	12	24	7	72	22
51	12	5	7	3	22	9
52	19	9	12	5	35	17
53	1	1	1	1	2	2
54	31	24	19	15	58	45
55	1	1	1	1	2	2
56	34	14	21	9	63	26
57	1	1	1	1	2	2
58	33	8	20	5	61	15
59	46	18	28	11	85	33
60	31	10	19	6	58	19
61	13	0	8	0	24	0
62	15	0	9	0	28	0
63	26	11	16	7	48	20
64	26	11	16	7	48	20
65	37	25	23	15	69	46
66	1	1	1	1	2	2
67	34	12	21	7	63	22
68	40	16	24	10	74	30
69	53	7	32	4	98	13
70	7	1	4	1	13	2
71	9	1	5	1	17	2
72	32	4	20	2	59	7

73	21	9	13	5	39	17
74	26	12	16	7	48	22
75	48	10	29	6	89	19
76	12	8	7	5	22	15
77	22	3	13	2	41	6
78	28	9	17	5	52	17
79	19	4	12	2	35	7
80	9	3	5	2	17	6
81	20	9	12	5	37	17
82	27	9	16	5	50	17
83	32	4	20	2	59	7
84	17	6	10	4	32	11
85	25	11	15	7	46	20
86	11	3	7	2	20	6
87	20	6	12	4	37	11
88	29	15	18	9	54	28
89	5	2	3	1	9	4
90	26	9	16	5	48	17
91	16	6	10	4	30	11
92	12	2	7	1	22	4
93	51	25	31	15	95	46
94	27	9	16	5	50	17
95	5	1	3	1	9	2
96	3	1	2	1	6	2
97	15	6	9	4	28	11
98	16	9	10	5	30	17
99	10	1	6	1	19	2
100	20	15	12	9	37	28
101	24	9	15	5	45	17
102	7	5	4	3	13	9
103	20	27	12	16	37	50
104	28	27	17	16	52	50
105	23	5	14	3	43	9
106	30	8	18	5	56	15
107	29	13	18	8	54	24
108	4	0	2	0	7	0
109	1	1	1	1	2	2
110	4	0	2	0	7	0
111	16	4	10	2	30	7
112	17	4	10	2	32	7
113	13	1	8	1	24	2
114	13	3	8	2	24	6
115	41	7	25	4	76	13
116	26	5	16	3	48	9
117	29	12	18	7	54	22
118	24	5	15	3	45	9
119	23	8	14	5	43	15
120	3	0	2	0	6	0
121	12	1	7	1	22	2
122	1	0	1	0	2	0
123	7	4	4	2	13	7
124	2	0	1	0	4	0
125	6	0	4	0	11	0

126	9	5	5	3	17	9
127	19	2	12	1	35	4
128	23	10	14	6	43	19
129	12	5	7	3	22	9
130	16	5	10	3	30	9
131	16	5	10	3	30	9
132	8	3	5	2	15	6
133	10	6	6	4	19	11
134	12	6	7	4	22	11
135	23	6	14	4	43	11
136	22	10	13	6	41	19
137	6	1	4	1	11	2
138	8	2	5	1	15	4
139	8	4	5	2	15	7
140	12	3	7	2	22	6
141	1	0	1	0	2	0
142	34	13	21	8	63	24
143	19	10	12	6	35	19
144	1	0	1	0	2	0
145	18	9	11	5	33	17
146	7	1	4	1	13	2
147	24	15	15	9	45	28
148	15	6	9	4	28	11
149	4	0	2	0	7	0
150	20	9	12	5	37	17
151	16	3	10	2	30	6
152	2	0	1	0	4	0
153	9	1	5	1	17	2
154	4	1	2	1	7	2
155	13	5	8	3	24	9
156	2	0	1	0	4	0
157	2.7	1.8	2	1	5	3
158	3.7	2.2	2	1	7	4
159	3.6	1.6	2	1	7	3
160	3.4	2.4	2	1	6	4
161	2.7	1.5	2	1	5	3
162	2.5	1.5	2	1	5	3
163	7	1	4	1	13	2
164	1	0	1	0	2	0
165	0.34	0.25	0	0	1	0
166	0.29	0.22	0	0	1	0
167	0.32	0.24	0	0	1	0
168	1	0.5	1	0	2	1
169	0.98	1	1	1	2	2
170	1	1	1	1	2	2
171	1.8	1.41	1	1	3	3
172	2	1.5	1	1	4	3
173	11	5.4	7	3	20	10
174	16	14	10	9	30	26
175	10	8	6	5	19	15
176	9.1	7.5	6	5	17	14
177	17	14.3	10	9	32	27
178	1.4	0.9	1	1	3	2

179	0.48	0.36	0	0	1	1
180	0.48	0.36	0	0	1	1
181	0.62	0.97	0	1	1	2
182	1.1	1.12	1	1	2	2
183	0.3	0.2	0	0	1	0
184	1.9	1.3	1	1	4	2
185	0.3	0.2	0	0	1	0
186	0.3	0.2	0	0	1	0
187	0.3	0.4	0	0	1	1
188	2.2	2	1	1	4	4
189	16.01	10.98	10	7	30	20
190	14.54	11.17	9	7	27	21
191	14.45	10.04	9	6	27	19
192	13.49	9.99	8	6	25	19
193	13.15	8.4	8	5	24	16
194	20.14	15.1	12	9	37	28
195	20.86	15.65	13	10	39	29
196	19.53	14.65	12	9	36	27
197	0.2	0.1	0	0	0	0
198	1.3	1.4	1	1	2	3
199	1.5	1.8	1	1	3	3
200	0.5	0.8	0	0	1	1
201	20.3	14.6	12	9	38	27
202	16	10.8	10	7	30	20
203	19.4	13.5	12	8	36	25
204	5.85	5.37	4	3	11	10
205	12.8	8.5	8	5	24	16
206	5	2	3	1	9	4
207	20	10	12	6	37	19
208	20	10	12	6	37	19
209	20	10	12	6	37	19
	3274	**1272**	**1998**	**776**	**6083**	**2364**